A semi-Lagrangian ϵ-monotone Fourier method for continuous withdrawal GMWBs under jump-diffusion with stochastic interest rate

Yaowen Lu * Duy-Minh Dang†

July 28, 2023

Abstract

We develop an efficient pricing approach for guaranteed minimum withdrawal benefits (GMWBs) with continuous withdrawals under a realistic modeling setting with jump-diffusions and stochastic interest rate. Utilizing an impulse stochastic control framework, we formulate the no-arbitrage GMWB pricing problem as a time-dependent Hamilton-Jacobi-Bellman (HJB) Quasi-Variational Inequality (QVI) having three spatial dimensions with cross derivative terms. Through a novel numerical approach built upon a combination of a semi-Lagrangian method and the Green's function of an associated linear partial integro-differential equation, we develop an ϵ-monotone Fourier pricing method, where $\epsilon > 0$ is a monotonicity tolerance. Together with a provable strong comparison result for the HJB-QVI, we mathematically demonstrate convergence of the proposed scheme to the viscosity solution of the HJB-QVI as $\epsilon \to 0$. We present a comprehensive study of the impact of simultaneously considering jumps in the sub-account process and stochastic interest rate on the no-arbitrage prices and fair insurance fees of GMWBs, as well as on the holder's optimal withdrawal behaviors.

Keywords: Variable annuity, guaranteed minimum withdrawal benefit, impulse control, viscosity solution, monotonicity, stochastic interest rate, jump-diffusion

AMS Classification 65N06, 93C20

1 Introduction

Variable annuities are a class of insurance products that provide the holder with particular guaranteed stream of income without requiring him/her to sacrifice full control over the funds invested, and hence, allowing the holder to enjoy potentially favorable market conditions. Therefore, these products are particularly popular among investors who need to manage their own spending plans, especially among retirees, considering the on-going rapid word-wide trend of replacing defined benefit pension plans by defined contribution ones. The current era of increased market volatility and growing inflation has significantly boosted annuity sales. In some countries, such as the US, annuity sales are at highest levels since the 2007-2008 Global Financial Crisis. Specifically, the US annuity market in 2021 was valued at US$231.63 billion, and the market is expected to grow at a compound annual growth rate of 4.7% during the forecast period of 2022-2026, reaching US$298.70 billion by 2026 [71].

To attract investors, variable annuities are often incorporated with additional features, among which Guaranteed Minimum Withdrawal Benefits (GMWBs) are popular. Since first introduced in the early 2000's, GBMWs have captured great attention from both industry and academia alike, as evidenced by a substantial and growing body of literature; see [61, 17, 19, 22, 6, 42, 44, 45, 29, 37, 40, 62, 4, 83, 1, 65, 43, 57], among many other publications.

*School of Mathematics and Physics, The University of Queensland, St Lucia, Brisbane 4072, Australia, yaowen.lu@uq.edu.au

†School of Mathematics and Physics, The University of Queensland, St Lucia, Brisbane 4072, Australia, duyminh.dang@uq.edu.au

In its simplest form, a GMWB is a long-dated contract, with maturity of 10 years or more, between the policy holder (e.g. a retiree) and the insurer (e.g. an insurance company), according to which the holder makes an up-front payment, i.e. the premium, into a (personal) sub-account for investment in risky assets. In return, by means of a guarantee account, the insurer is stipulated to provide the holder with a stream of guaranteed cash withdrawals whose amounts (and possibly timing) are to be determined by the holder, all of which cumulatively sum up to *at least* the premium, regardless of the performance of the risky investment. The holder may also withdraw more than the specified amount, subject to certain penalties and conditions. Upon contract expiry, the holder can convert the remaining investment in the risky assets to cash, and withdraw this amount. For protection from the downside in a GMWB, the insurer typically charges the holder an insurance fee by deducting an ongoing fraction of the risky investment as opposed to an up-front one-off fee. Underpricing typically results in undercalculated insurance fee, which adversely affects the insurer's risk management, potentially impacting the long-term sustainability of the market. The reader is referred to, for example, [20, 61, 19, 22, 12], for discussions in relation to GMWB underpricing in practice and its potential consequences.

Guaranteed Minimum Withdrawal Benefits are studied under two withdrawal scenarios, namely discrete and continuous. It is reported in the literature that no-arbitrage prices and fair insurance fees of GMWBs, as well as the holder's optimal withdrawal behaviors are highly sensitive to modeling assumptions and parameters, in particular, jumps in the sub-account's balance process [19, 14, 52, 57]. Under a discrete withdrawal scenario, fair prices and insurance fees are found to be remarkably sensitive to interest rates, in particular, in the case of (instantaneous) short rate dynamics, such as the Vasicek model [66, 74], the Hull-White [37, 30, 38, 55], and the the Cox-Ingersoll-Ross model [7, 40]. Substantial impact of short rate dynamics on the holder's optimal withdrawal behavior is recently reported in [62]. We highlight that the combined effects of jumps and stochastic interest rate in the context of GMWBs have not been previously studied in the literature.

Numerical methods for GMWBs in a continuous withdrawal scenario is studied through a stochastic optimal control framework. In this withdrawal scenario, the pricing problem can be formulated using either impulse control or singular control. This typically results in a Hamilton-Jacobi-Bellman Quasi-Variational Inequality (HJB-QVI) of at least two spatial dimensions, namely the balances of the sub- and guarantee accounts, which must be solved numerically. Convergence to viscosity solutions forms the main challenge in the development of numerical methods for HJB equations. This is typically built upon the convergence framework established by Barles and Souganidis in [11]; also, see [21, 81, 50, 10, 73, 15, 9] for relevant discussions. Specifically, provided that a strong comparison result holds, convergence to viscosity solution is ensured if numerical methods are (i) monotone (in the viscosity sense), (ii) stable, and (iii) consistent. When a finite difference method is used, monotonicity is ensured by a positive coefficient discretization method [69, 82, 59, 34]. The reader is referred to [22, 44, 43, 42, 61, 12] and [17, 19, 4, 57] for an analysis of singular control and impulse control formulations, respectively. For GMWB contracts, impulse control is more convenient than singular control in handling complex contract features, such as is the reset provision[22, 61, 65, 1, 40, 83].[1]

In contrast to continuous withdrawals, a discrete withdrawal scenario is relatively much simpler to tackle. Specifically, between fixed withdrawal (intervention) times, the pricing of GMWB contracts typically involves solving an either (i) associated linear Partial (Integro)-Differential Equation (P(I)DE) using finite differences [17, 22, 57], or (ii) an expectation problem using numerical integration [58, 75, 12, 1, 48, 47] or regression-type Monte Carlo [7, 46]. Across withdrawal times, an optimization problem needs to be solved to determine the optimal withdrawal amount, by which the balance of the guarantee account is then adjusted accordingly. We note that existing numerical integration or regression-type Monte Carlo are typically not suitable to tackle continuous withdrawals.

[1]Generally speaking, the impulse control approach is suitable for many complex situations in stochastic optimal control [64, 76, 77, 78, 79, 53, 39, 5, 32, 2, 13, 24].

In light of the current era of wildly fluctuating interest rates and economic turbulence, it is of enormous importance to apply realistic modelling for popular pension-related products. In addition, it is also equally important to develop mathematically reliable numerical methods for those products, enabling realistic and useful conclusions to be drawn from the numerical results. For GMWBs, it is highly desirable to simultaneously incorporate jumps (in the sub-account balance) and stochastic interest rate dynamics. Although in practice, only discrete withdrawals are possible, through no-arbitrage arguments, it is arguable that the prices and insurance fees in the associated continuous withdrawal scenario can serve as worst-case bounds for the respective values in a discrete withdrawal one, which are important for risk-management purposes.

Nonetheless, the continuous withdrawal scenario brings about significant mathematical challenges. As noted earlier, for GMWBs under a low-dimensional model, existing numerical integration and regression-type Monte Carlo methods are computationally expensive. With respect to the PIDE approach, due to the short rate factor, the no-arbitrage pricing of GMWBs gives rise to a HJB-QVI of three spatial dimensions with cross derivative terms, which is very challenging to solve efficiently numerically. In particular, while finite difference methods can be used to solve this HJB-QVI, due to cross derivative terms, to ensure monotonicity through a positive coefficient discretization method, a wide-stencil method based on a local coordinate rotation is needed. However, this is very computationally expensive [59, 26].

In general, Fourier-based methods, if applicable, offer several important advantages over finite differences, such as no timestepping error between intervention times, and the capability of straightforward handling of realistic underlying dynamics, such as jump diffusion and regime-switching. In particular, the well-known Fourier cosine series expansion method [33, 72] can achieve high order convergence for piecewise smooth problems. However, optimal control problems are often non-smooth, and hence high order convergence cannot be expected. Convergence issues, especially montonicity considerations are of primary importance. A novel Fourier-based method is introduced in our paper [57] for an impulse control formulation of the GMWB pricing problem in which the sub-account's balance process follows jump-diffusion dynamics with a constant interest rate. Central to the method is a combination of (i) the Green's function of an associated multi-dimensional PIDE and (ii) an ϵ-monotone Fourier method to approximate a pricing convolution integral through a known closed-form expression of the Fourier transform of the Green function. Here, the monotonicity of the method is achieved within an ϵ tolerance, where $\epsilon > 0$, as opposed to strictly monotone. In this work, a Barles-Souganidis-type analysis in [11] is utilized to rigorously prove the convergence of the scheme the unique viscosity solution of the HJB-QVI as the discretization parameter and the monotonicity tolerance ϵ approach zero. Nonetheless, for the case of jump-diffusion dynamics having a non-trivial correlation with the short rate, a closed-form expression of the Fourier transform of the Green function is not know to exist. Therefore, the approach in [57], while promising, is not directly applicable. This mathematical and computational challenge of continuous withdrawals forms another motivation for our work.

The objective of the paper is (i) to develop a provably convergent and computationally efficient PDE method for the no-arbitrage GMWB pricing problem with continuous withdrawals under realistic modeling assumptions, namely jumps and stochastic interest rate, and (ii) to study the combined impacts of these modelling assumptions on the no-arbitrage prices and fair insurance fees of GMWBs, as well as the holder's optimal withdrawal behaviors. For clarity of presentation, we focus on the GMWB pricing problem with basic contract features. We emphasize that we do not to advocate for a specific jump-diffusion and/or stochastic interest rate model, but rather, we aim to study the impact of realistic modeling on GWMB. In particular, to model stochastic interest rate, we use the Vasicek short rate dynamics [80]. Due to a Gaussian nature, the Vasicek short rate dynamics are often criticized for allowing negative interest rates, which is considered a highly undesirable, and perhaps, also highly improbable, scenario for any economy. However, in recent times, it has become evident that negative interest rates are employed as a monetary policy tool by central banks, such as the European Central Bank, against extreme financial crises. For example, see [51, 27, 56] and references therein.

The main contribution of the paper are as follows.

- We propose a comprehensive and systematic impulse control formulation and pricing approach for GMWBs when the sub-account process follows a jump-diffusion process [60, 54] with the Vasicek short rate dynamics [80].
  - We derive and define the pricing problem in a form of an HJB-QVI with three spatial dimensions posed on an infinite definition domain with appropriate boundary conditions. Through a novel approach built upon a combination of a semi-Lagrangian method and the Green's function of an associated PIDE, we obtain a properly truncated computational domain for which loss of information in the boundary is controllably negligible.
  - Starting from a discrete withdrawal scenario, we develop a semi-Lagrangian ϵ-monotone Fourier method to solve an associated two-dimensional PIDE on a finite computation domain, together with an efficient padding technique to control wrap-around errors.
  - With a provable strong comparison result, we rigorously prove the convergence of our scheme the unique viscosity solution of the HJB-QVI as the discretization parameter and the monotonicity tolerance ϵ approach zero. That is, our proposed method can be used for discrete withdrawals, and can also be shown to converge to the viscosity solution of the HJB-QVI arising in the continuous withdrawal setting.
- With a provably convergent numerical method, which allows realistic and useful conclusions to be drawn from the numerical results, we carry out a comprehensive study of the impact of considering jumps and stochastic short rate. Our numerical results suggest that, compared to stochastic interest rate dynamics, using a constant interest rate results in underpricing of fair insurance fees for GMWBs. Furthermore, the simultaneous application of jumps and stochastic interest rates results in (i) a much lower fair insurance fee, and (ii) significantly different optimal withdrawal behaviors than those obtained from a comparable pure-diffusion model with a comparable constant interest rate. These findings underscore the importance of realistic modelling and mathematically reliable numerical methods in reducing potential underpricing and overpricing of GMWBs, contributing to the long-term sustainability of the financial markets.

The remainder of the paper is organized as follows. Section 2 describes the impulse control framework and the underlying processes. We present in Section 3 an impulse control formulation of the GMWB pricing problem in the form of a three-dimensional HJB-QVI. Also therein, we also prove a strong comparison result. A numerical method for solving the HJB-QVI is discussed in Section 4. The convergence of the proposed numerical method is demonstrated in Section 5. In Section 6, we present and discuss extensive numerical results of GMWBs and the combined impact of jumps and stochastic interest rates on the prices, insurance fees, and the holder's optimal withdrawal behaviors. Section 7 concludes the paper and outlines possible future work.

2 Modeling

We consider a complete probability space $(\mathfrak{S}, \mathfrak{F}, \mathfrak{F}_{0\leq t\leq T}, \mathfrak{Q})$, with sample space $\mathfrak{S}$, sigma-algebra $\mathfrak{F}$, filtration $\mathfrak{F}_{0\leq t\leq T}$, where $T > 0$ is a fixed investment maturity, and a risk-neutral measure $\mathfrak{Q}$ defined on $\mathfrak{F}$. We discuss the underlying dynamics with an impulse control formulation framework in mind [64, 53].

Broadly speaking, using an impulse control argument [17], the holder's optimal withdrawal strategy involves choosing either (i) withdraw continuously at a rate determined by the holder, but no greater than a cap on the maximum allowed continuous withdrawal rate, hereinafter denoted by C_r; or (ii) withdraw finite amounts at specific times, both determined by the holder, subject to a penalty charge which is proportional to the withdrawal amount and is calculated at the rate μ, where $0 < \mu < 1$, as well as a strictly positive fixed cost c. Due to the associated penalty charge, (ii) is only optimal at some stopping times. To this end, let $\{t^\iota\}_{\iota\leq\iota_{\max}}$, $\iota_{\max}\leq\infty$, is any sequence of stopping times with respect to the filtration $\mathfrak{F}_{0\leq t\leq T}$ satisfying $0\leq t\leq t^1\leq t^2<\cdots<t^{\iota_{\max}}\leq T$.

We denote by (i) $\hat{\gamma}(t)$, $\hat{\gamma}(t)\in[0,C_r]$, a continuous control representing continuous withdrawal rate at time t, and by (ii) an impulse control $\{(t^\iota,\gamma^\iota)\}_{\iota\leq\iota_{\max}}$, representing withdrawal/intervention times $\{t^\iota\}_{\iota\leq\iota_{\max}}$ and associated impulses $\{\gamma^\iota\}_{\iota\leq\iota_{\max}}$, where γ^ι is a $\mathfrak{F}_{t^\iota}$-measurable random variable. Here, each t^ι corresponds to a time at which the holder instantaneously withdraws a finite amount, and γ^ι, $\gamma^\iota\in[0,A(t_\iota^-)]$, corresponds to the withdrawal amount at that time. The net revenue cash flow provided to the holder at time t^ι is $(1-\mu)\gamma^\iota-c$.

We respectively denote by $Z(t)$, $A(t)$, and $R(t)$, $t\in[0,T]$, the time-t balance of the sub-account, the guarantee account, and the instantaneous short-rate. Due to continuous withdrawals and withdrawing finite amounts, the dynamics of $A(t)$ are given by

$$\begin{aligned} dA(t) &= -\hat{\gamma}(t)\mathbf{1}_{\{A(t)>0\}}dt, \quad \text{for} \;\; t\neq t^\iota, \quad \iota=1,2,\ldots,\iota_{\max}, \\ A(t) &= A(t^-)-\gamma^\iota, \qquad\quad \text{for} \;\; t=t^\iota, \quad \iota=1,2,\ldots,\iota_{\max}. \end{aligned} \tag{2.1}$$

Let the dynamics of $Z(t)$ and $R(t)$ be given by

$$\begin{cases} \dfrac{dZ(t)}{Z(t)} = (R(t)-\beta-\lambda\kappa)\,dt+\sigma_z\rho dW_z(t)+\sigma_z\sqrt{1-\rho^2}dW_R(t)+dJ(t) \\ \qquad\qquad -\hat{\gamma}(t)\mathbf{1}_{\{Z(t),A(t)>0\}}dt, \quad \text{for } t\neq t^k, \quad \iota=1,2,\ldots,\iota_{\max}, & \text{(2.2a)} \\ Z(t) = \max\left(Z(t^-)-\gamma^\iota,0\right), \quad \text{for } t=t^\iota, \quad \iota=1,2,\ldots,\iota_{\max}, & \text{(2.2b)} \\ dR(t) = \delta\left(\theta-R(t)\right)dt+\sigma_R dW_R(t). & \text{(2.2c)} \end{cases}$$

We work under the following assumptions for model (2.1)-(2.2).

- Processes $\{W_z(t)\}_{0\leq t\leq T}$ and $\{W_R(t)\}_{0\leq t\leq T}$ are two independent standard Wiener processes.
- The process $\{J(t)\}_{0\leq t\leq T}$, where $J(t)=\sum_{k=1}^{\pi(t)}(Y_k-1)$, is a compound Poisson process. Specifically, $\{\pi(t)\}_{0\leq t\leq T}$ is a Poisson process with a constant finite jump intensity $\lambda\geq 0$; and, with Y being a positive random variable representing the jump multiplier, $\{Y_k\}_{k=1}^\infty$ are independent and identically distributed (i.i.d.) random variables having the same same distribution as Y. In the dynamics (2.2a), $\kappa=\mathbb{E}[Y-1]$ represents the expected percentage change in the sub-account balance, due to jumps. Here, $\mathbb{E}[\cdot]$ is the expectation operator taken under the risk-neutral measure $\mathfrak{Q}$.
- The Poisson process $\{\pi(t)\}_{0\leq t\leq T}$, and the sequence of random variables $\{Y_k\}_{k=1}^\infty$ are mutually independent, as well as independent of the Wiener processes $\{W_z(t)\}_{0\leq t\leq T}$ and $\{W_R(t)\}_{0\leq t\leq T}$.

In (2.2a), $\sigma_z>0$ is the instantaneous volatility of $Z(t)$ and $\beta>0$ is the proportional annual insurance rate paid by the policy holder. The constant ρ, where $|\rho|<1$, is a correlation coefficient between $Z(t)$ and $R(t)$.[2] In (2.2c), $\sigma_R>0$ is the instantaneous volatility of the short rate, $\delta>0$ is the speed of mean-reversion, θ is the long-term mean level. For simplicity, model parameters are assumed to be constant in time; however, the results of this paper can be generalized to the case of time-dependent parameters.

As a specific example, we consider two distribution for the jump multiplier Y, namely the log-normal distribution [60], and the log-double-exponential distribution [54]. Specifically, we denote by $b(y)$ the density function of the random variable $\ln(Y)$. In the former case, $\ln(Y)$ is normally distributed with mean ν and standard deviation ς, and

$$b(y)=\frac{1}{\varsigma\sqrt{2\pi}}\exp\left\{-\frac{(y-\nu)^2}{2\varsigma^2}\right\}. \tag{2.3}$$

In the latter case, $\ln Y$ has an asymmetric double-exponential distribution with

$$b(y)=p_u\eta_1 e^{-\eta_1 y}\mathbf{1}_{\{y\geq 0\}}+(1-p_u)\,\eta_2 e^{\eta_2 y}\mathbf{1}_{\{y<0\}}. \tag{2.4}$$

Here, $p_u\in[0,1]$, $\eta_1>1$ and $\eta_2>0$. Given that a jump occurs, p_u is the probability of an upward jump, and $(1-p_u)$ is the probability of a downward jump.

[2] Through a Cholesky factorization, the correlation coefficient between $W_R(t)$ and $\rho W_z(t)+\sqrt{1-\rho^2}W_R(t)$ is $|\rho|<1$.

3 Impulse control formulation

For the controlled underlying process $(Z(t), R(t), A(t))$, $t \in [0, T]$, let (z, r, a) be the state of the system. Let $\tau = T - t$, for $z > 0$, we apply the change of variable $w = \ln(z) \in (-\infty, \infty)$. With $\mathbf{x} = (w, r, a, \tau)$, we denote by $v(\mathbf{x}) \equiv v(w, r, a, \tau)$ the time-τ no-arbitrage price of a GMWB when $Z(t) = e^w$, $R(t) = r$ and $A(t) = a$. Using dynamic programming, we can show that, under dynamics (2.1)-(2.2), $v(w, r, a, \tau)$ satisfy the impulse control formulation [57, 17]

$$\min \Big\{ v_\tau - \mathcal{L}v - \mathcal{J}v - \sup_{\hat{\gamma} \in [0, C_r]} \hat{\gamma} \left(1 - e^{-w} v_w - v_a\right) \mathbf{1}_{\{a>0\}},$$

$$v - \sup_{\gamma \in [0,a]} \left[v\left(\ln\left(\max\left(e^w - \gamma, e^{w_{-\infty}}\right)\right), a - \gamma, \tau\right) + (1-\mu)\gamma - c \right] \Big\} = 0, \qquad (3.1)$$

where $(w, r, a, \tau) \in \Omega^\infty \equiv (-\infty, \infty) \times (-\infty, \infty) \times [a_{\min}, a_{\max}] \times [0, T)$, with $a_{\min} = 0$ and $a_{\max} = z_0$, and

$$\mathcal{L}v(\mathbf{x}) = \frac{\sigma_Z^2}{2} v_{ww} + \rho \sigma_Z \sigma_R v_{wr} + \frac{\sigma_R^2}{2} v_{rr} + \left(r - \frac{\sigma_Z^2}{2} - \beta - \lambda\kappa\right) v_w + \delta(\theta - r) v_r - (r + \lambda) v,$$

$$\mathcal{J}v(\mathbf{x}) = \lambda \int_{-\infty}^{\infty} v(w + y, r, a, \tau)\, b(y)\, dy. \qquad (3.2)$$

Here, in (3.1), $w_{-\infty} \ll 0$ is a constant to avoid the indeterminate case of of $\ln(0)$, due to condition (2.2b); the constant positive fixed cost c is introduced as a technical tool to ensure uniqueness of the impulse formulation, as commonly done in the impulse control literature [64, 67, 81]; in (3.2), $b(\cdot)$ is the probability density function of $\ln Y$.

3.1 Localization

The GMWB impulse control formulation (3.1) is posed on the infinite domain Ω^∞. For problem statement and convergence analysis of numerical schemes, we define a localized GMWB impulse formulation. To this end, with $w_{\min} < 0 < w_{\max}$, $r_{\min} < 0 < r_{\max}$, and $|w_{\min}|$, $w_{\max}$, $|r_{\min}|$, $r_{\max}$ sufficiently large, we define the following sub-domains:

$$\begin{aligned}
\Omega_{\text{in}} &= (w_{\min}, w_{\max}) \times (r_{\min}, r_{\max}) \times (a_{\min}, a_{\max}] \times (0, T], \\
\Omega_{\tau_0}^\infty &= (-\infty, \infty) \times (-\infty, \infty) \times [a_{\min}, a_{\max}] \times \{0\}, \\
\Omega_{w_{\max}}^\infty &= [w_{\max}, \infty) \times (r_{\min}, r_{\max}) \times [a_{\min}, a_{\max}] \times (0, T], \\
\Omega_{w_{\min}}^\infty &= (-\infty, w_{\min}] \times (r_{\min}, r_{\max}) \times (a_{\min}, a_{\max}] \times (0, T], \qquad (3.3) \\
\Omega_{a_{\min}} &= (w_{\min}, w_{\max}) \times (r_{\min}, r_{\max}) \times \{a_{\min}\} \times (0, T], \\
\Omega_{wa_{\min}}^\infty &= (-\infty, w_{\min}] \times (r_{\min}, r_{\max}) \times \{a_{\min}\} \times (0, T], \\
\Omega_{\text{c}}^\infty &= \Omega^\infty \setminus \Omega_{\text{in}} \setminus \Omega_{\tau_0}^\infty \setminus \Omega_{w_{\max}}^\infty \setminus \Omega_{w_{\min}}^\infty \setminus \Omega_{a_{\min}} \setminus \Omega_{wa_{\min}}^\infty.
\end{aligned}$$

An illustration of the sub-domains for the localized problem corresponding to a fixed $a \in [a_{\min}, a_{\max}]$ is given in Figure 3.1.

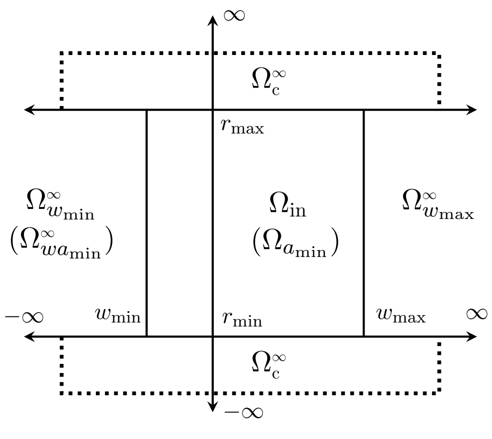

FIGURE 3.1: *Spatial computational domain at each τ and for a fixed $a \in [a_{\min}, a_{\max}]$; at $a = 0$, $\Omega_{in} \equiv \Omega_{a_{\min}}$ and $\Omega_{w_{\min}}^\infty \equiv \Omega_{wa_{\min}}^\infty$.*

We now present equations for sub-domains defined in (3.3).

- For $(w, r, a, \tau) \in \Omega_{\text{in}}$, we have (3.1).
- For $(w, r, a, \tau) \in \Omega_{\tau_0}^\infty$, we use the initial condition $v(w, a, 0) = \max(e^w, (1-\mu)a - c) \wedge e^{w_\infty}$ for a finite $w_\infty \gg w_{\max}$, where $x \wedge y = \min(x, y)$.
- For $(w, r, a, \tau) \in \Omega_{w_{\max}}^\infty$, we follow [22, 17] to impose the Dirichelet-type boundary condition

$$v = e^{-\beta\tau}(e^w \wedge e^{w_\infty}). \qquad (3.4)$$

We note that the theoretical quantity w_∞ is needed to indicate that the solutions $\Omega^\infty_{\tau_0}$ and $\Omega^\infty_{w_{\max}}$ are bounded as $w \to \infty$, and it does not need to be numerically specified.

- As $w \to -\infty$ (i.e. $z = e^w \to 0$) using the asymptotic forms of the HJB-QVI (3.1), for $(w, r, a, \tau) \in \Omega^\infty_{w_{\min}}$, (3.1) is reduced to the boundary condition

$$\min \left\{ v_\tau - \mathcal{L}_d v - \sup_{\hat{\gamma} \in [0, C_r]} (\hat{\gamma} - \hat{\gamma} v_a)\, \mathbf{1}_{\{a>0\}}, v - \sup_{\gamma \in [0,a]} [v(w, a-\gamma, \tau) + (1-\mu)\gamma - c] \right\} = 0, \quad (3.5)$$

where the degenerated differential operator $\mathcal{L}_d$ is defined by

$$\mathcal{L}_d v \;:=\; \frac{\sigma_R^2}{2} v_{rr} + \delta\,(\theta - r)\, v_r - rv. \quad (3.6)$$

This is essentially a Dirichlet boundary condition since it can be solved without using any information from $\Omega_{\text{in}} \cup \Omega_{a_{\min}}$.

- For $(w, r, a, \tau) \in \Omega_{a_{\min}}$, the impulse formulation (3.1) becomes the PIDE $v_\tau - \mathcal{L}v - \mathcal{J}v = 0$.

- For $(w, r, a, \tau) \in \Omega^\infty_{wa_{\min}}$, (3.5) becomes $v_\tau - \mathcal{L}_d v = 0$.

- For $(w, r, a, \tau) \in \Omega^\infty_{\text{c}}$, we note in this case, significant difficulty arises in choosing a boundary condition based on asymptotic forms of the HJB-QVI (3.1), or the holder's optimal withdrawal behaviours. Since a detailed analysis of the boundary conditions is not the focus of this paper, we leave it as a topic for future research. For simplicity, we follow [23, 28] to choose Dirichlet-type "stopped process" boundary conditions where we stop the processes $(Z(t), R(t), A(t))$ when $R(t)$ hits the boundary. Thus, $(w, r, a, \tau) \in \Omega^\infty_{\text{c}}$, the value is simply the discounted payoff for the current values of the state variables, i.e.

$$v(w, r, a, \tau) \;=\; p(w, r, a, \tau) \;=\; p_b(\bar{r}, \tau; T) \max(e^w, (1-\mu)a - c) \wedge e^{w_\infty}, \quad (3.7)$$

where $\bar{r} := \min(\max(r, r_{\min}), r_{\max})$. Here, $p_b(r, \tau; T)$ is the price at time $(T - \tau)$ of a zero coupon bond with maturity T given by the closed-form expression [16]

$$p_b(r, \tau; T) = \exp\left\{ \left(\theta - \frac{\sigma_R^2}{2\delta^2}\right)\left(\frac{1}{\delta}\left(1 - e^{-\delta\tau}\right) - \tau\right) - \frac{\sigma_R^2}{4\delta^3}\left(1 - e^{-\delta\tau}\right)^2 - \frac{r}{\delta}\left(1 - e^{-\delta\tau}\right) \right\}. \quad (3.8)$$

Note that no further information is needed along the boundary $a \to a_{\max}$ due to the hyperbolic nature of the variable a in the HJB-QVI (3.1). Although the above-mentioned artificial boundary conditions may induce additional approximation errors in the numerical solutions, we can make these errors arbitrarily small by choosing sufficiently large values for $|w_{\min}|$, $w_{\max}$, $|r_{\min}|$, and $r_{\max}$.

3.2 Definition of viscosity solution

We now write the GMWB pricing problem in a compact form, which includes the terminal and boundary conditions in a single equation. We define the intervention operator

$$\mathcal{M}(\gamma) v(\mathbf{x}) = \begin{cases} v(w, r, a-\gamma, \tau) + \gamma(1-\mu) - c & \mathbf{x} \in \Omega^\infty_{w_{\min}}, \quad (3.9\text{a}) \\ v\left(\ln(\max(e^w - \gamma, e^{w_{-\infty}})), r, a-\gamma, \tau\right) + \gamma(1-\mu) - c & \mathbf{x} \in \Omega_{\text{in}}. \quad (3.9\text{b}) \end{cases}$$

With $\mathbf{x} = (w, r, a, \tau)$, we let $Dv(\mathbf{x})$ and $D^2 v(\mathbf{x})$ represent the first-order and second-order partial derivatives of $v(\mathbf{x})$, and define

$$F_{\Omega^\infty}(\mathbf{x}, v) \equiv F_{\Omega^\infty}\left(\mathbf{x}, v(\mathbf{x}), Dv(\mathbf{x}), D^2 v(\mathbf{x}), \mathcal{J}v(\mathbf{x}), \mathcal{M}v(\mathbf{x})\right) \quad (3.10)$$

where

$$F_{\Omega^\infty}(\mathbf{x}, v) \;=\; \begin{cases} F_{\text{in}}(\mathbf{x}, v) & \equiv & F_{\text{in}}\left(\mathbf{x}, v(\mathbf{x}), Dv(\mathbf{x}), D^2 v(\mathbf{x}), \mathcal{J}v(\mathbf{x}), \mathcal{M}v(\mathbf{x})\right), & \mathbf{x} \in \Omega_{\text{in}}, \\ F_{a_{\min}}(\mathbf{x}, v) & \equiv & F_{a_{\min}}\left(\mathbf{x}, v(\mathbf{x}), Dv(\mathbf{x}), D^2 v(\mathbf{x}), \mathcal{J}v(\mathbf{x})\right), & \mathbf{x} \in \Omega_{a_{\min}}, \\ F_{w_{\min}}(\mathbf{x}, v) & \equiv & F_{w_{\min}}(\mathbf{x}, v(\mathbf{x}), Dv(\mathbf{x}), \mathcal{M}v(\mathbf{x})), & \mathbf{x} \in \Omega^\infty_{w_{\min}}, \\ F_{wa_{\min}}(\mathbf{x}, v) & \equiv & F_{wa_{\min}}(\mathbf{x}, v(\mathbf{x}), Dv(\mathbf{x})), & \mathbf{x} \in \Omega^\infty_{wa_{\min}}, \\ F_{w_{\max}}(\mathbf{x}, v) & \equiv & F_{w_{\max}}(\mathbf{x}, v(\mathbf{x})), & \mathbf{x} \in \Omega^\infty_{w_{\max}}, \\ F_{\text{c}}(\mathbf{x}, v) & \equiv & F_{\text{c}}(\mathbf{x}, v(\mathbf{x})), & \mathbf{x} \in \Omega^\infty_{\text{c}}, \\ F_{\tau_0}(\mathbf{x}, v) & \equiv & F_{\tau_0}(\mathbf{x}, v(\mathbf{x})), & \mathbf{x} \in \Omega^\infty_{\tau_0}, \end{cases}$$

with operators

$$
\begin{aligned}
F_{\text{in}}\left(\mathbf{x}, v\right) &= \min \left[v_\tau - \mathcal{L}v - \mathcal{J}v - \sup_{\hat{\gamma}\in[0,C_r]} \left(\hat{\gamma} - \hat{\gamma} e^{-w} v_w - \hat{\gamma} v_a\right) \mathbf{1}_{\{a>0\}}, v - \sup_{\gamma\in[0,a]} \mathcal{M}v \right], &(3.11)\\
F_{w_{\min}}\left(\mathbf{x}, v\right) &= \min \left[v_\tau - \mathcal{L}_d v - \sup_{\hat{\gamma}\in[0,C_r]} \left(\hat{\gamma} - \hat{\gamma} v_a\right) \mathbf{1}_{\{a>0\}}, v - \sup_{\gamma\in[0,a]} \mathcal{M}v \right], &(3.12)\\
F_{a_{\min}}\left(\mathbf{x}, v\right) &= v_\tau - \mathcal{L}v - \mathcal{J}v, &(3.13)\\
F_{wa_{\min}}\left(\mathbf{x}, v\right) &= v_\tau - \mathcal{L}_d v, &(3.14)\\
F_{w_{\max}}\left(\mathbf{x}, v\right) &= v - e^{-\beta\tau}(e^{w} \wedge e^{w_\infty}), &(3.15)\\
F_{c}\left(\mathbf{x}, v\right) &= v - p(w, r, a, \tau), &(3.16)\\
F_{\tau_0}\left(\mathbf{x}, v\right) &= v - \max(e^{w}, (1-\mu)a - c) \wedge e^{w_\infty}. &(3.17)
\end{aligned}
$$

Definition 3.1 (Impulse control GMWB pricing problem)**.** *The pricing problem for the GMWB under an impulse control formulation is defined as*

$$
F_{\Omega^\infty}\left(\mathbf{x}, v(\mathbf{x}), Dv(\mathbf{x}), D^2 v(\mathbf{x}), \mathcal{J}v(\mathbf{x}), \mathcal{M}v(\mathbf{x})\right) = 0, \tag{3.18}
$$

where the operator $F_{\Omega^\infty}(\cdot)$ *is defined in* (3.10)*.*

Next, we recall the notions of the upper semicontinuous (u.s.c. in short) and the lower semicontinuous (l.s.c. in short) envelops of a function $u : \mathbb{X} \to \mathbb{R}$, where $\mathbb{X}$ is a closed subset of $\mathbb{R}^n$. They are respectively denoted by $u^*(\cdot)$ (for the u.s.c. envelop) and $u_*(\cdot)$ (for the l.s.c. envelop), and are given by

$$
u^*(\hat{\mathbf{x}}) = \limsup_{\substack{\mathbf{x}\to\hat{\mathbf{x}} \\ \mathbf{x},\hat{\mathbf{x}}\in\mathbb{X}}} u(\mathbf{x}) \quad (\text{resp.} \quad u_*(\hat{\mathbf{x}}) = \liminf_{\substack{\mathbf{x}\to\hat{\mathbf{x}} \\ \mathbf{x},\hat{\mathbf{x}}\in\mathbb{X}}} u(\mathbf{x})).
$$

In general, the solution to impulse control problems are non-smooth, and we seek the viscosity solution of equation (3.18) [25, 73, 41]. Since equation (3.18) is defined on an infinite domain, we need to have a suitable growth condition at infinity for the solution [10, 73]. To this end, let $\mathcal{G}(\Omega^\infty)$ be the set of bounded functions defined by [10, 73]

$$
\mathcal{G}(\Omega^\infty) = \left\{ u : \Omega^\infty \to \mathbb{R}, \quad \sup_{\mathbf{x}\in\Omega^\infty} |u(\mathbf{x})| < \infty \right\}. \tag{3.19}
$$

Definition 3.2 (Viscosity solution of equation (3.18))**.** *A locally bounded function* $v \in \mathcal{G}(\Omega^\infty)$ *is a viscosity subsolution (resp. supersolution) of* (3.18) *in* Ω^∞ *if for all test function* $\phi \in \mathcal{G}(\Omega^\infty) \cap \mathcal{C}^\infty(\Omega^\infty)$ *and for all points* $\hat{\mathbf{x}} \in \Omega^\infty$ *such that* $v^* - \phi$ *has a* global *maximum on* Ω^∞ *at* $\hat{\mathbf{x}}$ *and* $v^*(\hat{\mathbf{x}}) = \phi(\hat{\mathbf{x}})$ *(resp.* $v_* - \phi$ *has a* global *minimum on* Ω^∞ *at* $\hat{\mathbf{x}}$ *and* $v_*(\hat{\mathbf{x}}) = \phi(\hat{\mathbf{x}})$*), we have*

$$
\begin{aligned}
&\left(F_{\Omega^\infty}\right)_* \left(\hat{\mathbf{x}}, \phi(\hat{\mathbf{x}}), D\phi(\hat{\mathbf{x}}), D^2\phi(\hat{\mathbf{x}}), \mathcal{J}\phi(\hat{\mathbf{x}}), \mathcal{M}\phi(\hat{\mathbf{x}})\right) \le 0, &(3.20)\\
\big(\textit{resp.} \quad &\left(F_{\Omega^\infty}\right)^* \left(\hat{\mathbf{x}}, \phi(\hat{\mathbf{x}}), D\phi(\hat{\mathbf{x}}), D^2\phi(\hat{\mathbf{x}}), \mathcal{J}\phi(\hat{\mathbf{x}}), \mathcal{M}\phi(\hat{\mathbf{x}})\right) \ge 0, \big)
\end{aligned}
$$

where the operator $F_{\Omega^\infty}(\cdot)$ *is defined in* (3.10)*.*

(ii) A locally bounded function $v \in \mathcal{G}(\Omega^\infty)$ *is a viscosity solution of* (3.18) *in* $\Omega_{in} \cup \Omega_{a_{\min}}$ *if* v *is a viscosity subsolution and a viscosity supersolution in* $\Omega_{in} \cup \Omega_{a_{\min}}$*.*

3.3 A strong comparison result

In the context of numerical solutions to HJB-QVIs, convergence of numerical methods to the viscosity typically requires stability, consistency, monotonicity, provided that a strong comparison result [21, 81, 50, 10, 73, 15, 11, 9]. Specifically, using stability, consistency, and monotonicity of a numerical scheme, the common route is to establish the candidate for u.s.c. subsolution (resp. l.s.c. supersolution) of the HJB-QVI using lim sup (resp. lim inf) of the numerical solutions as a discretization parameter approaches zero. We respectively denote by $\hat{u}$ the subsolution (resp. $\hat{v}$ the supersolution) in a target convergence region $\mathcal{S}$ which is a non-empty subset of Ω^∞. By construction, we have $\hat{u}(\mathbf{x}) \ge \hat{v}(\mathbf{x})$ for all $\mathbf{x} \in \mathcal{S}$. If a strong comparison result holds in $\mathcal{S}$, it means that for subsolution $\hat{u}(\mathbf{x})$ and supersolution $\hat{v}(\mathbf{x})$, we have $\hat{u}(\mathbf{x}) \le \hat{v}(\mathbf{x})$ for all $\mathbf{x} \in \mathcal{S}$. Therefore, a unique continuous viscosity solution exists in $\mathcal{S}$. We note that, while stability, consistency and monotonicity are required properties of numerical methods, a strong comparison result is problem dependent.

In our paper [57, Lemma B.1 and Theorem B.1], we present a framework for proving a strong comparison result for HJB-QVIs of a form similar to (3.18) where jump-diffusion dynamics with a positive constant interest rate are considered. For the HJB-QVI (3.18), using the aforementioned framework, we are able to show a strong comparison result for $\Omega_{\text{in}} \cup \Omega_{a_{\min}}$, where $\Omega_{a_{\min}} \subset \partial\Omega_{\text{in}}$. This result is presented in Theorem 3.1 below.

Theorem 3.1. *If function $\hat{u}$ (resp. $\hat{v}$) is a u.s.c. viscosity subsolution (resp. l.s.c. supersolution) of the HJB-QVI* (3.18) *in Ω in the sense of Definition 3.2, then we have $\hat{u} \le \hat{v}$ in $\Omega_{in} \cup \Omega_{a_{\min}}$.*

Proof of Theorem 3.1. We follow the framework presented in [57][Lemma B.1 and Theorem B.1]. With the target region being $\mathcal{S} = \Omega_{\text{in}} \cup \Omega_{a_{\min}}$, we rewrite Definition 3.2 into an equivalent definition as follows.

(i) In the non-local terms $\mathcal{J}(\cdot)$ and $\mathcal{M}(\cdot)$, the smooth test function $\phi(\hat{\mathbf{x}})$ is replaced by $v^*(\hat{\mathbf{x}})$ for subsolution (resp. $v_*(\hat{\mathbf{x}})$ for supersolution),

(ii) The envelopes $(F_{\Omega^\infty})_*$ (resp. $(F_{\Omega^\infty})^*$) is eliminated from the definition of subsolution (resp. supersolution).

We refer to this definition as Def-A, and it is the definition we use to prove a strong comparison result.[3]

Unlike the setting in [57], where a positive constant interest rate is used, a Gaussian stochastic interest rate is considered in the present paper, which could be negative. Therefore, the framework in [57] is not directly applicable without an important preprocessing step (shown below).

- Given the HJB-QVI with $F_{\Omega^\infty}(\cdot) = 0$ in (3.18), let $q > -r_{\min}$ be fixed, implying $r + q > 0$ for all $r \in (r_{\min}, r_{\max})$, we introduce an HJB-QVI $F_{\Omega^\infty}(\cdot; q) = 0$ which is similar to $F_{\Omega^\infty}(\cdot) = 0$ except in $\Omega_{\text{in}} \cup \Omega_{a_{\min}}$, where $F_{\text{in}}(\cdot; q)$ and $F_{a_{\min}}(\cdot; q)$ are defined by

$$\begin{aligned}
F_{\text{in}}(\mathbf{x}, v; q) &= \min\Bigg[v_\tau - \mathcal{L}v + qv - \mathcal{J}v - \sup_{\hat{\gamma} \in [0, C_r]} \hat{\gamma}\left(e^{-q\tau} - e^{-w} v_w - v_a\right) \mathbf{1}_{\{a>0\}}, \\
&\qquad v - \sup_{\gamma \in [0,a]} \left[v\left(\ln\left(\max\left(e^w - \gamma, e^{w_{-\infty}}\right)\right), a - \gamma, \tau\right) + \left((1-\mu)\gamma - c\right) e^{-q\tau} \right] \Bigg], \\
F_{a_{\min}}(\mathbf{x}, v; q) &= v_\tau - \mathcal{L}v + qv - \mathcal{J}v.
\end{aligned}$$

- It is straightforward to show that: in the sense of Def-A, if $\hat{u}$ is a u.s.c. viscosity subsolution (resp. $\hat{v}$ is a l.s.c. viscosity supersolution) of $F_{\Omega^\infty}(\cdot) = 0$ in $\Omega_{\text{in}} \cup \Omega_{a_{\min}}$, then $e^{-q\tau}\hat{u}$ is a u.s.c. viscosity subsolution (resp. $e^{-q\tau}\hat{v}$ is a l.s.c. viscosity subsolution) of $F_{\Omega^\infty}(\cdot; q) = 0$ in $\Omega_{\text{in}} \cup \Omega_{a_{\min}}$.

Finally, using the same steps as in Lemma B.1 and Theorem B.1 of [57] for the HJB-QVI $F_{\Omega^\infty}(\cdot; q) = 0$, we can prove that a strong comparison results holds for $\Omega_{\text{in}} \cup \Omega_{a_{\min}}$, i.e. $e^{-q\tau}\hat{u} \le e^{-q\tau}\hat{v}$, or equivalently, $\hat{u} \le \hat{v}$ in $\Omega_{\text{in}} \cup \Omega_{a_{\min}}$, which is the desired outcome. □

We conclude this subsection by noting that, as well-noted in the literature [81, 17, 24, 57, 42, 67], it is usually the case that a strong comparison result does not hold on the whole definition domain including boundary sub-domains, because this would imply the continuity of the value function across the boundary regions, which is not true for some impulse control problems, including the HJB-QVI (3.18). In particular, it is possible that loss of boundary data can occur over parts of $\Gamma = \partial\Omega_{\text{in}} \setminus \Omega_{a_{\min}}$, i.e. as

[3] For the purpose of verifying consistency of a numerical scheme, it is convenient to use Definition 3.2. However, it turns out more convenient to use the equivalent definition to prove a strong comparison result for the HJB-QVI (3.18). Similar arguments can be also referred to [25, 73, 3].

$\tau \to 0$, $w \to \{w_{\min}, w_{\max}\}$ and $r \to \{r_{\min}, r_{\max}\}$, hence, we cannot hope that a strong comparison result holds on Γ. However, these problematic parts of Γ are trivial to handle in the sense that either the boundary data is used or is irrelevant. In all cases, we consider the computed solution on those parts of Γ as the limiting value approaching Γ from the interior.

4 Numerical methods

4.1 Overview

Similar to the approach taken in our papers [57, 17], we will tackle the HJB-QVI (3.18) from a discrete withdrawal scenario which was first suggested in [22]. To this end, we first introduce a set of discrete intervention (withdrawal) times as follows. Let $\{\tau_m\}$, $m = 0, \ldots, M$, be a partition of $[0, T]$, where for simplicity, an uniform spacing is used, i.e. $\tau_m = m\Delta\tau$ and $\Delta\tau = T/M$. Following [22, 17], there is no withdrawal allowed at time $t = 0$, or equivalently, at $\tau_M = T$; therefore, the set of intervention times is $\{\tau_m\}$, $m = 0, \ldots, M-1$.

Broadly speaking, over the time interval $[\tau_m, \tau_{m+1}]$, $m = 0, \ldots, M-1$, our numerical approach consists of two steps, namely intervention in $[\tau_m, \tau_m^+]$. and time-advancement in $[\tau_m^+, \tau_{m+1}]$. Central to our method is the time-advancement step for the target region of convergence $\Omega_{\text{in}} \cup \Omega_{a_{\min}}$. For this step, $a \in [a_{\min}, a_{\max}]$ is fixed, and our starting point is a linear PIDE in (w, r) of the form

$$v_\tau - \mathcal{L}v - \mathcal{J}v = 0, \quad w \in (-\infty, \infty),\ r \in (-\infty, \infty),\ \tau \in (\tau_m^+, \tau_{m+1}]. \tag{4.1}$$

where the operators $\mathcal{L}$ and $\mathcal{J}$ are given in (3.2), subject to a generic initial condition at time τ_m^+ given by $\hat{v}(w, r, a, \tau_m^+)$ obtained from the intervention step above. Here,

$$\hat{v}(w, r, a, \tau_m^+) = \begin{cases} v(w, r, a, \tau_m^+) & (w, r, a, \tau_{m+1}) \in \Omega_{\text{in}} \cup \Omega_{a_{\min}}, \quad (4.2\text{a}) \\ v_{bc}(w, r, a, \tau_m) & (w, r, a, \tau_{m+1}) \in \Omega^\infty \setminus (\Omega_{\text{in}} \cup \Omega_{a_{\min}}). \quad (4.2\text{b}) \end{cases}$$

In (4.2a), $v(w, r, a, \tau_m^+)$ is the intermediate results from the intervention step, and $v_{bc}(w, r, a, \tau_m^+)$ in (4.2b) is the boundary conditions at time-τ_m satisfying (3.5), (3.4), (3.7) in $\Omega^\infty_{w_{\min}} \cup \Omega^\infty_{wa_{\min}} \cup \Omega^\infty_{w_{\max}} \cup \Omega^\infty_{c}$.

The key challenge in solving the PIDE (4.1) is that a closed-form expression for its Green's function is not known to exist, due to the v_r term arising from the short rate. (Also see [49] for relevant discussions related to similar difficulties). To handle the above challenge, we consider a combination of a semi-Lagrangian (SL) method and a Green's function approach. In particular, we consider writing $\mathcal{L}v = \mathcal{L}_g v + \mathcal{L}_s v - rv$, where

$$\mathcal{L}_g v := \frac{\sigma_Z^2}{2} v_{ww} + \rho\sigma_Z\sigma_R v_{wr} + \frac{\sigma_R^2}{2} v_{rr} - \lambda\kappa v_w - \lambda v,\ \mathcal{L}_s v := (r - \frac{\sigma_Z^2}{2} - \beta) v_w + \delta(\theta - r) v_r. \tag{4.3}$$

To solve the PIDE (4.1) in $\Omega_{\text{in}} \cup \Omega_{a_{\min}}$, we first handle the term $\mathcal{L}_s v - rv$ by an SL discretization method in $\Omega_{\text{in}} \cup \Omega_{a_{\min}}$. (This is discussed in Subsection 4.5.1.). We then effectively solve the PIDE of the form

$$(v_{\text{SL}})_\tau - \mathcal{L}_g v_{\text{SL}} - \mathcal{J} v_{\text{SL}} = 0, \quad w \in (-\infty, \infty),\ r \in (-\infty, \infty),\ \tau \in (\tau_m^+, \tau_{m+1}], \tag{4.4}$$

where v_{SL} is the unknown function, subject to a generic initial condition $\hat{v}_{\text{SL}}(w, r, a, \tau_m)$ given as follows. Letting $\mathbf{x} = (w, r, a, \tau_{m+1})$, for $\mathbf{x} \in \Omega_{\text{in}} \cup \Omega_{a_{\min}}$, $\hat{v}_{\text{SL}}(\mathbf{x})$ given by an SL discretization method combined with $\hat{v}(w, r, a, \tau_m^+)$ provided in (4.2a)-(4.2b); otherwise, $\hat{v}_{\text{SL}}(\mathbf{x})$ is given by $v_{bc}(\mathbf{x})$ as in (4.2b).

To numerically solve the PIDE (4.4) for $v_{\text{SL}}(w, r, a, \tau_{m+1})$, we start from a Green's function approach. It is a known fact that the Green's function $g(\cdot)$ associated with the PIDE (4.4) has the form $g(w, w', r, r', \Delta\tau) \equiv g(w - w', r - r', \Delta\tau)$ [36, 31]. Therefore, the solution $v_{\text{SL}}(w, r, a, \tau_{m+1})$ for $(w, r) \in \mathbf{D} \equiv (w_{\min}, w_{\max}) \times (r_{\min}, r_{\max})$ can be represented as the convolution integral of the Green's function $g(\cdot, \Delta\tau)$ and the initial condition $\hat{v}_{\text{SL}}(w, r, a, \tau_m^+)$ as follows [36, 31]

$$v_{\text{SL}}(w, r, \cdot, \tau_{m+1}) = \iint_{\mathbb{R}^2} g(w - w', r - r', \Delta\tau)\ \hat{v}_{\text{SL}}(w', r', \cdot, \tau_m^+)\, dw'\, dr', \qquad (w, r) \in \mathbf{D}. \tag{4.5}$$

The solution $v_{\text{SL}}(w, r, \cdot, \tau_{m+1})$ for $(w, r) \notin \mathbf{D}$ are given by the boundary conditions (3.5), (3.4), (3.7).

For computational purposes, we truncate the infinite region of integration of (4.5) to

$$\mathbf{D}^\dagger \equiv [w^\dagger_{\min}, w^\dagger_{\max}] \times [r^\dagger_{\min}, r^\dagger_{\max}], \tag{4.6}$$

where, for $x \in \{w, r\}$, $x^\dagger_{\min} \ll x_{\min} < 0 < x_{\max} \ll x^\dagger_{\max}$ and $|x^\dagger_{\min}|$ and $x^\dagger_{\max}$ are sufficiently large. This results in the approximation

$$v_{\text{SL}}\left(w, r, \cdot, \tau_{m+1}\right) \;\simeq\; \iint_{\mathbf{D}^\dagger} g\left(w - w', r - r', \Delta\tau\right)\; \hat{v}_{\text{SL}}(w', r', \cdot, \tau_m^+)\; dw'\; dr', \quad (w, r) \in \mathbf{D}. \tag{4.7}$$

The error arising from this truncation is discussed in Section 5.

With the above discussion in mind, we define a finite domain $\Omega = [w^\dagger_{\min}, w^\dagger_{\max}] \times [r^\dagger_{\min}, r^\dagger_{\max}] \times [a_{\min}, a_{\max}] \times [0, T]$, which consists of

$$\begin{aligned}
\Omega_{\text{in}} &= \text{defined in (3.3)}, \quad \Omega_{a_{\min}} = \text{defined in (3.3)},\\
\Omega_{\tau_0} &= [w^\dagger_{\min}, w^\dagger_{\max}] \times [r^\dagger_{\min}, r^\dagger_{\max}] \times [a_{\min}, a_{\max}] \times \{0\},\\
\Omega_{w_{\min}} &= [w^\dagger_{\min}, w_{\min}] \times (r_{\min}, r_{\max}) \times (a_{\min}, a_{\max}] \times (0, T],\\
\Omega_{wa_{\min}} &= [w^\dagger_{\min}, w_{\min}] \times (r_{\min}, r_{\max}) \times \{a_{\min}\} \times (0, T],\\
\Omega_{w_{\max}} &= [w_{\max}, w^\dagger_{\max}] \times (r_{\min}, r_{\max}) \times [a_{\min}, a_{\max}] \times (0, T],\\
\Omega_{\text{c}} &= \Omega \setminus \Omega_{\text{in}} \setminus \Omega_{a_{\min}} \setminus \Omega_{w_{\max}} \setminus \Omega_{wa_{\min}} \setminus \Omega_{w_{\min}} \setminus \Omega_{\tau_0}.
\end{aligned}$$

We stress that the region $\Omega_{w_{\min}} \cup \Omega_{wa_{\min}} \cup \Omega_{w_{\max}} \cup \Omega_{\text{c}}$ plays an important role in the proposed numerical method. In particular, the convolution integral (4.5) is typically approximated using efficient computation of an associated discrete convolution via Fast-Fourier Transform (FFT). It is well-documented that wraparound error (due to periodic extension) is an important issue for Fourier methods, particularly in the case of control problems (see, for example, [57]). Therefore, in (4.8), the region $\Omega_{w_{\min}} \cup \Omega_{wa_{\min}} \cup \Omega_{w_{\max}} \cup \Omega_{\text{c}}$ is also set up to serve as padding areas for nodes in $\Omega_{\text{in}} \cup \Omega_{a_{\min}}$. For this purpose, we assume that $|w_{\min}|$, $w_{\max}$, $|r_{\min}|$ and $r_{\max}$ are chosen sufficiently large so that

$$\begin{aligned}
w^\dagger_{\min} = w_{\min} - \frac{w_{\max} - w_{\min}}{2} \qquad &\text{and} \qquad w^\dagger_{\max} = w_{\max} + \frac{w_{\max} - w_{\min}}{2},\\
r^\dagger_{\min} = r_{\min} - \frac{r_{\max} - r_{\min}}{2} \qquad &\text{and} \qquad r^\dagger_{\max} = r_{\max} + \frac{r_{\max} - r_{\min}}{2}.
\end{aligned} \tag{4.8}$$

As elaborated in [57], this padding technique is efficient in controlling wraparound error (also Remark 4.3).

Due to withdrawals, the non-local impulse operator $\mathcal{M}(\cdot)$ for Ω_{in}, defined in (3.9b), requires evaluating a candidate value at point having $w = \ln(\max(e^w - \gamma, e^{w_{-\infty}}))$ which could be smaller than $w^\dagger_{\min}$, i.e. outside the finite computational domain, if $w_{-\infty} < w^\dagger_{\min}$. Therefore, with $w^\dagger_{\min}$ (and $w^\dagger_{\max}$) selected sufficiently large as above, we set $w_{-\infty} = w^\dagger_{\min}$. That is, $\mathcal{M}(\cdot)$ in (3.9b) becomes

$$\mathcal{M}v(\mathbf{x}) \equiv \mathcal{M}(\gamma)v(\mathbf{x}) = v\left(\ln(\max(e^w - \gamma, e^{w^\dagger_{\min}})), r, a - \gamma, \tau\right) + \gamma(1 - \mu) - c, \quad \mathbf{x} \in \Omega_{\text{in}}. \tag{4.9}$$

This is the intervention operator we use in F_{in} for computation and convergence analysis.

Finally, for a semi-Lagrangian discretization in the setting of HJB equations, common computational difficulties lie in the boundary areas, which typically require a special treatment of computational grids and boundary conditions [70, 68]. In our case, a semi-Lagrangian discretization is only applied in the sub-domain $\Omega_{\text{in}} \cup \Omega_{a_{\min}}$. It may require information from boundary sub-domains, such as $\Omega_{w_{\min}}$ and $\Omega_{w_{\max}}$, which is readily available from the numerical solutions in these boundary sub-domains. With $|r^\dagger_{\min}|$, $r^\dagger_{\max}$, $|w^\dagger_{\min}|$ and $w^\dagger_{\max}$ chosen large enough, we can ensure that a semi-Lagrangian discretization never requires information outside the computational domain Ω.

4.2 Discretization

The computational grid is constructed as follows. We denote by N (resp. $N^\dagger$) the number of points of an uniform partition of $[w_{\min}, w_{\max}]$ (resp. $[w^\dagger_{\min}, w^\dagger_{\max}]$). For convenience, we typically choose $N^\dagger = 2N$

so that only one set of w-coordinates is needed. Also let $P = w_{\max} - w_{\min}$, and $P^\dagger = w^\dagger_{\max} - w^\dagger_{\min}$. We define $\Delta w = \frac{P}{N} = \frac{P^\dagger}{N^\dagger}$. We use an equally spaced partition in the w-direction, denoted by $\{w_n\}$, where

$$\begin{aligned} w_n &= \hat{w}_0 + n\Delta w; \quad n \; = \; -N^\dagger/2, \ldots, N^\dagger/2, \quad \text{where} \qquad (4.10)\\ \Delta w &= P/N \; = \; P^\dagger/N^\dagger, \quad \text{and} \quad \hat{w}_0 \; = \; (w_{\min} + w_{\max})/2 \; = \; (w^\dagger_{\min} + w^\dagger_{\max})/2. \end{aligned}$$

Similarly, for the r-dimension, with $K^\dagger = 2K$, $Q = r_{\max} - r_{\min}$, and $Q^\dagger = r^\dagger_{\max} - r^\dagger_{\min}$, we denote by $\{r_k\}$, an equally spaced partition in the r-direction, such that

$$\begin{aligned} r_k &= \hat{r}_0 + k\Delta r; \quad k \; = \; -K^\dagger/2, \ldots, K^\dagger/2, \quad \text{where} \qquad (4.11)\\ \Delta r &= Q/K \; = \; Q^\dagger/K^\dagger, \quad \text{and} \quad \hat{r}_0 \; = \; (r_{\min} + r_{\max})/2 \; = \; (r^\dagger_{\min} + r^\dagger_{\max})/2. \end{aligned}$$

We use an unequally spaced partition in the a-direction, denoted by $\{a_j\}$, $j = 0, \ldots, J$, with $a_0 = a_{\min}$, and $a_J = a_{\max}$. We set

$$\Delta a_{\max} = \max_{0 \le j \le J-1} (a_{j+1} - a_j), \quad \Delta a_{\min} = \min_{0 \le j \le J-1} (a_{j+1} - a_j). \qquad (4.12)$$

We use the same previously defined equally spaced partition in the τ-dimension with $\Delta\tau = T/M$ and $\tau_m = m\Delta\tau$, denoted by $\{\tau_m\}$, $m = 0, \ldots, M$. [4]

At each time τ_m, $m = 1, \ldots, M$, we denote by $v^m_{n,k,j}$ an approximation to the exact solution $v(w_n, r_k, a_j, \tau_m)$ at the reference node (w_n, r_k, a_j, τ_m) obtained by our numerical method. At time τ_m^+, unless otherwise stated, $v^{m+}_{n,k,j}$ refers to an intermediate value, and not an approximation to the exact solution at time τ_m^+.

For subsequent use, we define the following index sets for the spatial and temporal variables: $\mathbb{N} = \{-N/2+1, \ldots, N/2-1\}$, $\mathbb{N}^\dagger = \left\{-N^\dagger/2, \ldots, N^\dagger/2-1\right\}$, $\mathbb{K} = \{-K/2+1, \ldots, K/2-1\}$, $\mathbb{K}^\dagger = \left\{-K^\dagger/2, \ldots, K^\dagger/2-1\right\}$, $\mathbb{J} = \{0, \ldots, J\}$ and $\mathbb{M} = \{0, \ldots, M-1\}$, $\mathbb{N}^{\mathrm{c}}_{\min} = \left\{-N^\dagger/2, \ldots, -N/2\right\}$, $\mathbb{N}^{\mathrm{c}}_{\max} = \left\{N/2, \ldots, N^\dagger/2-1\right\}$, $\mathbb{N}^{\mathrm{c}} = \mathbb{N}^\dagger \setminus \mathbb{N}$, and $\mathbb{K}^{\mathrm{c}} = \mathbb{K}^\dagger \setminus \mathbb{K}$. For fixed $j \in \mathbb{J}$ and $m \in \mathbb{M}$, nodes $\mathbf{x}^{m+1}_{n,j}$ having (i) $n \in \mathbb{N}^{\mathrm{c}}_{\min}$ and $k \in \mathbb{K}$ are in $\Omega_{w_{\min}} \cup \Omega_{wa_{\min}}$, (ii) $n \in \mathbb{N}$ and $k \in \mathbb{K}$ are in $\Omega_{\mathrm{in}} \cup \Omega_{a_{\min}}$, (iii) $n \in \mathbb{N}^{\mathrm{c}}_{\max}$ and $k \in \mathbb{K}$ are in $\Omega_{w_{\max}}$, and (iv) $n \in \mathbb{N}^\dagger$ and $k \in \mathbb{K}^{\mathrm{c}}$ are in Ω_{c}.

In subsequent discussion, we denote by $\gamma^m_{n,k,j} \in [0, a_j]$ the control representing the withdrawal amount at node (w_n, r_k, a_j, τ_m), $n \in \mathbb{N}^{\mathrm{c}}_{\min} \cup \mathbb{N}$, $k \in \mathbb{K}$, $j \in \mathbb{J}$, $m \in \mathbb{M}$. We also define

$$\tilde{w}_n = \ln(\max(e^{w_n} - \gamma^m_{n,j,k}, e^{w^\dagger_{\min}})), \quad \tilde{a}_j = a_j - \gamma^m_{n,k,j}, \quad \gamma^m_{n,k,j} \in [0, a_j]. \qquad (4.13)$$

For a given withdrawal amount γ, let $f(\gamma)$ be the cash amount received by the holder defined as follows

$$f(\gamma) = \begin{cases} \gamma & \text{if } \; 0 \le \gamma \le C_r\Delta\tau, \\ \gamma(1-\mu) + \mu C_r\Delta\tau - c & \text{if } \; C_r\Delta\tau < \gamma. \end{cases} \qquad (4.14)$$

Remark 4.1 (Interpolation)**.** *Optimal controls are typically decided by comparing candidates obtained via interpolation using on available relevant discrete values in Ω, i.e. including discrete values are in boundary sub-domains. In this work, we use linear interpolation. To this end, let $s \in (0, T]$ be fixed. We denote by $\mathcal{I}\{u^s\}(w, r, a)$ a generic three-dimensional linear interpolation operator acting on the time-s discrete values $\left\{\left((w_l, r_d, a_q), u^s_{l,d,q}\right)\right\}$, $l \in \mathbb{N}^\dagger$, $d \in \mathbb{K}^\dagger$, $q \in \mathbb{J}$. Here, unless otherwise stated, values $u^s_{l,d,q}$ corresponding to points $\mathbf{x}^s_{l,d,q}$ in the boundary sub-domains $\Omega_{w_{\min}}$, $\Omega_{wa_{\min}}$, $\Omega_{w_{\max}}$ or Ω_c are given by the respective time-s boundary values.*

In its primary usage, the above interpolation operator degenerates to a two- or one-dimensional operator respectively when one or two of the following equalities hold: $w = w_n$, $r = r_k$, and $a = a_j$, for some $n \in \mathbb{N}^\dagger$, $k \in \mathbb{K}$, and $j \in \mathbb{J}$. Nonetheless, in these cases, to simplify notation, we still use the notation $\mathcal{I}\{u^s\}(w, r, a)$, with these degenerations being implicitly understood.

It is straightforward to show that, due to linear interpolation, for any constant ξ, we have

$$\mathcal{I}\{\varphi^s + \xi\}(w, r, a) = \mathcal{I}\{\varphi^s\}(w, r, a) + \xi. \qquad (4.15)$$

[4] While it is straightforward to generalized the numerical method to non-uniform partitioning of the τ-dimension, for the purposes of proving convergence, uniform partitioning suffices.

Furthermore, for a smooth test function $\varphi \in \mathcal{C}^\infty(\Omega^\infty)$, we have

$$\mathcal{I}\left\{\varphi^s\right\}(w,r,a) = \varphi(w,r,a) + \mathcal{O}\left((\Delta w + \Delta r)^2\right). \quad (4.16)$$

Finally, we note that linear interpolation is monotone in the viscosity sense.

For double summations, we use the short-hand notation: $\sum_{d\in\mathcal{D}}^{q\in\mathcal{Q}}{}^{*}(\cdot) := \sum_{d\in\mathcal{D}}\sum_{q\in\mathcal{Q}}(\cdot)$, unless otherwise noted. We are now ready to present the complete numerical schemes to solve the HJB-QVI (3.18). For any point $(w_n, r_k, a_j, \tau_{m+1})$ in Ω, unless otherwise stated, we let $j \in \mathbb{J}$ and $m \in \mathbb{M}$ be fixed, and focus on the index sets of n and k in subsequent discussion.

4.3 Ω_{τ_0}, $\Omega_{w_{\max}}$, and Ω_{c}

For $(w_n, r_k, a_j, \tau_0) \in \Omega_{\tau_0}$, we impose the initial condition (3.17).

$$v_{n,k,j}^0 = \max(e^{w_n}, (1-\mu)a_j - c), \quad n \in \mathbb{N}^\dagger,\ k \in \mathbb{K}^\dagger. \quad (4.17)$$

For $(w_n, r_k, a_j, \tau_{m+1})$ in $\Omega_{w_{\max}}$ and Ω_{c}, we respectively apply the Dirichlet boundary condition (3.4) and (3.7) as follows

$$v_{n,k,j}^{m+1} = e^{-\beta\tau_{m+1}} e^{w_n}, \quad n \in \mathbb{N}_{\max}^{\mathrm{c}},\ k \in \mathbb{K}, \quad (4.18)$$

$$v_{n,k,j}^{m+1} = p(w_n, r_k, a_j, \tau_{m+1}), \quad n \in \mathbb{N}^\dagger,\ k \in \mathbb{K}^{\mathrm{c}}, \quad (4.19)$$

where $p(w_n, r_k, a_j, \tau_{m+1})$ is given in (3.7).

4.4 $\Omega_{w_{\min}} \cup \Omega_{wa_{\min}}$

For $(w_n, r_k, a_j, \tau_{m+1})$ in $\Omega_{w_{\min}} \cup \Omega_{wa_{\min}}$, we let $\tilde{v}_{n,k,j}^m$ be an approximation to $v(w_n, r_k, a_j - \gamma_{n,j}^m, \tau_m)$ computed by linear interpolation as follows

$$\tilde{v}_{n,k,j}^m = \mathcal{I}\left\{v^m\right\}\left(w_n, r_k, a_j - \gamma_{n,k,j}^m\right), \quad n \in \mathbb{N}_{\min}^{\mathrm{c}},\ k \in \mathbb{K}. \quad (4.20)$$

We compute intermediate results $v_{n,k,j}^{m+}$ by solving the optimization problem

$$v_{n,k,j}^{m+} \;=\; \sup_{\gamma_{n,k,j}^m \in [0,a_j]} \left(\tilde{v}_{n,k,j}^m + f\left(\gamma_{n,k,j}^m\right)\right), \quad n \in \mathbb{N}_{\min}^{\mathrm{c}},\ k \in \mathbb{K}. \quad (4.21)$$

where $\tilde{v}_{n,k,j}^m$ is given in (4.20) and $f(\cdot)$ is defined in (4.14). To advance to time τ_{m+1}, we solve the PDE $v_\tau - \mathcal{L}_d v = 0$ with the time-τ_{m+} initial condition given by $v_{n,k,j}^{m+}$ in (4.21). This step is achieved by applying finite difference methods built upon a fully implicit timestepping scheme together with a positive coefficient discretization as follows [17, 18, 43, 24, 34]

$$v_{n,k,j}^{m+1} \;=\; v_{n,k,j}^{m+} + \Delta\tau(\mathcal{L}_d^h v)_{n,k,j}^{m+1}, \quad \text{where} \quad (4.22)$$

$$(\mathcal{L}_d^h v)_{n,k,j}^{m+1} \;=\; \alpha_k v_{n,k-1,j}^{m+1} + \beta_k v_{n,k+1,j}^{m+1} - (\alpha_k + \beta_k + r_k)\, v_{n,k,j}^{m+1}, \quad n \in \mathbb{N}_{\min}^{\mathrm{c}},\ k \in \mathbb{K},$$

$$\text{with} \quad \alpha_k \;\geq\; 0, \quad \beta_k \;\geq\; 0, \quad k \in \mathbb{K}. \quad (4.23)$$

4.5 $\Omega_{\mathrm{in}} \cup \Omega_{a_{\min}}$

For $(w_n, r_k, a_j, \tau_{m+1})$ in $\Omega_{\mathrm{in}} \cup \Omega_{a_{\min}}$ and $\gamma_{n,k,j}^m \in [0, a_j]$, we let $\tilde{v}_{n,k,j}^m$ be an approximation to $v(\tilde{w}_n, r_k, \tilde{a}_j, \tau_m)$, where $\tilde{w}_n$ and $\tilde{a}_j$ are defined in (4.13), computed by linear interpolation given by

$$\tilde{v}_{n,k,j}^m = \mathcal{I}\left\{v^m\right\}(\tilde{w}_n, r_k, \tilde{a}_j), \quad \gamma_{n,k,j}^m \in [0, a_j],\ n \in \mathbb{N},\ k \in \mathbb{K}. \quad (4.24)$$

We recall the control formulation (3.1), where the admissible control set is $[0, a]$. We observe that the $\min\{\cdot\}$ operator of (3.1) contains two terms, with the continuous control $\hat{\gamma}$ in the first term having a local nature ($\hat{\gamma} \in [0, C_r]$), while the impulse control γ in the second term having a non-local nature ($\gamma \in [0, a]$). Motivated by this observation, as in [57, 17], with the convention that $(C_r\Delta\tau, a_j] = \emptyset$ if $a_j \leq C_r\Delta\tau$, we partition $[0, a_j]$ into $[0, a_j \wedge C_r\Delta\tau]$ and $(C_r\Delta\tau, a_j]$, where $x \wedge y = \min(x, y)$. We compute respective intermediate results $(v^{(1)})_{n,k,j}^{m+}$ and $(v^{(2)})_{n,k,j}^{m+}$, $n \in \mathbb{N}$, $k \in \mathbb{K}$, by solving the optimization problems

$$(v^{(1)})_{n,k,j}^{m+} = \sup_{\gamma_{n,k,j}^m \in [0, a_j \wedge C_r\Delta\tau]} (\tilde{v}_{n,k,j}^m + f(\gamma_{n,k,j}^m)), \quad (v^{(2)})_{n,k,j}^{m+} = \sup_{\gamma_{n,k,j}^m \in (C_r\Delta\tau, a_j]} (\tilde{v}_{n,k,j}^m + f(\gamma_{n,k,j}^m)), \quad (4.25)$$

where $\tilde{v}_{n,k,j}^m$ is given in (4.24) and $f(\cdot)$ is defined in (4.14).

Remark 4.2 (Attainability of supremum)**.** *It is straightforward to show that, due to boundedness of nodal values used in* $\mathcal{I}\{v^m\}(\cdot)$ *(see Lemma 5.1 on stability), the interpolated value* $\tilde{v}^m_{n,k,j}$ *in* (4.24) *is uniformly continuous in* $\gamma^m_{n,k,j}$*. As a result, the supremum in the discrete equations for* $(v^{(1)})^{m+}_{n,k,j}$ *and* $(v^{(2)})^{m+}_{n,k,j}$ *in* (4.25) *can be achieved by a control in* $[0, \min(a_j, C_r\Delta\tau)]$ *and* $(C_r\Delta\tau, a_j]$*, respectively, with the latter case being made possible due to* $c > 0$ *[17].*

The next step in the numerical scheme for $\Omega_{\text{in}} \cup \Omega_{a_{\min}}$ is time advancement from τ_m^+ to τ_{m+1}. As briefly discussed previously, the time advancement step involves (i) an SL discretization for the term $\mathcal{L}_s v - rv$ of the PIDE (4.1) in $\Omega_{\text{in}} \cup \Omega_{a_{\min}}$, (ii) an ϵ-monotone Fourier method based on the Green function associated with the PIDE (4.4). We now discuss these steps in detail below.

4.5.1 Intuition of semi-Lagrangian discretization

We start by providing an intuition of an SL discretization method and the Green's function approach utilized for $\Omega_{\text{in}} \cup \Omega_{a_{\min}}$. The main idea employed to construct an SL discretization of the PIDE of the form (4.1) is to integrate the PIDE along an SL trajectory, which is to be defined subsequently. Recall from (4.3) that the differential operator $\mathcal{L}$ in the PIDE (4.1) can be written as $\mathcal{L} = \mathcal{L}_g + \mathcal{L}_s - rv$, where the operator $\mathcal{L}_s = (r - \frac{\sigma_z^2}{2} - \beta)v_w + \delta(\theta - r)v_r$. In subsequent discussion, we let $a \in [a_{\min}, a_{\max}]$ be fixed, and also let $x := (w, r)$ be arbitrary in $[w_{\min}, w_{\max}] \times [r_{\min}, r_{\max}]$. For any $s \in [\tau_m^+, \tau_{m+1}]$, and $\tau \le s$, we consider an SL trajectory, denoted by $\chi(\tau; s, x) = (\chi_1(\tau; s, x), \chi_2(\tau; s, x))$, which satisfies the ordinary differential equations

$$\begin{cases} \dfrac{\partial \chi_1(\tau; s, x)}{\partial \tau} = -(r - \dfrac{\sigma_z^2}{2} - \beta), & \tau < s, \\ \chi_1(s; s, x) = w, & \tau = s, \end{cases} \quad \text{and} \quad \begin{cases} \dfrac{\partial \chi_2(\tau; s, x)}{\partial \tau} = -\delta(\theta - r), & \tau < s, \\ \chi_2(s; s, x) = r, & \tau = s. \end{cases} \tag{4.26}$$

Using (4.26), we have $\frac{Dv}{D\tau} = v_\tau + \mathcal{L}_s v$, and therefore, the PIDE (4.1) can be written as

$$\frac{Dv}{D\tau} + rv - \mathcal{L}_g v - \mathcal{J} v = 0, \quad \tau \in (\tau_m^+, \tau_{m+1}], \tag{4.27}$$

subject to a generic initial condition of the form (4.2). We let $(\breve{w}(s), \breve{r}(s))$ be the (w, r)-departure point at time-τ_m for the trajectory $\chi(\tau; s, x)$, i.e. $(\breve{w}(s), \breve{r}(s)) = (\chi_1(\tau = \tau_m; s, x), \chi_2(\tau = \tau_m; s, x))$, and hence, they can be computed by solving (4.26) from $\tau = \tau_m$ to $\tau = s$, i.e.

$$\breve{w}(s) = w + r(e^{s-\tau_m} - 1) - \left(\frac{\sigma_z^2}{2} + \beta\right)(e^{s-\tau_m} - 1), \;\; \breve{r}(s) = re^{-\delta(s-\tau_m)} - \theta\left(e^{-\delta(s-\tau_m)} - 1\right). \tag{4.28}$$

We then integrate both sides of the equation (4.27) along the trajectory $\chi(\tau; s, x)$ from $\tau = \tau_m$ to $\tau = s$ with a being fixed. This gives

$$\int_{\tau_m}^{s} \left(\frac{Dv}{D\tau}(\chi(\tau; s, x), a, \tau) + rv(w, r, a, \tau) - (\mathcal{L}_g + \mathcal{J})\, v(w, r, a, \tau)\right) d\tau = 0. \tag{4.29}$$

In (4.29), using the identity

$$\int_{\tau_m}^{s} \frac{Dv}{D\tau}(\chi(\tau; s, x), a, \tau)\, d\tau = v(w, r, a, s) - v(\breve{w}(s), \breve{r}(s), a, \tau_m),$$

together with a simple left-hand-side rule for $\int_{\tau_m}^{s} rv(w, r, a, \tau)\, d\tau \simeq r(s - \tau_m)v(w, r, a, \tau_m)$, and rearranging, (4.29) becomes

$$v(w, r, a, s) - \int_{\tau_m}^{s} (\mathcal{L}_g + \mathcal{J})\, v(w, r, a, \tau)\, d\tau = v(\breve{w}(s), \breve{r}(s), a, \tau_m) - r(s - \tau_m)v(w, r, a, \tau_m). \tag{4.30}$$

Here, $v(w, r, a, s)$, $\tau_m \le s \le \tau_{m+1}$, is the unknown function at time-s. In particular, we are interested in finding $v(w, r, a, \tau_{m+1})$. To this end, we approximate $v(w, r, a, \tau_{m+1})$ by $v_{\text{SL}}(w, r, a, \tau_{m+1})$ where the function $v_{\text{SL}}(w, r, a, s)$, $\tau_m \le s \le \tau_{m+1}$, satisfies a variation of equation (4.30) obtained by fixing its right-hand-side at $s = \tau_{m+1}$. More specifically, with $(\breve{w}, \breve{r}) \equiv (\breve{w}(\tau_m^+), \breve{r}(\tau_m^+))$, $v_{\text{SL}}(w, r, a, s)$ satisfies

$$v_{\text{SL}}(w, r, a, s) - \int_{\tau_m}^{s} (\mathcal{L}_g + \mathcal{J})\, v_{\text{SL}}(w, r, a, \tau)\, d\tau = v(\breve{w}, \breve{r}, a, \tau_m) - r\Delta\tau v(w, r, a, \tau_m), \tag{4.31}$$

where, on the rhs, $v(\cdot,\cdot,a,\tau_m)$ is given by a known generic initial condition at time τ_m. We highlight that equation (4.30) agrees with equation (4.31) only when $s = \tau_{m+1}$, at which time we have $v_{\text{SL}}(w,r,a,\tau_{m+1}) = v(w,r,a,\tau_{m+1})$, as wanted.

The form of equation (4.31) suggests that $v_{\text{SL}}(w,r,a,s)$ satisfies the PIDE of the form (4.4), i.e.

$$(v_{\text{SL}})_\tau - \mathcal{L}_g v_{\text{SL}} - \mathcal{J} v_{\text{SL}} = 0, \quad w \in (-\infty,\infty),\ r \in (-\infty,\infty),\ \tau \in (\tau_m^+, \tau_{m+1}], \tag{4.32}$$

subject to the initial condition

$$\hat{v}_{\text{SL}}(w,r,a,\tau_m^+ o) = \begin{cases} v\left(w,r,a,\tau_m^+\right) = \dfrac{v\left(\breve{w},\breve{r},a,\tau_m^+\right)}{1+\Delta\tau r} & (w,r,a,\tau_m) \in \Omega_{\text{in}} \cup \Omega_{a_{\min}}, \quad (4.33\text{a}) \\ v_{bc}(w,r,a,\tau_m^+) & (w,r,a,\tau_m) \in \Omega \setminus \left(\Omega_{\text{in}} \cup \Omega_{a_{\min}}\right), \quad (4.33\text{b}) \end{cases}$$

where, in (4.33a), $(\breve{w},\breve{r}) \equiv (\breve{w}(\tau_{m+1}), \breve{r}(\tau_{m+1}))$ given by (4.28). From here, as previously discussed in Subsection 4.1, the solution $v_{\text{SL}}(w,r,\cdot,\tau_{m+1})$ is approximated by the convolution integral (4.7).

For subsequent discussions, we investigate equation (4.31) and the initial condition (4.33) from a standpoint that involves discrete grid points. Specifically, for a Lagrangian trajectory which ends at (w_n, r_k) at time τ_{m+1}, the departure point $(\breve{w}_n, \breve{r}_k)$ at time-τ_m^+, computed by (4.28) with $w = w_n$, $r = r_k$, and $s = \tau_{m+1}$, does not necessarily coincide with a grid point. Therefore, to approximate (4.33a) corresponding to (w_n, r_k, a_j), i.e. $\frac{v\left(\breve{w}_n,\breve{r}_k,a_j,\tau_m^+\right)}{1+\Delta\tau r}$, linear interpolation can be used. Specifically, we denote by $(v_{\text{SL}})_{n,k,j}^{m+}$ the interpolation result given by

$$(v_{\text{SL}})_{n,k,j}^{m+} = \frac{\mathcal{I}\left\{v^{m+}\right\}(\breve{w}_n, \breve{r}_k, a_j)}{1+\Delta\tau r_k}, \quad n \in \mathbb{N},\ k \in \mathbb{K}, \tag{4.34}$$

$$\text{where } \breve{w}_n = w_n + r_k\left(e^{\Delta\tau} - 1\right) - \left(\frac{\sigma_z^2}{2} + \beta\right)\left(e^{\Delta\tau} - 1\right),\ \breve{r}_k = r_k e^{-\delta\Delta\tau} - \theta\left(e^{-\delta\Delta\tau} - 1\right).$$

Here, $\mathcal{I}\{\cdot\}$ is the discrete interpolation operator defined in (4.1). If the departure point $(\breve{w}_n, \breve{r}_k, a_j)$ falls outside $\Omega_{\text{in}} \cup \Omega_{a_{\min}}$, discrete solutions in the boundary sub-domains are used for interpolation. We emphasize the SL discretization is not applied to grid points outside $\Omega_{\text{in}} \cup \Omega_{a_{\min}}$.

4.5.2 Time advancement scheme: $\tau \in [\tau_m^+, \tau_{m+1}]$

To prepare for time advancement, we combine the time-τ_m boundary values in $\Omega_{w_{\min}}$, $\Omega_{wa_{\min}}$, $\Omega_{w_{\max}}$, and Ω_{c} with the time-τ_m^+ intermediate results obtained by the SL discretization discussed above and results from (4.25). With a slight abuse of notation, for $(i) \in \{(1),(2)\}$, this is done as follows

$$\left(v_{\text{SL}}^{(i)}\right)_{l,d,j}^{m+} = \begin{cases} \dfrac{\mathcal{I}\left\{(v^{(i)})^{m+}\right\}(\breve{w}_l, \breve{r}_d, a_j)}{1+\Delta\tau r_d} & \breve{w}_l \text{ and } \breve{r}_d \text{ defined in (4.34)} \quad l \in \mathbb{N} \text{ and } d \in \mathbb{K}, \\ v_{l,d,j}^m & \text{in (4.18), (4.19), and (4.22), otherwise.} \end{cases} \tag{4.35}$$

For $\tau \in [\tau_m^+, \tau_{m+1}]$, our timestepping method for solving the PIDE (4.32) is built upon the convolution integral (4.5), with the initial condition $\hat{v}_{\text{SL}}^{(i)}(w,r,\cdot,\tau_m^+)$, $(i) \in \{(1),(2)\}$, approximated by a projection of discrete values in (4.35). onto linear basis functions for the w- and r-dimensions. Specifically, $\hat{v}_{\text{SL}}^{(i)}(w,r,\cdot,\tau_m^+)$, $(i) \in \{(1),(2)\}$, is approximated by the projection

$$\hat{v}_{\text{SL}}^{(i)}\left(w,r,\cdot,\tau_m^+\right) \simeq \sum_{l\in\mathbb{N}^\dagger}^{d\in\mathbb{K}^\dagger}{}^{*} \varphi_l(w)\ \psi_d(r)\ \left(v_{\text{SL}}^{(i)}\right)_{l,d,j}^{m+}, \quad (w,r) \in \mathbf{D} \equiv (w_{\min}, w_{\max}) \times (r_{\min}, r_{\max}), \tag{4.36}$$

where $\{\varphi_l(w)\}_{l\in\mathbb{N}^\dagger}$ and $\{\psi_d(r)\}_{d\in\mathbb{K}^\dagger}$ are piecewise linear basis functions defined by

$$\varphi_l(w) = \begin{cases} (w_{l+1} - w)/\Delta w, & w_l \le w \le w_{l+1}, \\ (w - w_{l-1})/\Delta w, & w_{l-1} \le w \le w_l, \\ 0, & \text{otherwise,} \end{cases} \quad \psi_d(r) = \begin{cases} (r_{d+1} - r)/\Delta r, & r_d \le r \le r_{d+1}, \\ (r - r_{d-1})/\Delta r, & r_{d-1} \le r \le r_d, \\ 0, & \text{otherwise.} \end{cases} \tag{4.37}$$

In the convolution integral (4.7), we substitute $\hat{v}_{\text{SL}}^{(i)}(w, r, \cdot, \tau_m^+)$, $(i) \in \{(1), (2)\}$, by the projection (4.36) and rearrange the resulting equation. We obtain the discrete convolution for $\left(v_{\text{SL}}^{(i)}\right)_{n,k,j}^{m+1}$, $(i) \in \{(1), (2)\}$, as follows

$$\left(v_{\text{SL}}^{(i)}\right)_{n,k,j}^{m+1} = \Delta w \Delta r \sum_{l \in \mathbb{N}^\dagger}^{d \in \mathbb{K}^\dagger} {}^{*} \, \tilde{g}_{n-l,k-d} \;\; \left(v_{\text{SL}}^{(i)}\right)_{l,d,j}^{m+}, \quad n \in \mathbb{N},\ k \in \mathbb{K}. \tag{4.38}$$

Here, $\left(v_{\text{SL}}^{(i)}\right)_{l,d,j}^{m+}$ is given by the linear interpolation in (4.34), and $\tilde{g}_{n-l,k-d}$ is given by

$$\begin{aligned} \tilde{g}_{n-l,k-d} &\equiv \tilde{g}(w_n - w_l, r_k - r_d, \Delta\tau) \\ &= \frac{1}{\Delta w} \frac{1}{\Delta r} \iint_{\mathbf{D}^\dagger} \varphi_l(w)\ \psi_d(r)\ g(w_n - w, r_k - r, \Delta\tau)\ dw\ dr. \end{aligned} \tag{4.39}$$

That is, in the discrete convolution (4.38), the exact weights $\tilde{g}_{n-l,k-d}$, $n \in \mathbb{N}$, $k \in \mathbb{K}$, $l \in \mathbb{N}^\dagger$, $d \in \mathbb{K}^\dagger$, are obtained by a projection of the Green's function $g(\cdot, \Delta\tau)$ onto the piecewise linear basis functions $\{\varphi_l(w)\}_{l \in \mathbb{N}^\dagger}$ and $\{\psi_d(r)\}_{d \in \mathbb{K}^\dagger}$.

Finally, we compute the discrete solution $v_{n,k,j}^{m+1}$ by

$$v_{n,k,j}^{m+1} = \max\left(\left(v_{\text{SL}}^{(1)}\right)_{n,k,j}^{m+1}, \left(v_{\text{SL}}^{(2)}\right)_{n,k,j}^{m+1}\right) \quad n \in \mathbb{N},\ k \in \mathbb{K}, \tag{4.40}$$

where $\left(v_{\text{SL}}^{(1)}\right)_{n,k,j}^{m+1}$ and $\left(v_{\text{SL}}^{(2)}\right)_{n,k,j}^{m+1}$ are given by (4.38).

4.5.3 Approximation of exact weights $\tilde{g}$ and ϵ-monotonicity

We need to approximate the exact weights $\tilde{g}_{n-l,k-d}$ defined in the convolution integral (4.39). To this end, we adapt steps in [35, 57] for two-dimensional Green's functions. We let $G(\eta, \xi, \Delta\tau)$ be the Fourier transform of the Green's function $g(w, r, \Delta\tau)$. A closed-form expression for $G(\eta, \xi, \Delta\tau)$ is given by

$$\begin{aligned} G(\eta, \xi, \Delta\tau) &= \exp\left(\Psi(\eta, \xi)\, \Delta\tau\right), \quad \text{with} \\ \Psi(\eta, \xi) &= -\frac{\sigma_{\scriptscriptstyle Z}^2}{2}(2\pi\eta)^2 - \rho\sigma_{\scriptscriptstyle Z}\sigma_{\scriptscriptstyle R}(2\pi\eta)(2\pi\xi) - \frac{\sigma_{\scriptscriptstyle R}^2}{2}(2\pi\xi)^2 - \lambda\kappa(2\pi i\eta) - \lambda + \lambda\overline{B}(\eta), \end{aligned} \tag{4.41}$$

where, $\overline{B}(\eta)$ is the complex conjugate of the integral $B(\eta) = \int_{-\infty}^{\infty} b(y) e^{-2\pi i\eta y}\ dy$, noting $b(y)$ is the density function of $\ln(Y)$, where Y is the random variable representing the jump multiplier.

The idea in approximating the integral (4.39) is to replace $g(w, r, \Delta\tau)$ therein by its localized, periodic approximation $\hat{g}(w, r, \Delta\tau)$ given by

$$\hat{g}(w, r, \Delta\tau) \;=\; \frac{1}{P^\dagger} \frac{1}{Q^\dagger} \sum_{s \in \mathbb{Z}}^{z \in \mathbb{Z}} {}^{*} \, e^{2\pi i\eta_s w} e^{2\pi i\xi_z r} G(\eta_s, \xi_z, \Delta\tau) \;\; \text{with} \;\; \eta_s = \frac{s}{P^\dagger},\ \xi_z = \frac{z}{Q^\dagger}. \tag{4.42}$$

where we denote $\mathbb{Z}$ to be the set of all integers.[5] Then, assuming uniform convergence of Fourier series, we integrate (4.39) to obtain

$$\tilde{g}_{n-1,k-d} \equiv \tilde{g}_{n-1,k-d}(\infty) = \frac{1}{P^\dagger} \frac{1}{Q^\dagger} \sum_{s \in \mathbb{Z}}^{z \in \mathbb{Z}} {}^{*} \, e^{2\pi i\eta_s(n-l)\Delta w} e^{2\pi i\xi_z(k-d)\Delta r}\ \text{tg}(s, z)\ G(\eta_s, \xi_z, \Delta\tau), \tag{4.43}$$

where the trigonometry term $\text{tg}(s, z)$ is defined by[6]

$$\text{tg}(s, z) = \left(\frac{\sin^2 \pi\eta_s \Delta w}{(\pi\eta_s\Delta w)^2}\right)\left(\frac{\sin^2 \pi\xi_z \Delta r}{(\pi\xi_z\Delta r)^2}\right), \quad s \in \mathbb{Z}, z \in \mathbb{Z}. \tag{4.44}$$

[5]We note that the coefficients $G(\eta_s, \xi_z\Delta\tau)$ in (4.42) are the exact coefficients corresponding to the Green's function of the PIDE (4.4) with suitable periodic boundary conditions; hence, $\hat{g}(w, r, \Delta\tau)$ is a valid Green's function, and in particular $\hat{g}(\cdot) \geq 0$.

[6]For $\eta_s = 0$ and $\xi_z = 0$, we take the limit $\eta_s \to 0$ and $\xi_z \to 0$.

For $\alpha \in \{2, 4, 8, \ldots\}$, (4.43) is truncated to $\alpha N^\dagger$ and $\alpha K^\dagger$ terms for the outer and the inner summations, respectively, resulting in an approximation

$$\tilde{g}_{n-l,k-d}\left(\alpha\right) = \frac{1}{P^\dagger}\frac{1}{Q^\dagger}\sum_{s\in\mathbb{N}^\alpha}^{z\in\mathbb{K}^\alpha}{}^{*} e^{2\pi i \eta_s (n-l)\Delta w} e^{2\pi i \xi_z (k-d)\Delta r} \ \mathrm{tg}(s,z)\ G(\eta_s, \xi_z, \Delta\tau), \tag{4.45}$$

where $\mathbb{N}^\alpha = \{-\alpha N^\dagger/2 - 1, \ldots, \alpha N^\dagger/2 - 1\}$ and $\mathbb{K}^\alpha = \{-\alpha K^\dagger/2 - 1, \ldots, \alpha K^\dagger/2 - 1\}$.[7]

As $\alpha \to \infty$, replacing $\tilde{g}_{n-l,k-d}$ by $\tilde{g}_{n-l,k-d}\left(\alpha\right)$ in the discrete convolution (4.38) results in no loss of information. However, for any finite α, there is an error due to the use of a truncated Fourier series, although, as $\alpha \to \infty$, this error vanishes very quickly due a rapid convergence of truncated Fourier series. This is discussed in Subsection (5.2). Due to the above truncation error of Fourier series, strict monotonicity is not guaranteed for a finite α. To control this potential loss of monotonicity for a finite α, as in [35, 57], the selected α must satisfy

$$\Delta w \Delta r \sum_{l\in\mathbb{N}^\dagger}^{d\in\mathbb{K}^\dagger}{}^{*} \left|\min\left(\tilde{g}_{n-l,k-d}(\alpha), 0\right)\right| \ < \ \epsilon \frac{\Delta\tau}{T}, \quad \forall n \in \mathbb{N},\ k \in \mathbb{K}, \tag{4.46}$$

where $0 < \epsilon \ll 1/2$ is an user-defined monotonicity tolerance. We note that the left-hand-side of the monotonicity test (4.46) is scaled by Δw so that it is bounded as $\Delta w, \Delta\tau \to 0$. In addition, ϵ is scaled by $\frac{\Delta\tau}{T}$ in order to eliminate the number of timesteps from the bounds of potential loss of monotonicity.

4.5.4 Efficient implementation via FFT and algorithms

Note that, for a fixed $\alpha \in \{2, 4, 8, \ldots\}$, the sequence $\{\tilde{g}_{-N^\dagger/2,k}(\alpha), \ldots, \tilde{g}_{N^\dagger/2-1,k}(\alpha)\}$ for a fixed $k \in \mathbb{K}^\dagger$ is $N^\dagger$-periodic, and the sequence $\{\tilde{g}_{n,-K^\dagger/2}(\alpha), \ldots, \tilde{g}_{n,K^\dagger/2-1}(\alpha)\}$ for a fixed $n \in \mathbb{N}^\dagger$ is $K^\dagger$-periodic. With these in mind, we let $p = n - l$ and $q = k - d$ in the discrete convolution (4.45), and, for a fixed α, the set of approximate weights in the physical domain to be determined is $\tilde{g}_{p,q}(\alpha)$, $p \in \mathbb{N}^\dagger$, $q \in \mathbb{K}^\dagger$. Using this notation, in (4.45), with $p = n - l$ and $q = k - d$, we rewrite $e^{2\pi i \eta_s (n-l)\Delta w} = e^{2\pi i s\alpha p/(\alpha N^\dagger)}$, $e^{2\pi i \xi_z (k-d)\Delta r} = e^{2\pi i z\alpha q/(\alpha K^\dagger)}$, and obtain

$$\begin{aligned} \tilde{g}_{p,q}(\alpha) &= \frac{1}{P^\dagger}\frac{1}{Q^\dagger}\sum_{s\in\mathbb{N}^\alpha}^{z\in\mathbb{K}^\alpha}{}^{*} e^{2\pi i s\alpha p/(\alpha N^\dagger)} e^{2\pi i z\alpha q/(\alpha K^\dagger)}\ y_{s,z}, \quad p \in \mathbb{N}^\dagger,\ q \in \mathbb{K}^\dagger, \\ \text{where } y_{s,z} &= \mathrm{tg}(s,z)\ G(\eta_s, \xi_z \Delta\tau), \qquad\qquad s \in \mathbb{N}^\alpha,\ z \in \mathbb{K}^\alpha, \end{aligned} \tag{4.47}$$

and $\mathrm{tg}(s,z)$ is given in (4.44). It is observed from (4.47) that, given $\{y_{s,z}\}$, $\{\tilde{g}_{p,q}(\alpha)\}$ can be computed efficiently via a single two-dimensional FFT of size $(\alpha N^\dagger, \alpha K^\dagger)$. A suitable value for α, i.e. satisfying the ϵ-monotonicity condition (4.46), can be determined through an iterative procedure based on formula (4.47). Let this value be α_ϵ. We also observe that, once α_ϵ is found, the discrete convolution (4.38) can also be computed efficiently using an FFT. This suggests that we only need to compute the weights in the Fourier domain, i.e. the DFT of $\{\tilde{g}_{p,q}(\alpha_\epsilon)\}$, only once, and reuse them for all timesteps. We define $\{\tilde{G}_{p,q}(\alpha_\epsilon)\}$ to be the DFT of $\{\tilde{g}_{p,q}(\alpha_\epsilon)\}$ given by

$$\tilde{G}(\eta_s, \xi_z, \Delta\tau, \alpha_\epsilon) = \frac{P^\dagger}{N^\dagger}\frac{Q^\dagger}{K^\dagger}\sum_{p\in\mathbb{N}^\dagger}^{q\in\mathbb{K}^\dagger}{}^{*} e^{-2\pi i p s/N^\dagger} e^{-2\pi i q z/K^\dagger}\ \tilde{g}_{p,q}(\alpha_\epsilon), \quad s \in \mathbb{N}^\dagger,\ z \in \mathbb{K}^\dagger. \tag{4.48}$$

An iterative procedure for computing $\{\tilde{G}_{p,q}(\alpha_\epsilon)\}$ is given in Algorithm 4.1, where we also use the stopping criterion $\Delta w \Delta r \sum_{p\in\mathbb{N}^\dagger}^{q\in\mathbb{K}^\dagger}{}^{*} |\tilde{g}_{p,q}(\alpha) - \tilde{g}_{p,q}(\alpha/2)| < \epsilon_1$, $\epsilon_1 > 0$.

[7] We can use different numbers of terms in the truncation for the outer and the inner summations, i.e. $\alpha_1 N^\dagger$ and $\alpha_2 K^\dagger$, respectively. Here, we use a single α to simplify the presentation.

Algorithm 4.1 Computation of weights $\tilde{G}_{p,q}(\alpha_\epsilon)$, $p \in \mathbb{N}^\dagger$, $q \in \mathbb{K}^\dagger$, in Fourier domain.

1: set $\alpha = 1$ and compute $\tilde{g}_{p,q}(\alpha)$, $p \in \mathbb{N}^\dagger$, $q \in \mathbb{K}^\dagger$ using (4.47);
2: **for** $\alpha = 2, 4, \ldots$ until convergence **do**
3: compute $\tilde{g}_{p,q}(\alpha)$, $p \in \mathbb{N}^\dagger$, $q \in \mathbb{K}^\dagger$, using (4.47);
4: compute $\text{test}_1 = \Delta w \Delta r \sum_{p\in\mathbb{N}^\dagger} \sum_{q\in\mathbb{K}^\dagger} \min\left(\tilde{g}_{p,q}(\alpha), 0\right)$ for monotonicity test;
5: compute $\text{test}_2 = \Delta w \Delta r \sum_{p\in\mathbb{N}^\dagger} \sum_{q\in\mathbb{K}^\dagger} \left|\tilde{g}_{p,q}(\alpha) - \tilde{g}_{p,q}(\alpha/2)\right|$ for accuracy test;
6: **if** $|\text{test}_1| < \epsilon(\Delta\tau/T)$ and $\text{test}_2 < \epsilon_1$ **then**
7: $\alpha_\epsilon = \alpha$;
break from for loop;
8: **end if**
9: **end for**
10: use (4.48) to compute and output weights $\tilde{G}_{p,q}(\alpha_\epsilon)$, $p \in \mathbb{N}^\dagger$, $q \in \mathbb{K}^\dagger$, in Fourier domain.

For simplicity, unless otherwise state, we adopt the notional convention $\tilde{g}_{n-l,k-d} = \tilde{g}_{n-l,k-d}(\alpha_\epsilon)$ and $\tilde{G}(\eta_s, \xi_z, \Delta\tau) \equiv \tilde{G}(\eta_s, \xi_z, \Delta\tau, \alpha_\epsilon)$, where α_ϵ is selected by Algorithm 4.1. The discrete convolutions (4.38) can then be implemented efficiently via an FFT as follows

$$\left(v_{\text{SL}}^{(i)}\right)_{n,k,j}^{m+1} \simeq \sum_{p\in\mathbb{N}^\dagger}^{q\in\mathbb{K}^\dagger}{}^{*} e^{2\pi i p n/N^\dagger} e^{2\pi i q n/K^\dagger} \left(V_{\text{SL}}^{(i)}\right)(\eta_p, \xi_q, a_j, \tau_m^+)\, \tilde{G}(\eta_p, \xi_q, \Delta\tau), \tag{4.49}$$

$$\text{with } \left(V_{\text{SL}}^{(i)}\right)(\eta_p, \xi_q, a_j, \tau_m^+) = \frac{1}{N^\dagger}\frac{1}{K^\dagger} \sum_{l\in\mathbb{N}^\dagger}^{d\in\mathbb{K}^\dagger}{}^{*} e^{-2\pi i p l/N^\dagger} e^{-2\pi i q d/K^\dagger} \left(v_{\text{SL}}^{(i)}\right)_{l,d,j}^{m+}, \; p \in \mathbb{N}^\dagger, \; q \in \mathbb{K}^\dagger,$$

where $(i) \in \{(1), (2)\}$ and $\tilde{G}(\eta_p, \xi_q \Delta\tau)$ is given by (4.48). Putting everything together, an ϵ-monotone Fourier numerical algorithm for the HJB-QVI (3.18) on Ω is presented in Algorithm 4.2 below.

Algorithm 4.2 An ϵ-monotone Fourier algorithm for GMWB problem defined in Definition (3.1). $x \circ y$ is the Hadamard product of matrices x and y.

1: compute matrix $\tilde{G} = \left\{\tilde{G}(\eta_p, \xi_q, \Delta\tau)\right\}_{p\in\mathbb{N}^\dagger, q\in\mathbb{K}^\dagger}$, using Algorithm 4.1;
2: initialize $v_{n,k,j}^0 = \max\left(e^{w_n}, (1-\mu)a_j - c\right)$, $n \in \mathbb{N}^\dagger$, $k \in \mathbb{K}^\dagger$, $j \in \mathbb{J}$; $//\Omega_{\tau_0}$
3: **for** $m = 0, \ldots, M-1$ **do**
4: solve (4.25) to obtain $(v^{(1)})_{n,k,j}^{m+}$ and $(v^{(2)})_{n,k,j}^{m+}$, $n \in \mathbb{N}$, $k \in \mathbb{K}$, $j \in \mathbb{J}$; $//\Omega_{\text{in}} \cup \Omega_{a_{\min}}$
5: compute $\left(v_{\text{SL}}^{(1)}\right)_{n,k,j}^{m+}$ and $\left(v_{\text{SL}}^{(2)}\right)_{n,k,j}^{m+}$, $n \in \mathbb{N}$, $k \in \mathbb{K}$, $j \in \mathbb{J}$; using (4.34); $//\Omega_{\text{in}} \cup \Omega_{a_{\min}}$
6: combine results in Line-5 with $v_{n,k,j}^m$ in $\Omega_{w_{\min}}$, $\Omega_{wa_{\min}}$, $\Omega_{w_{\max}}$ and Ω_{c}, to obtain
$\left(v_{\text{SL}}^{(i)}\right)_j^{m+} = \left\{\left(v_{\text{SL}}^{(i)}\right)_{n,k,j}^{m+}\right\}_{n\in\mathbb{N}^\dagger, k\in\mathbb{K}^\dagger}$, $(i) \in \{(1), (2)\}$, $j \in \mathbb{J}$;
7: compute $\left\{\left(v_{\text{SL}}^{(i)}\right)_{n,k,j}^{m+1}\right\}_{n\in\mathbb{N}^\dagger, k\in\mathbb{K}^\dagger} = \text{IFFT}\left\{\text{FFT}\left\{\left(v_{\text{SL}}^{(i)}\right)_j^{m+}\right\} \circ \tilde{G}\right\}$, $(i) \in \{(1), (2)\}$, $j \in \mathbb{J}$;
8: discard FFT values in $\Omega_{w_{\min}}$, $\Omega_{wa_{\min}}$, $\Omega_{w_{\max}}$, and Ω_{c}, namely $\left(v_{\text{SL}}^{(1)}\right)_{n,k,j}^{m+1}$ and $\left(v_{\text{SL}}^{(2)}\right)_{n,k,j}^{m+1}$,
$n \in \mathbb{N}^{\text{c}}$, $k \in \mathbb{K}^{\text{c}}$, $j \in \mathbb{J}$;
9: set $v_{n,k,j}^{m+1} = \max\left(\left(v_{\text{SL}}^{(1)}\right)_{n,k,j}^{m+1}, \left(v_{\text{SL}}^{(2)}\right)_{n,k,j}^{m+1}\right)$, $n \in \mathbb{N}$, $k \in \mathbb{K}$, $j \in \mathbb{J}$; $//\Omega_{\text{in}} \cup \Omega_{a_{\min}}$
10: compute $v_{n,k,j}^{m+1}$, $n \in \mathbb{N}^{\text{c}}$, $k \in \mathbb{K}^{\text{c}}$, $j \in \mathbb{J}$ using (4.18), (4.19) and (4.22); $//\ \Omega \setminus (\Omega_{\text{in}} \cup \Omega_{a_{\min}})$
11: **end for**

Remark 4.3 (Wraparound error)**.** *The boundary sub-domains* $\Omega_{w_{\min}} \cup \Omega_{wa_{\min}}$, $\Omega_{w_{\max}}$ *and* Ω_c *are also set up to act as padding areas to minimize the wraparound error in the computation of discrete convolutions* (4.38) *via an FFT in Line 7 of Algorithm 4.2. After an FFT is applied, all results of auxiliary padding* *nodes in* $\Omega_{w_{\min}} \cup \Omega_{wa_{\min}}$*,* $\Omega_{w_{\max}}$ *and* Ω_c *are discarded to minimize the wraparound error at nodes in* $\Omega_{in} \cup \Omega_{a_{\min}}$ *(Line 8). Using similar techniques as in [57] for the case of one-dimensional Green's function, we can show that, with our choice of* $N^\dagger = 2N$ *and* $K^\dagger = 2K$*, where* N *and* K *are chosen large enough, our handling of wraparound described above is sufficiently effective. The reader is referred to [57][Section 4.4] for relevant details.*

4.6 Fair insurance fees

With respect to the insurance fee β, let $v(\beta; w, r, a, \tau)$ be the exact solution, i.e. $v(w, a, r, \tau)$, be parameterised by the insurance fee β. Then, the fair insurance fee for $t = 0$, or $\tau_M = T$, denoted by β_f, solves the equation $v(\beta_f; \ln(z_0), r_0, z_0, T) = z_0$. In a numerical setting, with a slight abuse of notation, let $v^M_{\ln(z_0), r_0, z_0}(\beta)$ be the numerical solution parametrized by β, then we need to solve $v^M_{\ln(z_0), r_0, z_0}(\beta_f) = z_0$, where $v^M_{\ln(z_0), r_0, z_0}$ is obtained by Algorithm 4.2. Finally, we apply the Newton iteration to solve for β_f.

5 Convergence to the viscosity solution

In this section, we appeal to a Barles-Souganidis-type analysis [11] to rigorously study the convergence of our scheme in $\Omega_{\text{in}} \cup \Omega_{a_{\min}}$ as $h \to 0$ by verifying three properties: ℓ_∞-stability, ϵ-monotonicity (as opposed to strict monotonicity), and consistency. We will show that convergence of our scheme is ensured if the monotonicity tolerance $\epsilon \to 0$ as $h \to 0$. We note that our proofs share some similarities with those in [57], but our proof techniques are more involved due to the SL discretization, especially for consistency of the numerical scheme. We will emphasize these key similarities and differences where suitable.

For subsequent use, we introduce several important results related to relevant properties of the weights $\tilde{g}_{n-l,k-d}$ in the discrete convolution (4.39).

Proposition 5.1. *For any* $(n, k) \in \{\mathbb{N} \times \mathbb{K}\}$*, we have*

$$\Delta w \Delta r \sum_{l \in \mathbb{N}^\dagger}^{d \in \mathbb{K}^\dagger} {}^{*}\, \tilde{g}_{n-l,k-d} \;=\; 1, \quad \text{with } \tilde{g}_{n-l,k-d} \text{ is given by (4.45).}$$

A proof of Proposition 5.1 is given Appendix B. Noting $\tilde{g} = \max(\tilde{g}, 0) + \min(\tilde{g}, 0)$, Proposition 5.1 and the monotonicity condition (4.46) give the bound

$$\Delta w \Delta r \sum_{l \in \mathbb{N}^\dagger}^{d \in \mathbb{K}^\dagger} {}^{*} \left(\max\left(\tilde{g}_{n-l,k-d}, 0\right) + \left|\min\left(\tilde{g}_{n-l,k-d}, 0\right)\right|\right) \;\leq\; 1 + 2\epsilon \frac{\Delta \tau}{T}. \tag{5.1}$$

Our scheme consists of the following equations: (4.17) for Ω_{τ_0}, (4.18) for $\Omega_{w_{\max}}$, (4.19) for Ω_{c}, (4.22) for $\Omega_{w_{\min}} \cup \Omega_{wa_{\min}}$, and finally (4.40) for $\Omega_{\text{in}} \cup \Omega_{a_{\min}}$. We start by verifying ℓ_∞-stability of our scheme.

5.1 Stability

Lemma 5.1 (ℓ_∞-stability)**.** *Suppose that (i) the discretization parameter* h *satisfies* (5.8)*, and (ii) the discretization* (4.22) *satisfies the positive coefficient condition* (4.23)*, (iii) linear interpolation in* (4.20)*,* (4.34)*, and* (4.24)*, and (iv)* $r_{\min} < 0$ *satisfies the condition*

$$1 + \Delta\tau r_{\min} \;>\; 0. \tag{5.2}$$

Then scheme (4.17)*,* (4.18)*,* (4.19)*,* (4.22)*, and* (4.40) *satisfies* $\sup\limits_{h>0} \|v^m\|_\infty < \infty$ *for all* $m = 0, \ldots, M$*, as the discretization parameter* $h \to 0$*. Here,* $\|v^m\|_\infty = \max_{n,k,j} |v^m_{n,k,j}|$*, where* $n \in \mathbb{N}^\dagger$*,* $k \in \mathbb{K}^\dagger$ *and* $j \in \mathbb{J}$*.*

Proof of Lemma 5.1. For fixed $h > 0$, we have $\left\|v^0\right\|_\infty < \infty$, and thus, $\sup_{h>0} \left\|v^0\right\|_\infty < \infty$. Motivated by this observation, to demonstrate ℓ_∞-stability of our scheme, we aim to demonstrate that, for a fixed $h > 0$, at any (w_n, r_k, a_j, τ_m) in Ω,

$$|v^m_{n,k,j}| < C'(\left\|v^0\right\|_\infty + a_j), \text{ where } C' = e^{2m\epsilon \frac{\Delta\tau}{T}} e^{Cm\Delta\tau}, \text{ with } C = |r_{\min}|(1 + \Delta\tau r_{\min})^{-1}, \tag{5.3}$$

where ϵ, $0 < \epsilon < 1/2$, is the monotonicity tolerance used in (4.46). Since $m\Delta\tau \le T$, C' is bounded above.

We now discuss the important point of how to the constant C' in (5.3) is determined. This choice is motivated by the stability bounds for $\Omega_{\text{in}} \cup \Omega_{a_{\min}}$, which primarily depend on the amplification factor of the time-advancement step. (Boundary sub-domains require smaller stability bounds as shown subsequently). In our proof techniques, through mathematical induction on m, the time-τ_m accumulative amplification factor of the time-advancement in $\Omega_{\text{in}} \cup \Omega_{a_{\min}}$ can be bounded by the product of the respective amplification factors of the SL discretization and of the ϵ-monotone Fourier method. For the SL discretization, from (4.34) and the condition (5.2), for all $k \in \mathbb{K}$, we have

$$0 \;<\; (1+\Delta\tau r_k)^{-1} \;\le\; (1+\Delta\tau r_{\min})^{-1} = 1+\Delta\tau C, \text{ where } C = |r_{\min}|(1+\Delta\tau r_{\min})^{-1} > 0, \qquad (5.4)$$

which results in the time-τ_m accumulative amplification factor bounded by $e^{Cm\Delta\tau}$. For the ϵ-monotone Fourier method, the bound (5.1) suggests the time-τ_m amplification factor is bounded by $e^{2m\epsilon\frac{\Delta\tau}{T}}$. Putting together, we obtain the constant $C' > 0$ given in (5.3).

We address ℓ-stability for the boundary and interior sub-domains separately. For (4.17), (4.18), it is straightforward to show $\max_{n,k,j} |v^m_{n,k,j}| \le \left\|v^0\right\|_\infty$, $n \in \mathbb{N} \cup \mathbb{N}^{c}_{\max}$, $k \in \mathbb{K}$, $j \in \mathbb{J}$, and $m = 0, \ldots, M$. For (4.19), since the T-maturity zero-coupon bond price $p_b(r_k, \tau_m; T)$ given in (3.7) is non-negative, the stability trivially to show. For (4.22), since the finite difference scheme is strictly monotone, the ℓ-stability can be demonstrated using the induction technique (on m) as in [17].

To prove (5.3) for (4.40), it is sufficient to show that for all $m \in \{0, \ldots, M\}$ and $j \in \mathbb{J}$, we have

$$\left[v^m_j\right]_{\max} \;\le\; e^{2m\epsilon\frac{\Delta\tau}{T}} e^{Cm\Delta\tau} \left(\left\|v^0\right\|_\infty + a_j\right), \qquad (5.5)$$

$$-2m\epsilon\frac{\Delta\tau}{T} e^{2m\epsilon\frac{\Delta\tau}{T}} e^{Cm\Delta\tau} \left(\left\|v^0\right\|_\infty + a_j\right) \;\le\; \left[v^m_j\right]_{\min}. \qquad (5.6)$$

where $\left[v^m_j\right]_{\max} = \max_{n,k}\left\{v^m_{n,k,j}\right\}$ and $\left[v^m_j\right]_{\min} = \min_{n,k}\left\{v^m_{n,k,j}\right\}$. To prove (5.5)-(5.6), motivated by the above reasoning regarding the choice C', we use mathematical induction on $m = 0, \ldots, M$, similar to the technique developed in [57][Lemma 5.1]. The details for this step are provided in Appendix C. □

5.2 Error analysis results

In this subsection, we identify errors arising in our numerical scheme and make assumptions needed for subsequent proofs.

1. Truncating the infinite region of integration in the convolution integral (4.5) to $\mathbf{D}^\dagger$ (defined in (4.6)) results in a boundary truncation error, denoted by $\mathcal{E}_b$, where

$$\mathcal{E}_b = \iint_{\mathbb{R}^2\backslash\mathbf{D}^\dagger} g(w-w', r-r', \Delta\tau)\; \hat{v}_{\text{SL}}(w', r', \cdot, \tau_m)\; dw'\; dr', \quad (w,r) \in \mathbf{D}. \qquad (5.7)$$

   Similar to the discussions in [57], we can show that $\mathcal{E}_b$ is bounded by

$$|\mathcal{E}_b| \;\le\; K_1\Delta\tau e^{-K_2\left(P^\dagger \wedge Q^\dagger\right)}, \quad \forall (w,r) \in \mathbf{D}, \quad K_1, K_2 > 0 \text{ independent of } \Delta\tau,\ P^\dagger \text{ and } Q^\dagger,$$

   where $P^\dagger = w^\dagger_{\max} - w^\dagger_{\min}$ and $Q^\dagger = r^\dagger_{\max} - r^\dagger_{\min}$. For fixed $P^\dagger$ and $Q^\dagger$, (5.8) shows $\mathcal{E}_b \to 0$, as $\Delta\tau \to 0$. However, as typically required for showing consistency, one would need to ensure $\frac{\mathcal{E}_b}{\Delta\tau} \to 0$ as $\Delta\tau \to 0$. Therefore, from (5.8), we need $P^\dagger \to \infty$ and $Q^\dagger \to \infty$ as $\Delta\tau \to 0$, which can be achieved by letting $P^\dagger = C/\Delta\tau$ and $Q^\dagger = C'/\Delta\tau$, for finite $C > 0$ and $C' > 0$.

2. The next error arises in approximating the Green's function $g(w, r, \Delta\tau)$ by its localized, periodic approximation $\hat{g}(w, r, \Delta\tau)$ defined in (4.42). We denote this error by $\mathcal{E}_{\hat{g}}$. While $\hat{g}(w, r, \Delta\tau) \neq g(w, r, \Delta\tau)$ for $(w, r) \in \mathbf{D}$. Nonetheless, if $P^\dagger = C_5/\Delta\tau$ and $Q^\dagger = C_5'/\Delta\tau$ as discussed above, then, as $\Delta\tau \to 0$, we have

$$\hat{g}(w, r, \Delta\tau) \overset{\text{(i)}}{=} \iint_{\mathbb{R}^2} e^{2\pi i\eta w} e^{2\pi i\xi r} G(\eta, \xi, \Delta\tau) d\eta d\xi + \mathcal{O}\left(1/\left(P^\dagger \wedge Q^\dagger\right)^2\right) \overset{\text{(ii)}}{=} g(w, r, \Delta\tau) + \mathcal{O}(\Delta\tau^2).$$

   Here, (i) is due to $P^\dagger \to \infty$ and $Q^\dagger \to \infty$ as $\Delta \to 0$, ensuring in an $\mathcal{O}\left(1/\left(P^\dagger \wedge Q^\dagger\right)^2\right) \sim \mathcal{O}((\Delta\tau)^2)$ error for the traperzoidal rule approximation of the integral, and (ii) is due to that $G(\cdot)$ is the Fourier transform of $g(\cdot)$. Therefore, $\mathcal{E}_{\hat{g}} = \mathcal{O}(\Delta\tau^2)$ as $\Delta\tau \to 0$.

3. Truncating $\tilde{g}_{n-l}(\infty)$, defined in (4.43), to to $\tilde{g}_{n-l}(\alpha)$, for a finite $\alpha \in \{2,4,8,\ldots\}$, in (4.45), gives rise to a Fourier series truncation error, denote by $\mathcal{E}_f$. As shown in Appendix A, as $\Delta\tau$, Δw and $\Delta r \to 0$, this error is

$$\mathcal{E}_f = \mathcal{O}\left(e^{-\frac{\Delta\tau}{(\Delta w)^2}}/(\Delta w \wedge \Delta r)^2\right) + \mathcal{O}\left(e^{-\frac{\Delta\tau}{(\Delta r)^2}}/(\Delta w \wedge \Delta r)^2\right), \quad \text{as } \Delta\tau,\ \Delta w,\ \Delta r \to 0.$$

4. Approximating a function in $\mathcal{G}(\Omega^\infty) \cap \mathcal{C}^\infty(\Omega^\infty)$ by its projection on the piecewise linear basis functions $\varphi_l(\cdot)$ and $\psi_d(\cdot)$, $l \in \mathbb{N}^\dagger$ ad $d \in \mathbb{K}^\dagger$, as in (4.36), as well as by linear interpolation, as in Remark (4.1), gives rise to a projection/interpolation error, collectively denoted by $\mathcal{E}_o$. Generally $\mathcal{E}_o = \mathcal{O}\left(\max(\Delta w, \Delta r, \Delta a)^2\right)$, as $\Delta w, \Delta r, \Delta a \to 0$.

Motivated by the above discussions, for convergence analysis, we make an assumption about the discretization parameter.

Assumption 5.1. *We assume that there is a discretization parameter h such that*

$$\Delta w = C_1 h, \quad \Delta r = C_2 h, \quad \Delta a_{\max} = C_3 h, \quad \Delta a_{\min} = C_3' h,$$
$$\Delta\tau = C_4 h, \quad P^\dagger = C_5/h, \quad Q^\dagger = C_5'/h, \tag{5.8}$$

where the positive constants C_1, C_2, C_3, C_3', C_4, C_5 and C_5' are independent of h.

Under Assumption 5.1, it is straightforward to obtain

$$\mathcal{E}_b = \mathcal{O}(he^{-\frac{1}{h}}), \quad \mathcal{E}_{\hat{g}} = \mathcal{O}(h^2), \quad \mathcal{E}_f = \mathcal{O}(e^{-\frac{1}{h}}/h^2), \quad \mathcal{E}_o = \mathcal{O}(h^2). \tag{5.9}$$

It is also straightforward to ensure the theoretical requirement $P^\dagger, Q^\dagger \to \infty$ as $h \to 0$. For example, with $C_5 = C_5' = 1$ in (5.8), we can quadruple $N^\dagger$ and $K^\dagger$ as we halve h. We emphasize that, for practical purposes, if $P^\dagger$ and $Q^\dagger$ are chosen sufficiently large, both can be kept constant for all $\Delta\tau$ refinement levels (as we let $\Delta\tau \to 0$). The effectiveness of this practical approach is demonstrated through numerical experiments in Section 6. Also see relevant discussions in [57].

To show convergence of the numerical scheme to the viscosity solution, our starting point is discrete convolutions of the form (4.38) which typically involve a generic function $\varphi \in \mathcal{G}(\Omega^\infty)$. There are two cases: (i) φ is not necessarily smooth, which corresponds to the SL discretization or non-local impulses, and (ii) φ is a test function in $\mathcal{G}(\Omega^\infty) \cap \mathcal{C}^\infty(\Omega^\infty)$, which corresponds to local impulses. In subsequent discussions, we present results relevant to these two cases in Lemma 5.2 below. For differential and jump operators, we use the notation $[\cdot]_{n,k,j}^m := [\cdot](\mathbf{x}_{n,k,j}^m)$.

Lemma 5.2. *Suppose the discretization parameter h satisfies Assumption 5.1. Let ϕ and χ be in $\mathcal{G}(\Omega^\infty) \cap \mathcal{C}^\infty(\Omega^\infty)$ and $\mathcal{G}(\Omega^\infty)$, respectively. For $\mathbf{x}_{n,k,j}^m$, $n \in \mathbb{N}$, $j \in \mathbb{J}$, $k \in \mathbb{K}$, $m \in \{0,\ldots,M\}$, we have*

$$\Delta w \Delta r \sum_{l\in\mathbb{N}^\dagger}^{d\in\mathbb{K}^\dagger} {}^{*}\, \tilde{g}_{n-l,k-d}\ \phi_{l,d,j}^m = \phi_{n,k,j}^m + \Delta\tau \left[\mathcal{L}_g\phi + \mathcal{J}\phi\right]_{n,k,j}^m + \mathcal{O}(h^2), \tag{5.10}$$

$$\Delta w \Delta r \sum_{l\in\mathbb{N}^\dagger}^{d\in\mathbb{K}^\dagger} {}^{*}\, \tilde{g}_{n-l,k-d}\ \chi_{l,d,j}^m = \chi_{n,k,j}^m + \mathcal{O}(h^2) + \mathcal{E}_\chi(\mathbf{x}_{n,k,j}^m, h),\ \text{where } \mathcal{E}_\chi(\mathbf{x}_{n,k,j}^m, h) \to 0 \text{ as } h \to 0. \tag{5.11}$$

Proof of Lemma 5.2. Lemma 5.2 can be proved using similar techniques in [57][Lemmas 5.3 and 5.4] for the one-dimensional Greens' function case. For completeness, we provide the key steps below. We let $a = a_j$ and $\tau{=}\tau_m$ be fixed, and with a slight abuse of notation, we view ϕ and χ as functions of (w,r). Let $\xi \in \{\phi, \chi\}$. Starting from the discrete convolutions on the left-hand-side of (5.10)-(5.11), we need to recover an associated convolution integrals of the form (4.5) which is posed on an infinite integration region. Since $\xi \in \{\chi, \phi\}$ is not necessarily in $L^1(R^2)$, standard mollification techniques can be used to obtain $\xi' \in L^1(R^2)$ which agrees with ξ on $\mathbf{D}^\dagger$. Then, with $\xi \in \{\phi, \chi\}$, using error analysis, we have

$$\Delta w \Delta r \sum_{l\in\mathbb{N}^\dagger}^{d\in\mathbb{K}^\dagger} {}^{*}\, \tilde{g}_{n-l,k-d}\ \xi_{l,d,j}^m = \iint_{R^2} \xi''(w,r) g(w_n - w, r_k - r, \Delta\tau)\, dw\, dr + \mathcal{E}_b + \mathcal{E}_{\hat{g}} + \mathcal{E}_f + \mathcal{E}_o. \tag{5.12}$$

where ξ'' is a projection of ξ' onto the piecewise linear basis functions $\varphi_l(\cdot)$ and $\psi_d(\cdot)$, $l \in \mathbb{N}^\dagger$ ad $d \in \mathbb{K}^\dagger$. By Assumption 5.1 and (5.9), $\mathcal{E}_b + \mathcal{E}_{\hat{g}} + \mathcal{E}_f + \mathcal{E}_o = \mathcal{O}(h^2)$.

For $\xi = \phi$, and since ϕ is smooth, we then apply the Fourier Transform and inverse Fourier Transform to $\iint_{R^2} \xi''(w,r) g(w_n - w, r_k - r, \Delta\tau) dw dr$ in (5.12) to recover the differential and jump operators.

For $\xi = \chi$ which is not smooth, we write the convolution integral in (5.12) as

$$\iint_{R^2} \chi''(w,r) g(w_n - w, r_k - r, \Delta\tau) = \chi''(w_n, r_k) + \iint_{\mathbb{R}^2} g(w_n - w, r_k - r, \Delta\tau) \left(\chi''(w,r) - \chi''(w_n, r_k)\right) \, dw dr.$$

Note that $\chi''(w_n, r_k) = \chi_{l,d,j}^m$, and letting $\mathcal{E}_\chi(\mathbf{x}_{n,k,j}^m, h) = \iint_{\mathbb{R}^2} (\cdot) dw dr$ gives (5.11), due to the "cancelation properties" of the Green's function [36, 31]. This concludes the proof. □

We now consider a special case of the discrete convolution (4.38) that involves interpolation of values of a smooth test function evaluated at the departure points of the SL trajectory presented in Subsection 4.5.1. Specifically, given $\phi \in \mathcal{G}(\Omega^\infty) \cap \mathcal{C}^\infty(\Omega^\infty)$, for $\mathbf{x}_{l,d,q}^{m+1} \in \Omega$, $0 < \tau_{m+1} \le T$, we define discrete values $(\phi_{\text{SL}})_{l,d,q}^m$ as follows

$$(\phi_{\text{SL}})_{l,d,q}^m = \begin{cases} \mathcal{I}\{\phi^m\}(\breve{w}_l, \breve{r}_d, a_q)(1 + \Delta\tau r_d)^{-1} & \mathbf{x}_{l,d,q}^{m+1} \in \Omega_{\text{in}} \cup \Omega_{a_{\min}}, \\ \phi_{l,d,q}^m & \text{otherwise.} \end{cases} \tag{5.13}$$

Here, as described in Remark 4.1, $\mathcal{I}\{\phi^m\}(\cdot)$ is the linear interpolation operator acting on discrete data $\left\{(w_l, r_d, a_q), \phi_{l,d,q}^m\right\}$ and $(\breve{w}_l, \breve{r}_d)$ is given by (4.34), while a_q is fixed.

Lemma 5.3. *Let $\phi \in \mathcal{G}(\Omega^\infty) \cap \mathcal{C}^\infty(\Omega^\infty)$ and $\{(w_l, r_d, a_q), (\phi_{SL})_{l,d,q}^m\}$ be given by (5.13). For any fixed $\mathbf{x}_{n,k,j}^m \in \Omega_{in} \cup \Omega_{a_{\min}}$, i.e. $n \in \mathbb{N}$, $j \in \mathbb{J}$, $k \in \mathbb{K}$, and $m \in \{1, \ldots, M\}$, we have*

$$\Delta w \Delta r \sum_{l \in \mathbb{N}^\dagger}^{d \in \mathbb{K}^\dagger} {}^{*} \, \tilde{g}_{n-l,k-d} \, (\phi_{\text{SL}})_{l,d,j}^m = \phi_{n,k,j}^m + \Delta\tau \left[\mathcal{L}\phi + \mathcal{J}\phi\right]_{n,k,j}^m + \mathcal{O}(h^2) + \Delta\tau \mathcal{E}(\mathbf{x}_{n,k,j}^m, h). \tag{5.14}$$

Here, $\tilde{g}_{n-l,k-d}$ is given by (4.45), $\mathcal{L}$ and $\mathcal{J}$ are defined in (3.2), and $\mathcal{E}(\mathbf{x}_{n,k,j}^{m+1}, h) \to 0$ as $h \to 0$..

Proof of Lemma 5.3. We let $j \in \mathbb{J}$ be fixed in this proof. We start by investigating the interpolation result $\mathcal{I}\{\phi^m\}(\breve{w}_l, \breve{r}_d, a_j)$ for $\mathbf{x}_{l,d,j}^m \in \Omega_{\text{in}} \cup \Omega_{a_{\min}}$ in (5.13). Remark 4.1

$$\begin{aligned} \mathcal{I}\{\phi^m\}(\breve{w}_l, \breve{r}_d, a_j) &\overset{(i)}{=} \phi(\breve{w}_l, \breve{r}_d, a_j, \tau_m) + \mathcal{O}(h^2) \\ &\overset{(ii)}{=} \phi_{l,d,j}^m + \Delta\tau \left[(r_d - \frac{\sigma_z^2}{2} - \beta)(\phi_w)_{l,d,j}^m + \delta(\theta - r_d)(\phi_r)_{l,d,j}^m \right] + \mathcal{O}(h^2) \\ &= \phi_{l,d,j}^m + \Delta\tau \left[\mathcal{L}_s \phi\right]_{l,d,j}^m + \mathcal{O}(h^2). \end{aligned} \tag{5.15}$$

Here, (i) follows from Remark 4.1[equation (4.16)], noting $\phi \in \mathcal{C}^\infty(\Omega^\infty)$; in (ii), we apply a Taylor series to expand the term $\phi(\breve{w}_l, \breve{r}_d, a_j, \tau_m)$ about the point (w_l, r_d, a_j, τ_m), and then use $e^{\Delta\tau} = 1 + \Delta\tau + \mathcal{O}(h^2)$ and $e^{-\delta\Delta\tau} = 1 - \delta\Delta\tau + \mathcal{O}(h^2)$. We note that, for $\mathbf{x}_{l,d,q}^m \in \Omega_{\text{in}} \cup \Omega_{a_{\min}}$, we have

$$(1 + \Delta\tau r_d)^{-1} = 1 - \Delta\tau r_d + \mathcal{O}\left((\Delta\tau)^2\right), \quad r_d \in [r_{\min}, r_{\max}]. \tag{5.16}$$

Using (5.16) and (5.15), we arrive at

$$\mathcal{I}\{\phi^m\}(\breve{w}_l, \breve{r}_d, a_j)(1 + \Delta\tau r_d)^{-1} = \phi_{l,d,j}^m + \Delta\tau \left[\mathcal{L}_s\phi - r\phi\right]_{l,d,j}^m + \mathcal{O}(h^2), \quad \mathbf{x}_{l,d,j}^m \in \Omega_{\text{in}} \cup \Omega_{a_{\min}}. \tag{5.17}$$

Next, letting $\mathbf{x}' = (w', a', r', \tau')$, we define a function $\psi(\mathbf{x}') : \Omega^\infty \to \mathbb{R}$ by

$$\psi(\mathbf{x}') = \begin{cases} (r' - \frac{\sigma_z^2}{2} - \beta)\phi_w(\mathbf{x}') + \delta(\theta - r')\phi_r(\mathbf{x}') - r'\phi(\mathbf{x}'), & \mathbf{x}' \in \Omega_{\text{in}} \cup \Omega_{a_{\min}}, \\ 0 & \text{otherwise.} \end{cases} \tag{5.18}$$

Note that $\psi \in \mathcal{G}(\Omega^\infty)$, and that $\psi_{l,d,j}^m = [\mathcal{L}_s\phi - r\phi]_{l,d,j}^m$ for $\mathbf{x}_{l,d,j}^m \in \Omega_{\text{in}} \cup \Omega_{a_{\min}}$. Now, we consider the discrete convolution on the rhs of (5.14): $\Delta w \Delta r \sum_{l\in\mathbb{N}^\dagger}^{d\in\mathbb{K}^\dagger} {}^{*}\, \tilde{g}_{n-l,k-d}\ (\phi_{\text{SL}})_{l,d,j}^m = \ldots$

$$
\begin{aligned}
\ldots &\overset{(i)}{=} \Delta w \Delta r \sum_{l\in\mathbb{N}^\dagger}^{d\in\mathbb{K}^\dagger} {}^{*}\, \tilde{g}_{n-l,k-d}\ \phi_{l,d,j}^m + \Delta\tau\big(\Delta w \Delta r \sum_{l\in\mathbb{N}^\dagger}^{d\in\mathbb{K}^\dagger} {}^{*}\, \tilde{g}_{n-l,k-d}\ \psi_{l,d,j}^m\big) + \mathcal{O}(h^2)\\
&\overset{(ii)}{=} \phi_{n,k,j}^m + \Delta\tau\, [\mathcal{L}_g\phi + \mathcal{J}\phi]_{n,k,j}^m + \Delta\tau\, [\mathcal{L}_s\phi - r\phi]_{n,k,j}^m + \Delta\tau\mathcal{E}(\mathbf{x}_{n,k,j}^m, h) + \mathcal{O}(h^2)\\
&\overset{(iii)}{=} \phi_{n,k,j}^m + \Delta\tau\, [\mathcal{L}\phi + \mathcal{J}\phi]_{n,k,j}^m + \mathcal{O}(h^2) + \Delta\tau\mathcal{E}(\mathbf{x}_{n,k,j}^m, h).
\end{aligned}
$$

Here, (i) is due to the definition of $(\phi_{\text{SL}})_{l,d,j}^m$ given in (5.13), together with (5.17)-(5.18), and Proposition 5.1 to get $\mathcal{O}(h^2)$. In (ii), we use Lemma 5.2[equation (5.11)] on the discrete convolution involving $\psi_{l,d,j}^m$, noting its definition (5.18) and $\mathcal{E}(\mathbf{x}_{n,k,j}^m, h) \to 0$ as $h \to 0$; and in (iii), we use $\mathcal{L}\phi = \mathcal{L}_g\phi + \mathcal{L}_s\phi - r\phi$. This concludes the proof. □

5.3 Consistency

While equations (4.17), (4.18), (4.19), (4.22), and (4.40) are convenient for computation, they are not in a form amendable for analysis. For purposes of proving consistency, it is more convenient to rewrite them in a single equation. To this end, we recall that we partition $[0, a_j]$ into $[0, a_j \wedge C_r\Delta\tau]$ and $(C_r\Delta\tau, a_j]$, with the convention that $(C_r\Delta\tau, a_j] = \emptyset$ if $a_j \leq C_r\Delta\tau$. Subsequently in this subsection, the aforementioned partition of $[0, a_j]$ is used to write (4.17), (4.18), (4.19), (4.22), and (4.40) into an equivalent single equation convenient for analysis. Unless noted otherwise, in the following, let $j \in \mathbb{J}$ and $m \in \mathbb{M}$ be fixed.

For $(w_n, r_k, a_j, \tau_{m+1}) \in \Omega_{w_{\min}} \cup \Omega_{wa_{\min}}$, i.e. $n \in \mathbb{N}_{\min}^{\text{c}}$ and $k \in \mathbb{K}$, we define the following operators: $\mathcal{A}_{n,k,j}^{m+1}\left(h, v_{n,k,j}^{m+1}, \left\{v_{l,d,p}^m\right\}_{p\leq j}\right) \equiv \mathcal{A}_{n,k,j}^{m+1}(\cdot)$ and $\mathcal{B}_{n,k,j}^{m+1}\left(h, v_{n,k,j}^{m+1}, \left\{v_{l,d,p}^m\right\}_{p\leq j}\right) \equiv \mathcal{B}_{n,k,j}^{m+1}(\cdot)$, where

$$
\begin{aligned}
\mathcal{A}_{n,k,j}^{m+1}(\cdot) &= \frac{1}{\Delta\tau}\left[v_{n,k,j}^{m+1} - \sup_{\gamma_{n,k,j}^m \in [0, a_j \wedge C_r\Delta\tau]} \left(\tilde{v}_{n,k,j}^m + f\left(\gamma_{n,k,j}^m\right)\right) + \Delta\tau(\mathcal{L}_d^h v)_{n,k,j}^{m+1}\right],\\
\mathcal{B}_{n,k,j}^{m+1}(\cdot) &= v_{n,k,j}^{m+1} - \sup_{\gamma_{n,k,j}^m \in (C_r\Delta\tau, a_j]} \left(\tilde{v}_{n,k,j}^m + f\left(\gamma_{n,k,j}^m\right)\right) + \Delta\tau(\mathcal{L}_d^h v)_{n,k,j}^{m+1},
\end{aligned} \tag{5.19}
$$

where $\tilde{v}_{n,k,j}^m$, $n \in \mathbb{N}_{\min}^{\text{c}}$ and $k \in \mathbb{K}$, is given in (4.20), and $f(\cdot)$ is defined in (4.14).

For $(w_n, r_k, a_j, \tau_{m+1}) \in \Omega_{\text{in}} \cup \Omega_{a_{\min}}$, i.e. $n \in \mathbb{N}$ and $k \in \mathbb{K}$, we define the following operators: $\mathcal{C}_{n,k,j}^{m+1}\left(h, v_{n,k,j}^{m+1}, \left\{v_{l,d,p}^m\right\}_{p\leq j}\right) \equiv \mathcal{C}_{n,k,j}^{m+1}(\cdot)$ and $\mathcal{D}_{n,k,j}^{m+1}\left(h, v_{n,k,j}^{m+1}, \left\{v_{l,d,p}^m\right\}_{p\leq j}\right) \equiv \mathcal{D}_{n,k,j}^{m+1}(\cdot)$, where

$$
\begin{aligned}
\mathcal{C}_{n,k,j}^{m+1}(\cdot) &= \frac{1}{\Delta\tau}\left[v_{n,k,j}^{m+1} - \Delta w \Delta r \sum_{l\in\mathbb{N}}^{d\in\mathbb{K}} {}^{*}\, \tilde{g}_{n-l,k-d}\ \left(v_{\text{SL}}^{(1)}\right)_{l,d,j}^{m+} - \Delta w \Delta r \sum_{l\in\mathbb{N}^{\text{c}}}^{d\in\mathbb{K}^{\text{c}}} {}^{*}\, \tilde{g}_{n-l,k-d}\ v_{l,d,j}^m\right],\\
\mathcal{D}_{n,k,j}^{m+1}(\cdot) &= v_{n,k,j}^{m+1} - \Delta w \Delta r \sum_{l\in\mathbb{N}}^{d\in\mathbb{K}} {}^{*}\, \tilde{g}_{n-l,k-d}\left(v_{\text{SL}}^{(2)}\right)_{l,d,j}^{m+} - \Delta w \Delta r \sum_{l\in\mathbb{N}^{\text{c}}}^{d\in\mathbb{K}^{\text{c}}} {}^{*}\, \tilde{g}_{n-l,k-d}\ v_{l,d,j}^m.
\end{aligned} \tag{5.20}
$$

Here, for $(i) \in \{(1), (2)\}$, $\left(v_{\text{SL}}^{(i)}\right)_{l,d,j}^{m+} = \frac{\mathcal{I}\left\{(v^{(i)})^{m+}\right\}(\breve{w}_l, \breve{r}_d, a_j)}{1+\Delta\tau r_d}$, $l \in \mathbb{N}$ and $d \in \mathbb{K}$, are defined in (4.34), and $\mathcal{I}\{(v^{(i)})^{m+}\}$, a linear operator discussed in Remark 4.1.

In order to show local consistency, we split the sub-domains Ω_{in} and $\Omega_{w_{\min}}$ as follows: $\Omega_{\text{in}} = \Omega_{\text{in}}^{L} \cup \Omega_{\text{in}}^{U}$ and $\Omega_{w_{\min}} = \Omega_{w_{\min}}^{L} \cup \Omega_{w_{\min}}^{U}$, where

$$
\begin{aligned}
\Omega_{\text{in}}^{L} &= (w_{\min}, w_{\max}) \times (r_{\min}, r_{\max}) \times (a_{\min}, C_r\Delta\tau] \times (0, T],\\
\Omega_{\text{in}}^{U} &= (w_{\min}, w_{\max}) \times (r_{\min}, r_{\max}) \times (C_r\Delta\tau, a_{\max}] \times (0, T],\\
\Omega_{w_{\min}}^{L} &= [w_{\min}^{\dagger}, w_{\min}] \times (r_{\min}, r_{\max}) \times (a_{\min}, C_r\Delta\tau] \times (0, T],\\
\Omega_{w_{\min}}^{U} &= [w_{\min}^{\dagger}, w_{\min}] \times (r_{\min}, r_{\max}) \times (C_r\Delta\tau, a_{\max}] \times (0, T].
\end{aligned} \tag{5.21}
$$

Using $\mathcal{A}_{n,k,j}^{m+1}(\cdot)$, $\mathcal{B}_{n,k,j}^{m+1}(\cdot)$, $\mathcal{C}_{n,k,j}^{m+1}(\cdot)$ and $\mathcal{D}_{n,k,j}^{m+1}(\cdot)$ defined (5.19)-(5.3), our scheme at the reference node $\mathbf{x} = (w_n, r_k, a_j, \tau_{m+1})$ can be rewritten in an equivalent form as follows

$$0 = \mathcal{H}_{n,k,j}^{m+1}\left(h, v_{n,k,j}^{m+1}, \{v_{l,d,p}^{m}\}_{p\le j}\right) \equiv \begin{cases} \mathcal{A}_{n,k,j}^{m+1}(\cdot) & \mathbf{x} \in \Omega_{w_{\min}}^{L} \cup \Omega_{wa_{\min}}, \\ \min\left\{\mathcal{A}_{n,k,j}^{m+1}(\cdot), \mathcal{B}_{n,k,j}^{m+1}(\cdot)\right\} & \mathbf{x} \in \Omega_{w_{\min}}^{U}, \\ \mathcal{C}_{n,k,j}^{m+1}(\cdot) & \mathbf{x} \in \Omega_{\rm in}^{L} \cup \Omega_{a_{\min}}, \\ \min\left\{\mathcal{C}_{n,k,j}^{m+1}(\cdot), \mathcal{D}_{n,k,j}^{m+1}(\cdot)\right\} & \mathbf{x} \in \Omega_{\rm in}^{U}, \\ v_{n,k,j}^{m+1} - e^{-\beta\tau_{m+1}} e^{w_n} & \mathbf{x} \in \Omega_{w_{\max}}, \\ v_{n,k,j}^{m+1} - \max(e^{w_n}, (1-\mu)a_j - c) & \mathbf{x} \in \Omega_{\tau_0}, \\ v_{n,k,j}^{m} - p(w_n, r_k, a_j, \tau_m) & \mathbf{x} \in \Omega_{\rm c}, \end{cases} \tag{5.22}$$

where the sub-domains are defined in (3.3) and (5.21).

To demonstrate the consistency in viscosity sense of (5.22), we need some intermediate results on local consistency of our scheme. To this end, motivated by the aforementioned partitioning of $[0, a_j]$, we define operators $F_{\rm in'}$ and $F_{w'_{\min}}$, respectively associated with $F_{\rm in}$ and $F_{w_{\min}}$, for the case $0 \le a_j \le C_r\Delta\tau$, i.e. $0 \le a/\Delta\tau \le C_r$, as follows

$$\begin{aligned} F_{\rm in'}(\mathbf{x}, v) &= v_\tau - \mathcal{L}v - \mathcal{J}v - \sup_{\hat{\gamma}\in[0,a/\Delta\tau]} \hat{\gamma}\left(1 - e^{-w}v_w - v_a\right)\mathbf{1}_{\{a>0\}}, \quad 0 \le a/\Delta\tau \le C_r, \\ F_{w'_{\min}}(\mathbf{x}, v) &= v_\tau - \mathcal{L}_d v - \sup_{\hat{\gamma}\in[0,a/\Delta\tau]} \hat{\gamma}\left(1 - v_a\right)\mathbf{1}_{\{a>0\}}, \quad 0 \le a/\Delta\tau \le C_r. \end{aligned} \tag{5.23}$$

Below, we state the key supporting lemma related to local consistency of scheme (5.22).

Lemma 5.4 (Local consistency). *Suppose that (i) the discretization parameter h satisfies Assumption 5.1, (ii) linear interpolation in* (4.20), (4.34), *and* (4.24) *is used, and (iii)* $w_{\min}$ *satisfies*

$$e^{w_{\min}} - e^{w_{\min}^{\dagger}} \ge C_r\Delta\tau. \tag{5.24}$$

Then, for any function $\phi \in \mathcal{G}(\Omega^\infty) \cap \mathcal{C}^\infty(\Omega^\infty)$, with $\phi_{n,k,j}^{m} = \phi\left(\mathbf{x}_{n,k,j}^{m}\right)$ and $\mathbf{x} = (w_n, r_k, a_j, \tau_{m+1})$, and for a sufficiently small h, we have

$$\mathcal{H}_{n,k,j}^{m+1}\left(h, \phi_{n,k,j}^{m+1} + \xi, \{\phi_{l,d,p}^{m} + \xi\}_{p\le j}\right) = \begin{cases} F_{in}(\cdot,\cdot) & + c(\mathbf{x})\xi + \mathcal{O}(h) + \mathcal{E}(\mathbf{x}_{n,k,j}^{m}, h) & \mathbf{x} \in \Omega_{in}^{U}; \\ F_{in'}(\cdot,\cdot) & + c(\mathbf{x})\xi + \mathcal{O}(h) + \mathcal{E}(\mathbf{x}_{n,k,j}^{m}, h) & \mathbf{x} \in \Omega_{in}^{L}; \\ F_{a_{\min}}(\cdot,\cdot) & + c(\mathbf{x})\xi + \mathcal{O}(h) & \mathbf{x} \in \Omega_{a_{\min}} \\ F_{w_{\min}}(\cdot,\cdot) & + c(\mathbf{x})\xi + \mathcal{O}(h) & \mathbf{x} \in \Omega_{w_{\min}}^{U}; \\ F_{w'_{\min}}(\cdot,\cdot) & + c(\mathbf{x})\xi + \mathcal{O}(h) & \mathbf{x} \in \Omega_{w_{\min}}^{L}; \\ F_{wa_{\min}}(\cdot,\cdot) & + c(\mathbf{x})\xi + \mathcal{O}(h) & \mathbf{x} \in \Omega_{wa_{\min}}; \\ F_{w_{\max}}(\cdot,\cdot) & + c(\mathbf{x})\xi & \mathbf{x} \in \Omega_{w_{\max}}; \\ F_{\tau_0}(\cdot,\cdot) & + c(\mathbf{x})\xi & \mathbf{x} \in \Omega_{\tau_0}; \\ F_{c}(\cdot,\cdot) & + c(\mathbf{x})\xi & \mathbf{x} \in \Omega_{c}. \end{cases} \tag{5.25}$$

Here, ξ is a constant and $c(\cdot)$ is a bounded function satisfying $|c(\mathbf{x})| \le \max(|r_{\min}|, r_{\max}, 1)$ for all $\mathbf{x} \in \Omega$, and $\mathcal{E}(\mathbf{x}_{n,k,j}^{m}, h) \to 0$ as $h \to 0$. The operators $F_{in}(\cdot,\cdot)$, $F_{a_{\min}}(\cdot,\cdot)$, $F_{w_{\min}}(\cdot,\cdot)$, $F_{wa_{\min}}(\cdot,\cdot)$, $F_{w_{\max}}(\cdot,\cdot)$ $F_{\tau_0}(\cdot,\cdot)$, $F_{c}(\cdot,\cdot)$, defined in (3.11)-(3.16), *as well as $F_{in'}$ and $F_{w'_{\min}}$ defined in* (5.23), *are function of* $(\mathbf{x}, \phi(\mathbf{x}))$.

Proof of Lemma 5.4. Since $\phi \in \mathcal{C}^\infty(\Omega^\infty)$ and the computational domain Ω is bounded, ϕ has continuous and bounded derivatives of up to second-order in Ω. Given the smooth test function ϕ, with $j \in \mathbb{J}$ and $m \in \mathbb{M}$ being fixed and $(i) \in \{(1), (2)\}$, we define discrete values $(\phi^{(i)})_{l,d,j}^{m+}$, $l \in \mathbb{N}^\dagger$ and $d \in \mathbb{K}^\dagger$, as follows

$$\begin{aligned} &l \in \mathbb{N} \text{ and } d \in \mathbb{K}: \quad (\phi^{(1)})_{l,d,j}^{m+} = \sup_{\gamma_{l,d,j}^{m}\in[0,C_r\Delta\tau]} \tilde{\phi}_{l,d,j}^{m} + f(\gamma_{l,d,j}^{m}), \; (\phi^{(2)})_{l,d,j}^{m+} = \sup_{\gamma_{l,d,j}^{m}\in(C_r\Delta\tau,a_j]} \tilde{\phi}_{l,d,j}^{m} + f(\gamma_{l,d,j}^{m}), \\ &l \in \mathbb{N}^{c} \text{ or } d \in \mathbb{K}^{c}: \quad (\phi^{(1)})_{l,d,j}^{m+} = (\phi^{(2)})_{l,d,j}^{m+} = \phi_{l,d,j}^{m} + \xi, \end{aligned} \tag{5.26}$$

where $\tilde{\phi}_{l,d,j}^m$ is given by

$$\tilde{\phi}_{l,d,j}^m = \mathcal{I}\{\phi^m + \xi\}(\tilde{w}_l, r_d, \tilde{a}_j),\ \tilde{w}_l = \ln(\max(e^{w_l} - \gamma_{l,d,j}^m, e^{w_{\min}^\dagger})),\ \tilde{a}_j = a_j - \gamma_{l,d,j}^m. \tag{5.27}$$

Given the discrete data $\left\{\left(\left(w_l, r_d, a_j\right), (\phi^{(i)})_{l,d,j}^{m+}\right)\right\}$, $(i) \in \{(1),(2)\}$, where $(\phi^{(i)})_{l,d,j}^{m+}$, is given in (5.26)-(5.27), we define associated discrete values $(\phi_{\text{SL}}^{(i)})_{l,d,j}^m$ as follows

$$(\phi_{\text{SL}}^{(i)})_{l,d,j}^{m+} = \begin{cases} \mathcal{I}\left\{(\phi^{(i)})^{m+}\right\}(\breve{w}_l, \breve{r}_d, a_j)(1+\Delta\tau r_d)^{-1} & l \in \mathbb{N} \text{ and } d \in \mathbb{K} \quad (5.28\text{a}) \\ \phi_{l,d,j}^m + \xi & \text{otherwise,} \quad (5.28\text{b}) \end{cases}$$

where the departure point $(\breve{w}_l, \breve{r}_d)$ of an SL trajectory are defined in (4.34).

We now show that the first equation of (5.25) holds, that is, for $\mathbf{x} = (w_n, r_k, a_j, \tau_{m+1})$,

$$\mathcal{H}_{n,k,j}^{m+1}(\cdot) = \min\left\{\mathcal{C}_{n,k,j}^{m+1}(\cdot), \mathcal{D}_{n,k,j}^{m+1}(\cdot)\right\} = F_{\text{in}}(\mathbf{x}, \phi(\mathbf{x})) + c(\mathbf{x})\xi + \mathcal{O}(h) + \mathcal{E}(\mathbf{x}_{n,k,j}^m, h)$$
$$\text{if } w_{\min} < w_n < w_{\max},\ r_{\min} < r_k < r_{\max}, C_r\Delta\tau < a_j \le a_J,\ 0 < \tau_{m+1} \le T,$$

where operators $\mathcal{C}_{n,k,j}^{m+1}(\cdot)$ and $\mathcal{D}_{n,k,j}^{m+1}(\cdot)$ are defined in (5.3). First, we consider operator $\mathcal{C}_{n,k,j}^{m+1}(\cdot)$ which can be written as

$$\mathcal{C}_{n,k,j}^{m+1}(\cdot) = \frac{1}{\Delta\tau}\left[\phi_{n,k,j}^{m+1} + \xi - \Delta w \Delta r \sum_{l\in\mathbb{N}^\dagger}^{d\in\mathbb{K}^\dagger}{}^{*}\ \tilde{g}_{n-l,k-d}\ (\phi_{\text{SL}}^{(1)})_{l,d,j}^{m+}\right], \tag{5.29}$$

where the discrete values $(\phi_{\text{SL}}^{(1)})_{l,d,j}^{m+}$ are defined in (5.28) with $(i) = (1)$.

The key challenge in (5.29) is the discrete convolution $\sum^* \tilde{g}\ (\phi_{\text{SL}}^{(1)})_{l,d,j}^{m+}$. Our approach is to decompose it into the sum of two simpler discrete convolutions of the forms $\sum^* \tilde{g}\ (\phi_{\text{SL}})_{l,d,j}^m$ and $\sum^* \tilde{g}\ (\varphi_{\text{SL}})_{l,d,j}^m$ for which Lemmas 5.3 and 5.2 are respectively applicable. Here, $(\phi_{\text{SL}})_{l,d,j}^m$ is given in (5.13) and $(\varphi_{\text{SL}})_{l,d,j}^m$ is to be defined subsequently. To this end, we will start with the interpolated values $\tilde{\phi}_{l,d,j}^m$ in (5.27).

For operator $\mathcal{C}_{n,k,j}^{m+1}(\cdot)$, the admissible control set is $\gamma_{l,d,j}^m \in [0, C_r\Delta\tau]$. In this case, condition (5.24) implies that, for $w_l \in (w_{\min}, w_{\max})$, $e^{w_l} - \gamma_{l,d,j}^m > e^{w_{\min}^\dagger}$ for all $\gamma_{l,d,j}^m \in [0, C_r\Delta\tau]$. Therefore, we can eliminate the $\max(\cdot)$ operator in the linear interpolation operator in (5.27) when $\gamma_{l,d,j}^m \in [0, C_r\Delta\tau]$. Consequently, when $\gamma_{l,d,j}^m \in [0, C_r\Delta\tau]$, using (5.26) and recalling the cash flow function $f(\cdot)$ defined in (4.14), we have

$$\tilde{\phi}_{l,d,j}^m + f\left(\gamma_{l,d,j}^m\right) \overset{\text{(i)}}{=} \phi\left(\ln\left(e^{w_l} - \gamma_{l,d,j}^m\right), a_j - \gamma_{l,d,j}^m, \tau_m\right) + \xi + \mathcal{O}\left(h^2\right) + \gamma_{l,d,j}^m$$
$$\overset{\text{(ii)}}{=} \phi_{l,d,j}^m + \xi + \gamma_{l,d,j}^m\left(1 - e^{-w_l}(\phi_w)_{l,d,j}^m - (\phi_a)_{l,d,j}^m\right) + \mathcal{O}\left(h^2\right). \tag{5.30}$$

Here, (i) follows from Remark 4.1[eqns (4.15) and (4.16)], and $f\left(\gamma_{l,d,j}^m\right) = \gamma_{l,d,j}^m$ as defined in (4.14); and in (ii), we apply a Taylor series to expand $\phi\left(\ln\left(e^{w_l} - \gamma_{l,d,j}^m\right), r_d, a_j - \gamma_{l,d,j}^m, \tau_m\right)$ about (w_l, r_d, a_j, τ_m), noting $\gamma_{l,d,j}^m = \mathcal{O}(\Delta\tau)$. Therefore, using (5.30), $\sup_{\gamma_{l,d,j}^m \in [0, C_r\Delta\tau]} \tilde{\phi}_{l,d,j}^m + f(\gamma_{l,d,j}^m) = \ldots$

$$\ldots = \phi_{l,d,j}^m + \xi + \mathcal{O}\left(h^2\right) + \sup_{\gamma_{l,d,j}^m \in [0, C_r\Delta\tau]} \gamma_{l,d,j}^m(1 - e^{-w_l}(\phi_w)_{l,d,j}^m - (\phi_a)_{l,d,j}^m)$$
$$\overset{\text{(i)}}{=} \phi_{l,d,j}^m + \xi + \mathcal{O}(h^2) + \Delta\tau \sup_{\hat{\gamma}_{l,d,j}^m \in [0, C_r]} \hat{\gamma}_{l,d,j}^m(1 - e^{-w_l}(\phi_w)_{l,d,j}^m - (\phi_a)_{l,d,j}^m). \tag{5.31}$$

Here, in (i) of (5.31), since the control $\gamma_{l,d,j}^m$ can be factored out completely from the objective function $\gamma_{l,d,j}^m(1 - e^{-w_l}(\phi_w)_{l,d,j}^m - (\phi_a)_{l,d,j}^m)$, we define a new control variable $\hat{\gamma}_{l,d,j}^m = \gamma_{l,d,j}^m/\Delta\tau$ where $\hat{\gamma}_{l,d,j}^m \in [0, C_r]$. We also note that, as a result of this change of control variable, there is a factor of $\Delta\tau$ in front of the term $\sup_{\hat{\gamma}_{l,d,j}^m \in [0, C_r]}(\cdot)$ in (i) of (5.31).

For subsequent use, letting $\mathbf{x}' = (w', r', a', \tau') \in \Omega^\infty$, we define a function $\varphi(\mathbf{x}')$ as follows

$$\varphi(\mathbf{x}') = \begin{cases} \sup\limits_{\hat{\gamma}\in[0,C_r]} \varphi'(\hat{\gamma}, \mathbf{x}'), & w_{\min} < w' < w_{\max},\ r_{\min} < r' < r_{\max}, \\ \quad \text{where } \varphi'(\hat{\gamma}, \mathbf{x}') = \hat{\gamma}(1 - e^{-w}\phi_w(\mathbf{x}') - \phi_a(\mathbf{x}')) & C_r\Delta\tau < a' \le a_J,\ 0 \le \tau' < T, \\ 0 & \text{otherwise.} \end{cases} \tag{5.32}$$

Using (5.31)-(5.32), and recalling from (5.26) that $(\phi^{(1)})^{m+}_{l,d,j} = \sup_{\gamma^m_{l,d,j}\in[0,C_r\Delta\tau]} \tilde{\phi}^m_{l,d,j} + f(\gamma^m_{l,d,j})$, we have

$$(\phi^{(1)})^{m+}_{l,d,j} = \phi^m_{l,d,j} + \xi + \Delta\tau\varphi^m_{l,d,j} + \mathcal{O}\left(h^2\right), \quad l \in \mathbb{N},\ d \in \mathbb{K}. \tag{5.33}$$

The decomposition formula (5.33) allows us to write $(\phi^{(1)}_{\text{SL}})^{m+}_{l,d,j}$, defined in (5.28), as follows

$$(\phi^{(1)}_{\text{SL}})^{m+}_{l,d,j} = (\phi_{\text{SL}})^m_{l,d,j} + (\varphi_{\text{SL}})^m_{l,d,j} + \mathcal{O}\left(h^2\right), \quad l \in \mathbb{N}^\dagger,\ d \in \mathbb{K}^\dagger, \tag{5.34}$$

where $(\phi_{\text{SL}})^m_{l,d,q}$ is given in (5.13) and $(\varphi_{\text{SL}})^m_{l,d,q}$ is given by

$$(\varphi_{\text{SL}})^m_{l,d,q} = \begin{cases} (\xi + \Delta\tau\mathcal{I}\{\varphi^m\}(\breve{w}_l, \breve{r}_d, a_j))(1 + \Delta\tau r_d)^{-1} & l \in \mathbb{N} \text{ and } d \in \mathbb{K}, \quad (5.35\text{a}) \\ \xi & \text{otherwise,} \quad (5.35\text{b}) \end{cases}$$

where φ is defined in (5.32). Using (5.34)-(5.35), we rewrite operator $\mathcal{C}^{m+1}_{n,k,j}(\cdot)$, previously given in (5.29), into a convenient form below

$$\mathcal{C}^{m+1}_{n,k,j}(\cdot) = \frac{1}{\Delta\tau}\left[\phi^{m+1}_{n,k,j} + \xi - \Delta w\Delta r \sum_{l\in\mathbb{N}^\dagger}^{d\in\mathbb{K}^\dagger}{}^{*} \tilde{g}_{n-l,k-d}\left((\phi_{\text{SL}})^m_{l,d,j} + (\varphi_{\text{SL}})^m_{l,d,j} + \mathcal{O}\left(h^2\right)\right)\right]. \tag{5.36}$$

From here, respectively applying Lemma 5.3 and Lemma 5.2[equation (5.11)] on discrete convolutions involving $(\phi_{\text{SL}})^m_{l,d,j}$ and $(\varphi_{\text{SL}})^m_{l,d,j}$ gives

$$\Delta w\Delta r \sum_{l\in\mathbb{N}^\dagger}^{d\in\mathbb{K}^\dagger}{}^{*} \tilde{g}_{n-l,k-d}\ (\phi_{\text{SL}})^m_{l,d,j} = \phi^m_{n,k,j} + \Delta\tau\left[\mathcal{L}\phi + \mathcal{J}\phi\right]^m_{n,k,j} + \mathcal{O}(h^2) + \Delta\tau\mathcal{E}_\phi(\mathbf{x}^m_{n,k,j}, h), \tag{5.37}$$

$$\Delta w\Delta r \sum_{l\in\mathbb{N}^\dagger}^{d\in\mathbb{K}^\dagger}{}^{*} \tilde{g}_{n-l,k-d}\ (\varphi_{\text{SL}})^m_{l,d,j} = (\varphi_{\text{SL}})^m_{n,k,j} + \mathcal{O}(h^2) + \Delta\tau\mathcal{E}_\varphi(\mathbf{x}^m_{n,k,j}, h), \tag{5.38}$$

where $\mathcal{E}_\phi(\mathbf{x}^m_{n,k,j}, h), \mathcal{E}_\varphi(\mathbf{x}^m_{n,k,j}, h) \to 0$ as $h \to 0$.

We now investigate the rhs of (5.38). By the definition of $(\varphi_{\text{SL}})^m_{n,k,j}$ in (5.35), and since linear interpolation is used, together with (5.16), we can further write the term $(\varphi_{\text{SL}})^m_{n,k,j}$ for the case (5.35a) as

$$\begin{aligned} (\xi + \Delta\tau\mathcal{I}\{\varphi^m\}(\breve{w}_n, \breve{r}_k, a_j))(1 + \Delta\tau r_k)^{-1} &= (\xi + \Delta\tau\mathcal{I}\{\varphi^m\}(\breve{w}_n, \breve{r}_k, a_j))(1 - \Delta\tau r_k) + \mathcal{O}(h^2) \\ &= \xi + \Delta\tau\mathcal{I}\{\varphi^m\}(\breve{w}_n, \breve{r}_k, a_j) - \Delta\tau\xi r_k + \mathcal{O}(h^2). \end{aligned} \tag{5.39}$$

Suppose that $w_{n'} \le \breve{w}_n \le w_{n'+1}$ and $r_{k'} \le \breve{r}_k \le r_{k'+1}$. Then, $\mathcal{I}\{\varphi^m\}(\breve{w}_n, \breve{r}_k, a_j)$ can be written into

$$\begin{aligned} \mathcal{I}\left\{\varphi^m\right\}(\breve{w}_n, \breve{r}_k, a_j) &\overset{(i)}{=} x_r(x_w\varphi^m_{n',k',j} + (1 - x_w)\varphi^m_{n'+1,k',j}) + (1 - x_r)(x_w\varphi^m_{n',k'+1,j} + (1 - x_w)\varphi^m_{n'+1,k'+1,j}), \\ &\overset{(ii)}{=} \left[\sup_{\hat{\gamma}\in[0,C_r]} \hat{\gamma}(1 - e^{-w}\phi_w - \phi_a)\right]^m_{n,k,j} + \mathcal{O}(h). \end{aligned} \tag{5.40}$$

Here, in (i), $0 \le x_r \le 1$ and $0 \le x_w \le 1$ are linear interpolation weights. For (ii), we replace $\{\varphi^m_{n',k',j}, \ldots, \varphi^m_{n'+1,k'+1,j}\}$ by $\varphi^m_{n,k,j}$, resulting in an overall error of size $\mathcal{O}(h)$. Specifically, as an example, replacing $\varphi^m_{n',k',j}$ by $\varphi^m_{n,k,j}$ gives rise to an error bounded as follows

$$|\varphi^m_{n,k,j} - \varphi^m_{n',k',j}| \le \sup_{\hat{\gamma}\in[0,C_r]} \hat{\gamma}|e^{-w_n}(\phi_w)^m_{n,k,j} - e^{-w_{n'}}(\phi_w)^m_{n',k',j} + (\phi_a)^m_{n',k',j}) - (\phi_a)^m_{n,k,j}| = \mathcal{O}(h), \tag{5.41}$$

due to smooth test function ϕ and boundedness of $\hat{\gamma} \in [0, C_r]$, independently of h.

Substituting (5.37)-(5.38) and (5.40) into (5.36), and simplifying gives $\mathcal{C}_{n,k,j}^{m}(\cdot) = \ldots$

$$\ldots = \frac{\phi_{n,k,j}^{m+1} - \phi_{n,k,j}^{m}}{\Delta\tau} - \left[\mathcal{L}\phi + \mathcal{J}\phi + \sup_{\hat{\gamma}\in[0,C_r]} \hat{\gamma}(1 - e^{-w}\phi_w - \phi_a)\right]_{n,k,j}^{m} + \xi r_k + \mathcal{E}(\mathbf{x}_{n,k,j}^{m}, h) + \mathcal{O}(h)$$

$$\overset{(i)}{=} \left[\phi_\tau - \mathcal{L}\phi - \mathcal{J}\phi - \sup_{\hat{\gamma}\in[0,C_r]} \hat{\gamma}\left(1 - e^{-w}\phi_w - \phi_a\right)\right]_{n,k,j}^{m+1} + \xi r_k + \mathcal{E}(\mathbf{x}_{n,k,j}^{m}, h) + \mathcal{O}(h). \tag{5.42}$$

Here, in (i), $\mathcal{E}(\mathbf{x}_{n,k,j}^{m}, h) \to 0$ as $h \to 0$, and we use

$$(\phi_\tau)_{n,k,j}^{m} = (\phi_\tau)_{n,k,j}^{m+1} + \mathcal{O}\left(h\right), \ (\phi_w)_{n,k,j}^{m} = (\phi_w)_{n,k,j}^{m+1} + \mathcal{O}\left(h\right), \ (\phi_a)_{n,k,j}^{m} = (\phi_a)_{n,k,j}^{m+1} + \mathcal{O}\left(h\right).$$

This step results in an $\mathcal{O}\left(h\right)$ term inside $\sup_{\hat{\gamma}}(\cdot)$, which can be moved out of the $\sup_{\hat{\gamma}}(\cdot)$, because it has the form $C(\hat{\gamma})h$, where $C(\hat{\gamma})$ is bounded independently of h, due to boundedness of $\hat{\gamma} \in [0, C_r]$ independently of h.

We now consider operator $\mathcal{D}_{n,k,j}^{m+1}(\cdot)$ which can be written as

$$\mathcal{D}_{n,k,j}^{m+1}\left(\cdot\right) = \phi_{n,k,j}^{m+1} + \xi - \Delta w \Delta r \sideset{}{^*}\sum_{l\in\mathbb{N}^\dagger}^{d\in\mathbb{K}^\dagger} \tilde{g}_{n-l,k-d}\ (\phi_{\text{SL}}^{(2)})_{l,d,j}^{m+}, \tag{5.43}$$

where the discrete values $(\phi_{\text{SL}}^{(2)})_{l,d,j}^{m+}$ are defined in (5.28) with $(i) = (2)$. Adopting a similar approach as the one utilized for $\mathcal{C}_{n,k,j}^{m+1}(\cdot)$, we aim to decompose $\sum^* \tilde{g}\ (\phi_{\text{SL}}^{(2)})_{l,d,j}^{m+}$ into $\sum^* \tilde{g}\ (\psi_{\text{SL}})_{l,d,j}^{m}$ for which Lemma 5.3 is applicable. Here, $(\psi_{\text{SL}})_{l,d,j}^{m}$ is to be defined subsequently.

We first start from the interpolated value $\tilde{\phi}_{l,d,j}^{m}$ in (5.26). In this case, since $\gamma_{l,d,j}^{m} \in (C_r\Delta\tau, a_j]$, we cannot eliminate the $\max(\cdot)$ operator in $\tilde{w}_l$ of the linear interpolation in (5.26). Therefore, as noted in Remark 4.1[(4.15)-(4.16)], for $\gamma \in (C_r\Delta\tau, a_j]$, we have $\sup_{\gamma_{l,d,j}^{m}\in(C_r\Delta\tau,a_j]} \tilde{\phi}_{l,d,j}^{m} + f(\gamma_{l,d,j}^{m}) = \ldots$

$$\ldots = \sup_{\gamma_{l,d,j}^{m}\in(C_r\Delta\tau,a_j]} (\phi(\tilde{w}_l, r_d, \tilde{a}_j, \tau_m) + \gamma_{l,d,j}^{m}(1-\mu)) + \xi + \mu C_r\Delta\tau - c + \mathcal{O}(h^2). \tag{5.44}$$

Here, $(\tilde{w}_l, \tilde{a}_j)$ is given in (5.26), and $f(\gamma)$ is replaced by $\gamma(1-\mu) + \mu C_r\Delta\tau - c$, as per (4.14) for $\gamma \in (C_r\Delta\tau, a_j]$.

Recalling operator $\mathcal{M}(\cdot)$ defined in (3.9b), we define a function $\psi\left(\mathbf{x}'\right)$ as follows

$$\psi\left(\mathbf{x}'\right) = \begin{cases} \sup\limits_{\gamma\in[0,a']} \psi'(\gamma, \mathbf{x}') & w_{\min} < w' < w_{\max},\ r_{\min} < r' < r_{\max}, \quad (5.45\text{a}) \\ \quad \text{where } \psi'(\gamma, \mathbf{x}') = \mathcal{M}(\gamma)\phi(\mathbf{x}') + \mu C_r\Delta\tau & C_r\Delta\tau < a' \le a_J,\ 0 \le \tau' < T, \\ \phi(\mathbf{x}') & \text{otherwise.} \quad (5.45\text{b}) \end{cases}$$

We note that in (5.45a), the admissible control set is $\gamma \in [0, a']$. It is straightforward to show that, for a fixed $\mathbf{x}' \in \Omega$ satisfies (5.45a), function $\psi'\left(\gamma; \mathbf{x}'\right)$ defined in (5.45a) is (uniformly) continuous in $\gamma \in [0, a']$. Hence, for the case (5.45a)

$$\sup_{\gamma\in(C_r\Delta\tau,a']} \psi'\left(\gamma, \mathbf{x}'\right) - \sup_{\gamma\in(0,a']} \psi'\left(\gamma, \mathbf{x}'\right) = \max_{\gamma\in[C_r\Delta\tau,a']} \psi'\left(\gamma, \mathbf{x}'\right) - \max_{\gamma\in[0,a']} \psi'\left(\gamma, \mathbf{x}'\right) = \mathcal{O}\left(h\right), \tag{5.46}$$

since the difference of the optimal values of γ for the two $\max(\cdot)$ expressions is bounded by $C_r\Delta\tau = \mathcal{O}(h)$.

Using (5.45a) and (5.46), and recalling from (5.26) that $(\phi^{(2)})_{l,d,j}^{m+} = \sup_{\gamma_{l,d,j}^{m}\in(C_r\Delta\tau,a_j]} \tilde{\phi}_{l,d,j}^{m} + f(\gamma_{l,d,j}^{m})$, we have

$$(\phi^{(2)})_{l,d,j}^{m+} = \xi + (\psi)_{l,d,j}^{m} + \mathcal{O}(h), \quad l \in \mathbb{N},\ d \in \mathbb{K}, \tag{5.47}$$

where ψ is given in (5.45a). Equation (5.47) allows us to write $(\phi_{\text{SL}}^{(2)})_{l,d,j}^{m+}$, defined in (5.28), as follows

$$(\phi_{\text{SL}}^{(2)})_{l,d,j}^{m+} = (\psi_{\text{SL}})_{l,d,j}^{m} + \mathcal{O}\left(h\right), \quad l \in \mathbb{N}^\dagger \text{ and } d \in \mathbb{K}^\dagger, \tag{5.48}$$

where

$$(\psi_{\text{SL}})^m_{l,d,q} = \begin{cases} (\xi + \mathcal{I}\{(\psi)^m\}(\breve{w}_l, \breve{r}_d, a_q))(1+\Delta\tau r_d)^{-1} & l \in \mathbb{N} \text{ and } d \in \mathbb{K}, \\ \phi^m_{l,d,q} + \xi & \text{otherwise,} \end{cases} \tag{5.49}$$

where ψ is defined in (5.45). Using (5.48), we rewrite operator $\mathcal{D}^{m+1}_{n,k,j}(\cdot)$, previously given in (5.43), into a convenient form below

$$\mathcal{D}^{m+1}_{n,k,j}(\cdot) = \phi^{m+1}_{n,k,j} + \xi - \Delta w \Delta r \sum_{l\in\mathbb{N}^\dagger}^{d\in\mathbb{K}^\dagger} {}^{*}\, \tilde{g}_{n-l,k-d} (\psi_{\text{SL}})^m_{l,d,j} + \mathcal{O}\left(h\right). \tag{5.50}$$

Then, for the above discrete convolution, applying Lemma 5.2[eqn (5.11)], noting (5.16), gives

$$\begin{aligned}\Delta w \Delta r \sum_{l\in\mathbb{N}^\dagger}^{d\in\mathbb{K}^\dagger} {}^{*}\, \tilde{g}_{n-l,k-d}\ (\psi_{\text{SL}})^m_{l,d,j} &= (\psi_{\text{SL}})^m_{n,d,j} + \mathcal{E}_\psi(\mathbf{x}^m_{n,k,j}, h) + \mathcal{O}(h), \\ &= \xi + \mathcal{I}\{(\psi)^m\}(\breve{w}_n, \breve{r}_k, a_j) + \mathcal{E}_\psi(\mathbf{x}^m_{n,k,j}, h) + \mathcal{O}(h), \end{aligned} \tag{5.51}$$

where we used the definition of $(\psi_{\text{SL}})^m_{n,k,j}$ in (5.49), and $\mathcal{E}_\psi(\mathbf{x}^m_{n,k,j}, h) \to 0$ as $h \to 0$.

For the term $\mathcal{I}\{(\psi)^m\}(\breve{w}_n, \breve{r}_k, a_j)$ in (5.51), following the same arguments as those for (5.40)-(5.41), noting the definition of ψ in (5.45), we obtain

$$\begin{aligned}\mathcal{I}\{(\psi)^m\}(\breve{w}_n, \breve{r}_k, a_j) &= \sup_{\gamma\in[0,a_j]} \mathcal{M}(\gamma)\phi(\mathbf{x}^m_{n,k,j}) + \mu C_r \Delta\tau + \mathcal{O}(h) + \mathcal{E}_\psi(\mathbf{x}^m_{n,k,j}, h) \\ &= \sup_{\gamma\in[0,a_j]} \mathcal{M}(\gamma)\phi(\mathbf{x}^{m+1}_{n,k,j}) + \mathcal{O}(h) + \mathcal{E}_\psi(\mathbf{x}^m_{n,k,j}, h). \end{aligned} \tag{5.52}$$

Here, $\mathcal{M}(\gamma)\phi\left(\mathbf{x}^m_{n,k,j}\right) = \mathcal{M}(\gamma)\phi\left(\mathbf{x}^{m+1}_{n,k,j}\right) + \mathcal{O}\left(h\right)$, which is combined with $\mu C_r \Delta\tau = \mathcal{O}\left(h\right)$. Substituting (5.51) and (5.52) into (5.50) gives

$$\mathcal{D}^{m+1}_{n,j}\left(\cdot\right) = \phi^{m+1}_{n,k,j} - \sup_{\gamma\in[0,a]} \mathcal{M}(\gamma)\phi\left(\mathbf{x}^{m+1}_{n,k,j}\right) + \mathcal{O}(h) + \mathcal{E}(\mathbf{x}^m_{n,k,j}, h). \tag{5.53}$$

Overall, recalling $\mathbf{x} = \mathbf{x}^{m+1}_{n,k,j}$, we have

$$\begin{aligned}&\mathcal{H}^{m+1}_{n,k,j}\left(h, \phi^{m+1}_{n,k,j} + \xi, \left\{\phi^m_{l,d,p} + \xi\right\}_{p\le j}\right) - F_{\text{in}}\left(\mathbf{x}, \phi\left(\mathbf{x}\right), D\phi\left(\mathbf{x}\right), D^2\phi\left(\mathbf{x}\right), \mathcal{J}\phi\left(\mathbf{x}\right), \mathcal{M}\phi\left(\mathbf{x}\right)\right) \\ &\quad = \ c\left(\mathbf{x}\right)\xi + \mathcal{O}(h) + \mathcal{E}(\mathbf{x}^m_{n,k,j}, h), \quad \text{if } \mathbf{x} \in \Omega^{U}_{\text{in}}, \end{aligned}$$

where $c(\mathbf{x})$ is a bounded function satisfying $r_{\min} \le c(\mathbf{x}) \le r_{\max}$ and $\mathcal{E}(\mathbf{x}^m_{n,k,j}, h) \to 0$ as $h \to 0$. This proves the first equation in (5.25). The remaining equations in (5.25) can be proved using similar arguments with the first equation. $\square$

Remark 5.1. *We impose the condition* (5.24) *to ease the presentation of the proof, that is, we make sure the term* $\max(e^{w_l} - \gamma^m_{l,d,j}, e^{w^\dagger_{\min}})$ *in the operator* $\mathcal{C}^{m+1}_{n,k,j}(\cdot)$ *will never be triggered. However, we can avoid this condition by the similar procedures presented in [57].*

Lemma 5.5 (Consistency)**.** *Assuming all the conditions in Lemma 5.4 are satisfied, then the scheme* (5.22) *is consistent in the viscosity sense to the impulse control problem* (3.1) *in* Ω^∞*. That is, for all* $\hat{\mathbf{x}} = (\hat{w}, \hat{r}, \hat{a}, \hat{\tau}) \in \Omega^\infty$*, and for any* $\phi \in \mathcal{G}(\Omega^\infty) \cap \mathcal{C}^\infty(\Omega^\infty)$ *with* $\phi^{m+1}_{n,k,j} = \phi(w_n, r_k, a_j, \tau_{m+1})$ *and* $\mathbf{x} = (w_n, r_k, a_j, \tau_{m+1})$*, we have both of the following*

$$\limsup_{\substack{h\to0,\ \mathbf{x}\to\hat{\mathbf{x}} \\ \xi\to0}} \mathcal{H}^{m+1}_{n,k,j}\Big(h, \phi^{m+1}_{n,k,j} + \xi, \left\{\phi^m_{l,d,p} + \xi\right\}_{p\le j}\Big) \le (F_{\Omega^\infty})^*\left(\hat{\mathbf{x}}, \phi(\hat{\mathbf{x}}), D\phi(\hat{\mathbf{x}}), D^2\phi(\hat{\mathbf{x}}), \mathcal{J}\phi(\hat{\mathbf{x}}), \mathcal{M}\phi(\hat{\mathbf{x}})\right), \tag{5.54}$$

$$\liminf_{\substack{h\to0,\ \mathbf{x}\to\hat{\mathbf{x}} \\ \xi\to0}} \mathcal{H}^{m+1}_{n,k,j}\Big(h, \phi^{m+1}_{n,k,j} + \xi, \left\{\phi^m_{l,d,p} + \xi\right\}_{p\le j}\Big) \ge (F_{\Omega^\infty})_*\left(\hat{\mathbf{x}}, \phi(\hat{\mathbf{x}}), D\phi(\hat{\mathbf{x}}), D^2\phi(\hat{\mathbf{x}}), \mathcal{J}\phi(\hat{\mathbf{x}}), \mathcal{M}\phi(\hat{\mathbf{x}})\right). \tag{5.55}$$

Proof of Lemma 5.5. Lemma 5.5 can be proved using similar steps in Lemma 5.5 in [57]. For brevity, we outline key steps to prove (5.54) for Ω_{in} and $\Omega_{a_{\min}}$; other sub-domains can be treated similarly. We note the continuity in their parameters of operators defined in (3.17)-(3.11), which is needed for this proof.

Consider $\hat{\mathbf{x}} \in \Omega_{\text{in}}$. There exist sequences of discretization parameter $\{h_i\}_i \to 0$, constants $\{\xi_i\}_i \to 0$, and gridpoints $\{(w_{n_i}, r_{k_i}, a_{j_i}, \tau_{m_i+1})\}_i \equiv \mathbf{x}_i \to \hat{\mathbf{x}}$, as $i \to \infty$. For sufficiently small $\{\Delta\tau_i\}_i$, we assume $a_{j_i} \in (C_r\Delta\tau_i, a_{\max}]$ for each i, and hence, the sequence $\{\mathbf{x}_i\}_i$ is contained in Ω_{in}^{U}, defined in (5.21). Therefore, lhs of (5.54) $= \limsup_{i\to\infty} \mathcal{H}_{n_i,k_i,j_i}^{m_i+1}(h_i, \phi_{n_i,k_i,j_i}^{m_i+1} + \xi_i, \{\phi_{l_i,d_i,p_i}^{m_i} + \xi_i\}_{p_i \le j_i}) \ldots$

$$\ldots \underset{\text{(i)}}{\le} \limsup_{i\to\infty} F_{\text{in}}(\mathbf{x}_i, \phi(\mathbf{x}_i)) + \limsup_{i\to\infty}[c(\mathbf{x}_i)\xi_i + \mathcal{O}(h_i) + \mathcal{E}(\mathbf{x}_{n_i,j_i}^{m_i}, h_i)] \underset{\text{(ii)}}{=} F_{\text{in}}(\hat{\mathbf{x}}, \phi(\hat{\mathbf{x}})) = \text{rhs of (5.54)},$$

as wanted. Here, (i) is due to the local consistency result for Ω_{in}^{U} in the first equation of (5.25) (Lemma 5.4), and properties of lim sup; (ii) is because of continuity of F_{in}.

For $\hat{\mathbf{x}} \in \Omega_{a_{\min}}$, complications arise because $\{\mathbf{x}\}_i$ could converge to $\hat{\mathbf{x}}$ from two different sub-domains, $\Omega^{\text{in}} = \Omega_{\text{in}}^{U} \cup \Omega_{\text{in}}^{L}$ and $\Omega_{a_{\min}}$; however, on Ω_{in}^{L}, the second equation of (5.25) (Lemma 5.4) indicates local consistency with $F_{\text{in}}'(\mathbf{x}_i, \phi(\mathbf{x}_i))$, defined in (5.23) but is not part of F_{Ω^∞}. Nonetheless, since $\sup_{\hat{\gamma}\in[0,a/\Delta\tau]} \hat{\gamma}\,(1 - e^{-w}\phi_w - \phi_a) \ge 0$, $F_{\text{in}}'(\mathbf{x}_i, \phi(\mathbf{x}_i)) \le F_{a_{\min}}(\mathbf{x}_i, \phi(\mathbf{x}_i))$, we can eliminate $F_{\text{in}}'(\mathbf{x}_i, \phi(\mathbf{x}_i))$ when considering lim sup. Thus, lhs of (5.54) $= \limsup_{i\to\infty} \mathcal{H}_{n_i,k_i,j_i}^{m_i+1}(h_i, \phi_{n_i,k_i,j_i}^{m_i+1} + \xi_i, \{\phi_{l_i,d_i,p_i}^{m_i} + \xi_i\}_{p_i \le j_i}) \ldots$

$$\ldots \le \limsup_{i\to\infty} F_{\Omega^\infty}(\mathbf{x}_i, \phi(\mathbf{x}_i)) + \limsup_{i\to\infty}[c(\mathbf{x}_i)\xi_i + \ \mathcal{E}(\mathbf{x}_{n_i,j_i}^{m_i}, h_i)] \le (F_{\Omega^\infty})^*\,(\hat{\mathbf{x}}, \phi(\hat{\mathbf{x}})) = \text{rhs of (5.54)}.$$

□

5.4 Monotonicity

We present a result on the monotonicity of scheme (5.22).

Lemma 5.6 (ϵ-monotonicity). *Suppose that (i) the discretization* (4.22) *satisfies the positive coefficient condition* (4.23), *and (ii) linear interpolation in* (4.20), (4.24) *and (ii) the weight* $\tilde{g}_{n-l,k-d}$ *satisfies the monotonicity condition* (4.46)*; and (iii)* $r_{\min}$ *satisfies condition* (5.2)*. Then scheme* (5.22) *satisfies*

$$\mathcal{H}_{n,k,j}^{m+1}\left(h, v_{n,k,j}^{m+1}, \left\{x_{l,d,p}^{m}\right\}_{p\le j}\right) \ \le\ \mathcal{H}_{n,k,j}^{m+1}\left(h, v_{n,k,j}^{m+1}, \left\{y_{l,d,p}^{m}\right\}_{p\le j}\right) \ +\ K'\epsilon \tag{5.56}$$

for bounded $\{x_{l,d,p}^{m}\}$ *and* $\{y_{l,d,p}^{m}\}$ *having* $\{x_{l,d,p}^{m}\} \ge \{y_{l,d,p}^{m}\}$*, where the inequality is understood in the component-wise sense, and* K' *is a positive constant independent of* h*.*

A proof of Lemma 5.6 is similar to that of Lemma 5.6 in [57], and hence omitted for brevity.

5.5 Convergence to viscosity solution

We have demonstrated that the scheme (5.22) satisfies the three key properties in Ω: (i) ℓ_∞-stability (Lemma 5.1), (ii) consistency (Lemma 5.5) and (iii) ϵ-monotonicity (Lemma 5.6). With a strong comparison result in $\Omega_{\text{in}} \cup \Omega_{a_{\min}}$, we now present the main convergence result of the paper.

Theorem 5.1 (Convergence in $\Omega_{\text{in}} \cup \Omega_{a_{\min}}$). *Suppose that all the conditions for Lemmas 5.1, 5.5 and 5.6 are satisfied. Under the assumption that the monotonicity tolerance* $\epsilon \to 0$ *as* $h \to 0$*, scheme* (5.22) *converges locally uniformly in* $\Omega_{in} \cup \Omega_{a_{\min}}$ *to the unique bounded viscosity solution of the GMWB pricing problem in the sense of Definition 3.2.*

Proof of Theorem 5.1. To highlight the importance of the discretization parameter h, we let $\mathbf{x}_{n,k,j}^{m}(h) = (w_n, r_k, a_j, \tau_m; h)$, and denote by $v_{n,k,j}^{m}(h)$ the numerical solution at this node. The candidate for the viscosity subsolution (resp. supersolution) the GMWB pricing problem is given by the u.s.c function $\overline{v} : \Omega^\infty \to \mathbb{R}$ (resp. the l.s.c function $\underline{v} : \Omega^\infty \to \mathbb{R}$) defined as follows

$$\overline{v}\,(\mathbf{x}) = \limsup_{\substack{h\to 0 \\ \mathbf{x}_{n,k,j}^{m+1}(h)\to\mathbf{x}}} v_{n,k,j}^{m+1}(h) \qquad (\text{resp. } \underline{v}(\mathbf{x}) = \liminf_{\substack{h\to 0 \\ \mathbf{x}_{n,k,j}^{m+1}(h)\to\mathbf{x}}} v_{n,k,j}^{m+1}(h)) \qquad \mathbf{x} \in \Omega^\infty. \tag{5.57}$$

Here, lim sup and lim inf are finite due to stability of our scheme in Ω established in Lemma 5.1.

We appeal to a Barles-Souganidis-type analysis in [9, 11] to show that $\overline{v}$ (resp. $\underline{v}$) is a viscosity subsolution (resp. supersolution) of the HJB-QVI (3.18) in Ω^{∞} in the sense of Definition 3.2. In this step, we use (i) ℓ_{∞}-stability (Lemma 5.1), (ii) consistency (Lemma 5.5) and (iii) ϵ-monotonicity (Lemma 5.6) of the numerical scheme, noting the requirement $\epsilon \to 0$ as $h \to 0$. By 5.57, $\overline{v} \geq \underline{v}$ in Ω^{∞}. By a strong comparison result in Theorem 3.1, $\overline{v} \leq \underline{v}$ in $\Omega_{\text{in}} \cup \Omega_{a_{\min}}$. Therefore, $v(\mathbf{x}) = \overline{v}(\mathbf{x}) = \underline{v}(\mathbf{x})$ is the unique viscosity solution in $\Omega_{\text{in}} \cup \Omega_{a_{\min}}$ in the sense of Definition 3.2. The fact that convergence is locally uniform is automatically implied. This concludes the proof. □

6 Numerical experiments

In this section, we present selected numerical results for the no-arbitrage pricing problem (3.18). In addition to validation examples, we particularly focus on investigating the impact of jump-diffusion dynamics and stochastic interest rates on the prices/the fair insurance fees, as well as on the holder's optimal withdrawal behaviors.

A set of GMWB parameters commonly used for subsequent experiments is given in Table 6.1. These include expiry time T, the maximum allowed withdrawal rate C_r (for continuous withdrawals), the proportional penalty rate μ (for withdrawing finite amounts), the premium z_0 which is also the initial balance of the guarantee account and of the personal sub-account.

For experiments in this section, the computational domain is constructed with $w_{\min} = \ln(z_0) - 10$, $w_{\max} = \ln(z_0) + 10$, $r_{\min} = -0.2$, $r_{\max} = 0.3$, together with $w^{\dagger}_{\min}$, $w^{\dagger}_{\max}$, $r^{\dagger}_{\min}$, and $r^{\dagger}_{\max}$ computed as discussed in Section 4. Unless otherwise stated, relevant details about the refinement levels are given in Table 6.2. Here, the timestep $M = 20$ (resp. $M = 40$) corresponds to the case of $T = 5$ (resp. $T = 10$) in Table 6.1. Based on the choices of N and K, we have $N^{\dagger} = 2N$ and $K^{\dagger} = 2K$ as in (4.10) and (4.11), respectively. We emphasize that, increasing $|w_{\min}|$, $w_{\max}$, $|r_{\min}|$, or $r_{\max}$ virtually does not change the no-arbitrage prices/fair insurance fees. Therefore, for practical purposes, with $P^{\dagger} \equiv w^{\dagger}_{\max} - w^{\dagger}_{\min}$ and $K^{\dagger} \equiv r^{\dagger}_{\max} - r^{\dagger}_{\min}$ chosen sufficiently large as above, they can be kept constant for all refinement levels (as we let $h \to 0$).

Similar to [17, 42, 57], a sufficiently small fixed cost $c = 10^{-8}$ is used all numerical tests. For user-defined tolerances ϵ and ϵ_1 in Algorithm 4.1, we use $\epsilon = \epsilon_1 = 10^{-6}$ for all experiments and all refinement levels. We note that using smaller ϵ or ϵ_1 produces virtually identical numerical results.

Parameter	Value
Expiry time (T)	{5, 10} years
Maximum withdrawal rate (C_r)	$1/T$
Withdrawal penalty rate (μ)	0.10
Init. lump-sum premium (z_0)	100
Init. balance of guarantee a/c ($= z_0$)	100
Init. balance value of sub-a/c ($= z_0$)	100

TABLE 6.1: *GMWB parameters for numerical experiments.*

Refinement level	N (w)	K (r)	J (a)	M (τ)
0	2^9	2^5	26	{20, 40}
1	2^{10}	2^6	51	{40, 80}
2	2^{11}	2^7	101	{80, 160}
3	2^{12}	2^8	201	{160, 320}
4	2^{13}	2^9	401	{320, 640}

TABLE 6.2: *Grid and timestep refinement levels for numerical experiments.*

Unless otherwise stated, representative parameters to jump-diffusion dynamics and Vasicek short rate dynamics are respectively given in Tables 6.4 (taken from [57]) and 6.3 (from [58]).

Parameters	Merton	Kou
σ_z (risky asset volatility)	0.3	0.3
λ (jump intensity)	0.1	0.1
ν(log jump multiplier mean)	-0.9	n/a
ς (log jump multiplier std)	0.45	n/a
p_u (probability of up-jump)	n/a	0.3445
η_u (exp. parameter up-jump)	n/a	3.0465
η_d (exp. parameter down-jump)	n/a	3.0775

TABLE 6.3: *Parameters for the jump-diffusion dynamics* (2.2a). *Values are taken from [57].*

Parameters	Vasicek
r_0	0.05
θ	0.05
δ	0.0349
σ_R	0.02

TABLE 6.4: *Parameters for the Vasicek short rate dynamics* (2.2c). *Values are taken from [58].*

The correlation coefficient ρ is chosen from $\{-0.2, 0.2\}$. The value for ρ will be specified for each experiment subsequently.

6.1 Validation through Monte Carlo simulation

As previously mentioned, the no-arbitrage pricing of GMWB with continuous withdrawals under a jump-diffusion dynamics with with stochastic interest rate has not been previously studied in the literature, hence, reference prices/insurance fees are not available for the dynamics considered in this work. Therefore, for validation purposes, we compare no-arbitrage prices obtained by the proposed numerical method, hereafter referred to as "ϵ-mF", with those obtained by MC simulation.

Method	Level	Merton				Kou			
		$\rho=-0.2$		$\rho=0.2$		$\rho=-0.2$		$\rho=0.2$	
		price	ratio	price	ratio	price	ratio	price	ratio
ϵ-mF	0	115.4845		116.4466		109.1908		110.1039	
	1	114.2267		114.8675		109.1608		109.7832	
	2	113.6613	2.22	114.1549	2.22	109.1517	3.29	109.6396	2.23
	3	113.3921	2.10	113.8171	2.11	109.1483	2.62	109.5719	2.12
	4	113.2601	2.04	113.6524	2.05	109.1467	2.27	109.5388	2.05
MC	95%-CI	[112.61, 113.47]		[112.95, 113.79]		[108.64, 109.48]		[109.31, 110.15]	

TABLE 6.5: *Validation example with jump-diffusion and Vasicek short rate dynamics with parameters from Tables 6.3 and 6.4; expiry time $T = 5$, the insurance fee $\beta = 0.02$.*

To carry out Monte Carlo validation, we proceed in two steps outlined below.

- Step 1: we solve the GMWB pricing problem using the "ϵ-mF" method on a relatively fine computational grid (Refinement Level 2 in Table 6.2). During this step, the optimal control $\gamma_{l,d,q}^m$ is stored for each computational gridpoint $\mathbf{x}_{l,d,q}^m \in \Omega_{\text{in}} \cup \Omega_{a_{\min}} \cup \Omega_{w_{\min}} \cup \Omega_{aw_{\min}}$.

- Step 2: we carry out Monte Carlo simulation of dynamics (2.1), and (2.2), and (2.2c), for $A(t)$, $Z(t)$, and $R(t)$, respectively, following the stored PDE-computed optimal strategies $\{(\mathbf{x}_{l,d,q}^m, \gamma_{l,d,q}^m)\}$ obtained in Step 1.

  Specifically, let $t_{m'} = T - \tau_m$, $m' = M - m$, $m = M-1, \ldots, 0$, and $\hat{Z}_{m'}$, $\hat{R}_{m'}$ and $\hat{A}_{m'}$ be simulated values. Across each $t_{m'}$, if necessary, linear interpolation $\mathcal{I}\{\gamma^m\}(\ln(\hat{Z}_{m'}), \hat{R}_{m'}, \hat{A}_{m'})$ is applied to determine the optimal controls for simulated state values. (No linear interpolation across time is used.) For $t \in [t_{m'-1}, t_{m'}]$, a smaller timestep size than $\Delta\tau$ is utilized for MC simulation. For Step 2, a total of 10^5 paths and a timestep size $\Delta\tau/20$ is used. The antithetic variate technique is also employed to reduce the variance of MC simulation.

In Table 6.5, we present the no-arbitrage prices (in dollars) obtained by the "ϵ-mF" method and by the above-described MC simulation. These prices indicate indicate excellent agreement with those obtained by MC simulation. In addition, first-order convergence is observed for "ϵ-mF".

6.2 Modeling impact

In this subsection, we investigate the (combined) impact of jumps and stochastic interest rate dynamics on quantities of central importance to GMWBs, namely no-arbitrage prices and fair insurance fees, as well as on the holder's optimal withdrawal behaviors. In this study, we typically compare the aforementioned quantities obtained from different model types: (i) pure-diffusion (GBM) dynamics with a constant interest rate, (i) pure-diffusion (GBM) dynamics with Vasicek short rate, (ii) jump-diffusion dynamics with a constant interest rate, and (iii) jump-diffusion dynamics with Vasicek short rate. Hereinafter, these model types are respectively referred to as "GBM-C", "GBM-V", "JD-C" and "JD-V". As an illustrative example, we only consider the case of the Merton jump-diffusion dynamics; using the Kou jump-diffusion dynamics yield qualitatively similar conclusions, and hence omitted for brevity. We note that, the Merton jump parameters in Table (6.3) result in $\kappa = -0.5501$, indicating a bear stock market scenario, which is typical in an elavated interest rate setting.

With respect to interest rates, for fair comparisons, we establish an effective constant interest rate which is "comparable" to stochastic short rate dynamics. Hereinafter, this comparable rate is denoted by r_c. Inspired by [8], the comparable constant interest rate r_c is chosen to be the T-year Yield-to-Maturity (YTM) corresponding to the Vasicek dynamics (2.2c). The comparable constant rate r_c is obtained simply by solving $e^{-r_c T} = p_b(r_0, T; T)$, where $p_b(r_0, T; T)$ given by the formula (3.8). This gives

$$r_c = -\ln(p_b(r_0, T; T))/T, \quad p_b(r_0, \cdot; T) \text{ is given in (3.8).} \tag{6.1}$$

With respect to jumps, we consider an effective constant instantaneous volatility which approximates the behavior of the Merton jump-diffusion dynamics by pure-diffusion dynamics [63]. It is interesting to include this case as conventional wisdom asserts that over long times, jump-diffusions can be approximated by diffusions with enhanced volatility. In our experiments, the effective (enhanced) constant instantaneous volatility, denoted by σ_c, is computed by [63]

$$\sigma_c = \sqrt{\sigma_z^2 + \lambda(\nu^2 + \varsigma^2)}. \tag{6.2}$$

In Table 6.6, numerical values of parameters relatvant to different models are given. Regarding numerical methods for different model types, we note that the propsed SL ϵ-monotone Fourier method can be modified in a straightfoward manner to handle the GBM-V model. Concerning the GBM-C and JD-C models, the ϵ-monotone Fourier method for jump-diffusion dynamics with a constant interes rate proposed in our paper [57] is used.

Model	σ_c	r_c $T=5$	r_c $T=10$	Merton	Vasicek
GBM-C	0.437	0.0485	0.0448	n/a	n/a
GBM-V	0.437	n/a		n/a	Table 6.4
JD-C	n/a	0.0485	0.0448	Table 6.3	n/a
JD-V	n/a	n/a		Table 6.3	Table 6.4

Table 6.6: *Parametes for different models considered; r_c and σ_c are computed using* (6.1) *and* (6.2), *respectively.*

In subsequent discussions, to compare no-arbitrage prices (v) and fair insurance fees (β_f) across different model types, with $x \in \{v, \beta_f\}$, we denote by $\%\Delta x(\text{Model}_1, \text{Model}_2)$ the relative change in the quantity x between Model$_1$ and Model$_2$. It is defined by $\%\Delta x(\text{Model}_1, \text{Model}_2) = \dfrac{|x_1 - x_2|}{x_2}$, where x_1 and x_2 are respecitive x-values for Model$_1$ and Model$_2$.

6.2.1 No-arbitrage prices and fair insurance fees

In this experiment, we compare the no-arbitrage prices and the fair insurance fees obtained from different model types described above with parameters specified in Table 6.6 and the correlation coefficient $\rho = 0.2$ for the GBM-V and the JD-V models. In Table 6.7, we present selected selected results obtained from four different models. Here, the no-arbitrage prices (obtained with the insurance fee $\beta = 0.02$), and the fair insurance fees are numerically estimated as described in Subsection 4.6. The numerical results in Table 6.7 suggest that jumps and stochastic short rate have sub-

Model	no-arbitrage price (v)		fair insurance fee (β_f)	
	$T = 5$	$T = 10$	$T = 5$	$T = 10$
GBM-C	116.1926	115.1230	0.1070	0.0610
GBM-V	116.2775	115.7670	0.1079	0.0647
JD-C	113.0806	111.9754	0.0801	0.0487
JD-V	114.1549	114.4837	0.0841	0.0550

TABLE 6.7: *No-arbitrage prices and fair insurance fees obtained from different model types; parameters specified in Table 6.6; the insurance fee $\beta = 0.02$ used for no-arbitrage prices; for GBM-V and JD-V, the correlation is $\rho = 0.2$; refinement level 2.*

stantial combined impact on both no-arbitrage prices and fair insurance fees, with the impact being more pronounced on the latter (the fees) than on the former (prices). Also, the fair insurance fees under the GBM-C/V models are considerably more expensive than those obtained under JD-C/V models. Specifically, with GBM-C being the reference model, when $T = 5$, $\%\Delta\beta_f(\cdot, \text{GBM-C})$ ranges from 0.8% ($= \%\Delta\beta_f(\text{GBM-V}, \text{GBM-C})$) to 25.1% ($= \%\Delta\beta_f(\text{JD-C}, \text{GBM-C})$), which is much large than $\%\Delta v(\cdot, \text{GBM-C})$ ranging from 0.1% ($= \%\Delta v(\text{GBM-V}, \text{GBM-C})$) to 2.7%, which is $\%\Delta v(\text{JD-C}, \text{GBM-C})$. Similarly, for $T = 10$: $\%\Delta\beta_f(\cdot, \text{GBM-C})$ ranges from 6.0% ($= \%\Delta\beta_f(\text{GBM-V}, \text{GBM-C})$) to 20.1% ($= \%\Delta\beta_f(\text{JD-C}, \text{GBM-C})$), whereas, $\%\Delta v(\cdot, \text{GBM-C})$ is only from 0.6% ($= \%\Delta v(\text{GBM-V}, \text{GBM-C})$) to 2.7% ($= \%\Delta v(\text{JD-C}, \text{GBM-C})$).

We also observe that, all else being equal, the price and the fair insurance fee obtained with a constant interest rate (GBM-C, JD-C) are also smaller than those obtained from the Vasicek dynamics counterpart (resp. GBM-V, JD-V). For example, when $T = 10$, compare JD-C (0.0801) vs JD-V (0.0841), and GBM-C(0.1070) vs GBM-V(0.1079). On the other hand, application of jumps, all else being equal, results in a lower fair insurance fee. For example, when $T = 10$, compare JD-C (0.0801) vs GBM-C (0.1070) and JD-V (0.0841) vs GBM-V (0.1079)). We also observe that, all else being equal, the impact of jumps on the fair insurance fee (and the price) reduces as the maturity T increases, but that of stochastic interest rate appears to be more pronounced over a longer investment horizon. For example, regarding jumps, $\%\Delta\beta_f(\text{JD-C}, \text{GBM-C})$ is 25.1% when $T = 5$ (years), but reduces to 20.1% when $T = 10$ (years); regarding interest rate, $\%\Delta\beta_f(\text{JD-C}, \text{JD-V})$ is 4.7% when $T = 5$ (years), but is 11.4% when $T = 10$ (years) .

A possible explanation for the above observation is as follows. Stochastic interest rate constitutes an additional source of risk uncaught by using a constant interest rate, resulting in the fair insurance fee (and the no-arbitrage price) underpriced using a constant interest rate than using stochastic interest rate dynamics. Furthermore, using an effective volatility (σ_c) does not fully capture risk caused by (substantial) downward jumps, hence resulting in the fair insurance fee underpriced. To investigate further the combined impact of jumps and stochastic interes rates, in the following subsection, we study the holder's optimal withdrawal behaviors.

6.2.2 Optimal withdrawals

In this study, we use the fair insurance fees for the GBM-C, GBM-V, JD-C and JD-V models, respectively denoted by β_f^{gc}, β_f^{gV}, β_f^{c} and β_f^{V}. We use $T = 10$ and $\rho = 0.2$. As reported in Table 6.7, $\beta_f^{gc} = 0.0610$, $\beta_f^{gV} = 0.0647$, $\beta_f^{c} = 0.0487$ and $\beta_f^{V} = 0.0550$. In Figure 6.1, we present plots of optimal withdrawals for (calendar) time $t = 5$ (years) obtained using different models: the GBM-C in Figure 6.1(a), the JD-C model in Figure 6.1(b), the GBM-V in Figure 6.1(c), and the JD-V model in Figure 6.1(d). For the GBM-V and JD-V models, the control plots correspond to the spot rate $R(t = 5) = r_c = 0.0448$.

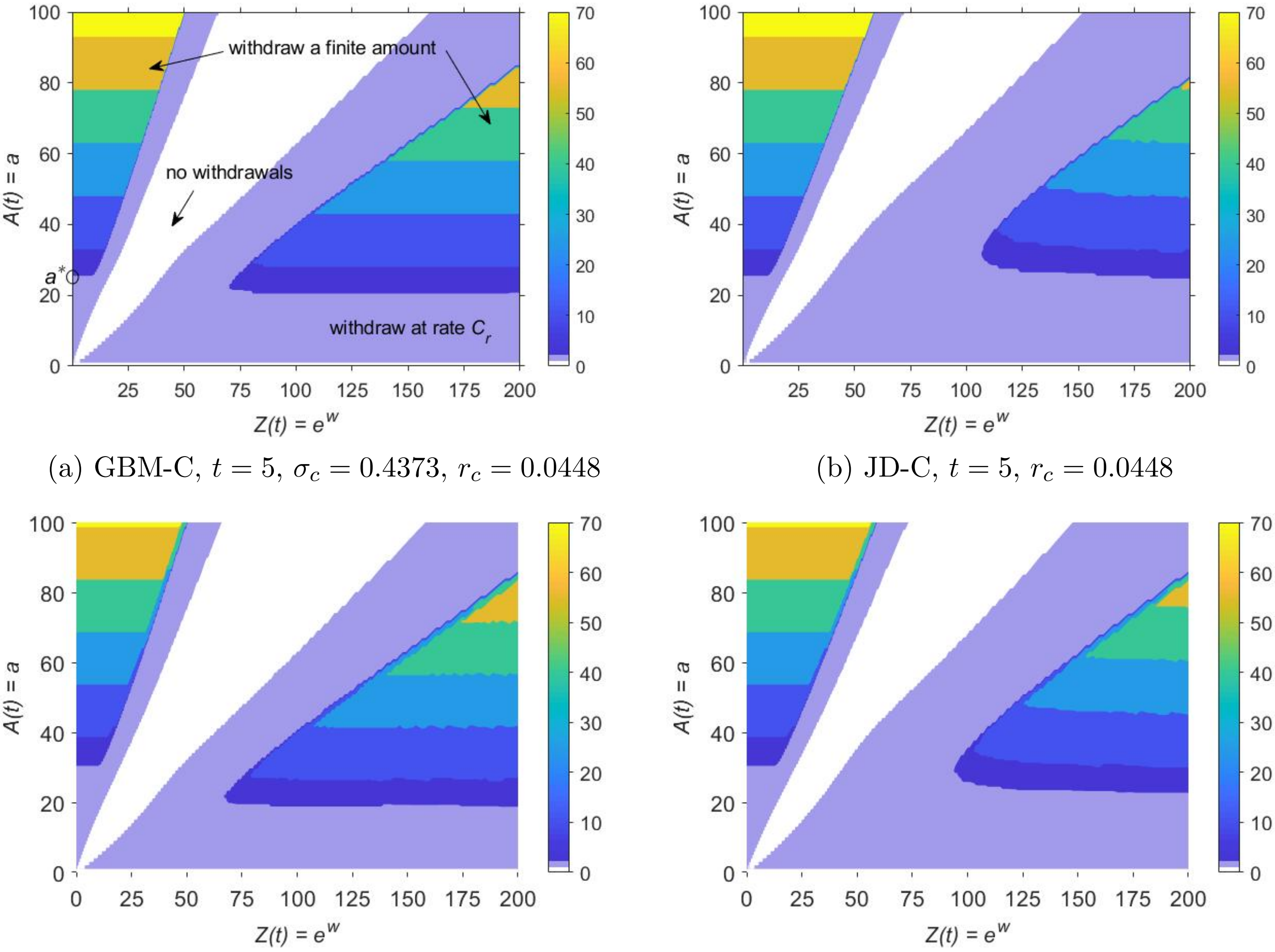

(a) GBM-C, $t = 5$, $\sigma_c = 0.4373$, $r_c = 0.0448$ (b) JD-C, $t = 5$, $r_c = 0.0448$

(c) GBM-V, $t = 5$, $R(t) = r_c = 0.0448$ (d) JD-V, $t = 5$, $R(t) = r_c = 0.0448$

FIGURE 6.1: *The holder's optimal withdrawals at (calendar) time $t = 5$ (years); parameters specified in Table 6.6; $T = 10$, $\rho = 0.2$; fair insurance fee $\beta_f^{gc} = 0.0610$, $\beta_f^{gV} = 0.0647$, $\beta_f^{c} = 0.0487$, $\beta_f^{V} = 0.0550$; refinement level 2.*

From Figure 6.1, we observe several key qualitative similarities across different models. Specifically, in the lower-right region, where $A(t) \ll z_0$ and $Z(t) \gg A(t)$, all optimal controls suggest the holder should withdraw continuously at rate C_r; however, withdrawing a finite amount becomes optimal when $A(t)$ becomes sufficiently large (upper-right region). Also, in the lower-left region, when both $A(t)$ and $Z(t)$ are small, optimal controls suggest to either withdrawal nothing or to withdraw continuously at rate C_r; however, in the upper-left region of Figure 6.1, where $A(t) \gg Z(t)$, optimal controls suggest withdraw a finite amount.

Nonetheless, significant quantitative differences are also observed, most notably in the upper-right and in the lower-left regions. For example, consider the upper-right region in Figure 6.1(a)-(d). At $(Z(t), A(t)) = (200, 80)$, our numerical results in Figure 6.1(b), indicate that, when the JD-C model is used, it is optimal to withdraw continuously at rate $C_r = 1/T = 0.1$; however, using other model, as shown in Figure 6.1(a), (c) and (d), it is suggested that withdrawing a finite amount (about \$60) is optimal.

In Figure 6.2, we present control plots for at $t = 5$ (years) when $R(t) \in \{0.03, 0.1\} \neq r_c$, and $R(t) = -0.0125 < 0$ obtained using the GBM-V and JD-V models. Comparing Figure 6.2(a), (c) and (e) with Figure 6.1(c), as well as comparing Figure 6.2(b), (d) and (f) with Figure 6.1(d)), suggests that the optimal withdrawal behaviours depend considerably on spot rates, and they are significantly different from those obtained using a comparable rate r_c, with a more conservative withdraw behaviours,

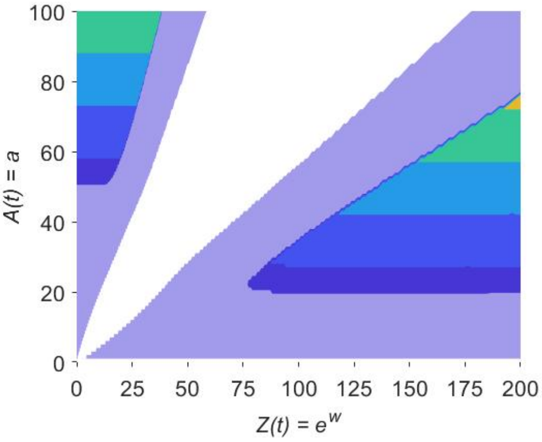

(a) GBM-V, $t = 5$, $R(t) = 0.03$

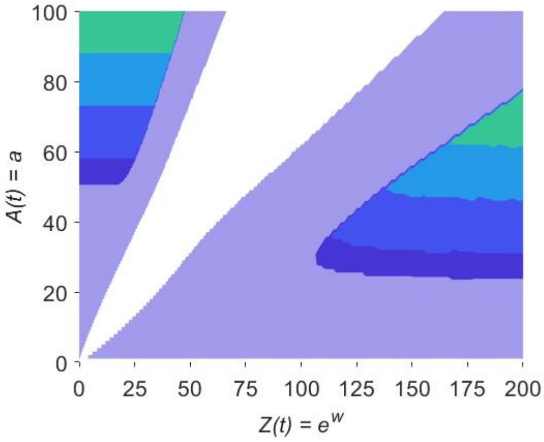

(b) JD-V, $t = 5$, $R(t) = 0.03$

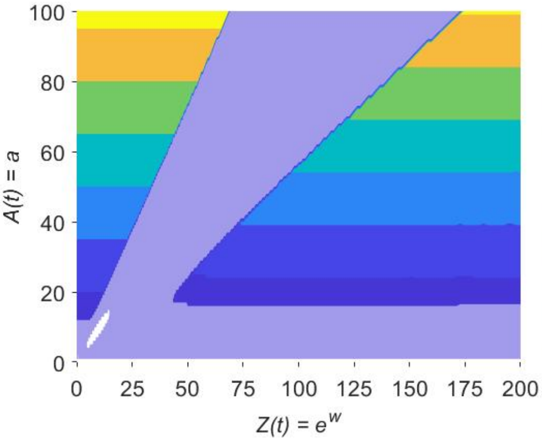

(c) GBM-V, $t = 5$, $R(t) = 0.1$

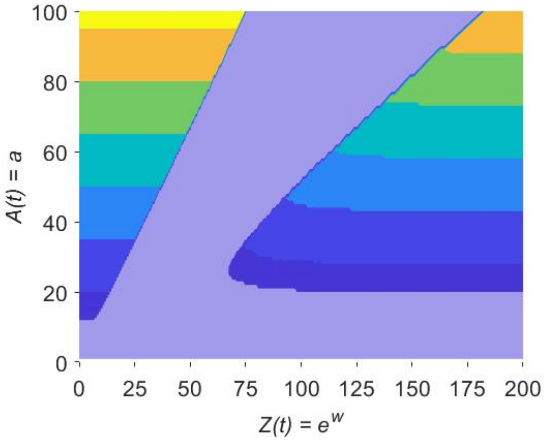

(d) JD-V, $t = 5$, $R(t) = 0.1$

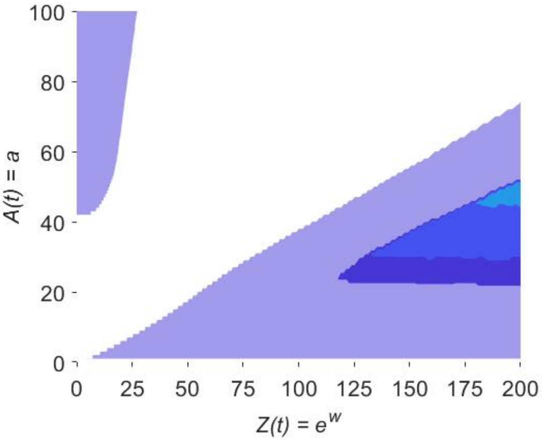

(e) GBM-V, $t = 5$, $R(t) = -0.0125$

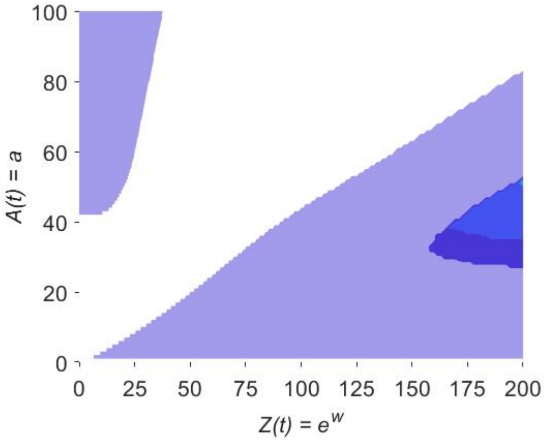

(f) JD-V, $t = 5$, $R(t) = -0.0125$

FIGURE 6.2: *The holder's optimal withdrawals at* $t = 5$ *(years) for different spot rates; parameters are from Table 6.3[Merton] and Table 6.4;* $T = 10$*, correlation coefficient* $\rho = 0.2$*, effective volatility* $\sigma_c = 0.4373$*, fair insurance fee* $\beta_f^{gV} = 0.0647$*,* $\beta_f^V = 0.0550$*; refinement level 2.*

especially in withdrawing a finite amount, when the spot interst rate is low.

We now turn our attention to the lower-left region of the control plots in Figure 6.1 and Figure 6.2, where $A(t)$ dominates $Z(t)$. In particular, with $Z(t)$ being zero, we study the value of a across which the optimal withdrawal behaviours change from withdrawing continuously at rate C_r to withdrawing a finite amount. For brevity, we only discuss the GBM-C and JD-V model. For the GBM-C model, we denote by a_c^* this special a-value, and it is given by $a_c^* = -\frac{C_r}{r_c}\ln(1-\mu)$, as shown in [22]. For the JD-V model, we denote by a_V^* the aforementioned special value of a (this is also the same a-value for the GBM-V model). A closed-form expression for a_V^* is not known to exist, and therefore, we estimate it using numerical results.

In Figure 6.3, we plot a_c^* and a_V^* against different spot rate $R(t)$ at $t = 5$. We note that, when $r < 0$ and $z = e^w \to 0$, Figure 6.3 suggests that never optimal to withdraw a finite amount (also see Figure 6.1(c)). It is observed from Figure 6.3 that when $R(t) \ll r_c$, a_V^* is significantly larger than a_c^*; however, when $R(t) \gg r_c$, a_V^* is considerably smaller than a_c^*. These suggest that, when the balance of sub-account balance is zero, the holder should be much more cautious with finite amount withdrawals from the guarantee account in a low interest rate environment than s/he is in a constant interest rate; however, the holder should be much more aggressive in a high interest rate environment.

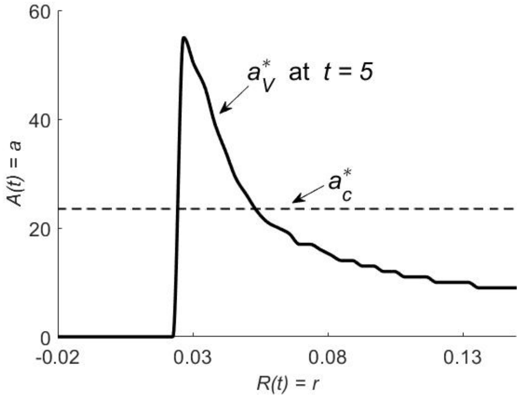

FIGURE 6.3: *A plot of a_V^* (for JD-V) and a_c^* (for GBM-C) against spot rate $R(t)$ at (calendar) time $t = 5$ (years); parameters are similar to those used for Figure 6.1;*

To summarize, our numerical results suggest a simultaneous application of jumps and stochastic interest rate result in considerably cheaper fair fees than those obtained under a comparable pure-diffusion model. In addition, under this realistic modeling setting, the holder's optimal withdrawal behaviour appears to be much more conservative (resp. aggressive) in withdrawing a finite amount when the balance of the sub-account is negligible (resp. considerable) than in the optimal behaviour under a pure-diffusion model would dictate. This is possibly because of combined risk due to (i) possible downsize jumps, and (ii) stochastic interest rate, which drives lower fair insurance fees for GMWBs. We plan to investigate these observations further in a future work.

7 Conclusion

In a continuous withdrawal scenario, using an impulse control framework, the GMWB pricing problem under a jump-diffusion dynamics with stochastic short rate is formulated as HJB-QVI of three spatial dimensions. The viscosity solution to this HJB-QVI is shown to satisfy a strong comparison result. Utilizing a semi-Lagrangian discretization, we develop an ϵ-monotone Fourier method to solve the HJB-QVI. We rigorously prove the convergence of the numerical solutions to the viscosity solution of the associated HJB-QVI. Numerical experiments demonstrate an excellent agreement with reference values obtained by the Monte Carlo simulation. Extensive analysis of numerical results indicate a significant (combined) impact of jumps and stochastic interest rate dynamics on the fair insurance fees and on the optimal withdrawal behaviors of policy holders. For future work, we plan to investigate further the impact of realistic modeling with various withdrawal settings and complex contract features.

Acknowledgement

The authors would like to thank George Labahn and Peter Forsyth of the University of Waterloo for very useful comments on earlier drafts of this paper.

References

[1] J. Alonso-Garcca, O. Wood, and J. Ziveyi. Pricing and hedging guaranteed minimum withdrawal benefits under a general Lévy framework using the COS method. *Quantitative Finance*, 18:1049–1075, 2018.

[2] B.E. Asri and S. Mazid. Stochastic impulse control problem with state and time dependent cost functions. *Mathematical Control & Related Fields*, 10(4):855–875, 2020.

[3] P. Azimzadeh, E. Bayraktar, and G. Labahn. Convergence of implicit schemes for Hamlton-Jacobi-Bellman quasi-variational inequalities. *SIAM Journal on Control and Optimization*, 56(6):3994–4016, 2018.

[4] P. Azimzadeh and P.A. Forsyth. The existence of optimal bang-bang controls for GMxB contracts. *SIAM Journal on Financial Mathematics*, pages 117–139, 02 2015.

[5] S. Baccarin. Optimal impulse control for a multidimensional cash management system with generalized cost functions. *European Journal of Operational Research*, (196):198–206, 2009.

[6] A.R. Bacinello, P. Millossovich, and A. Montealegre. The valuation of GMWB variable annuities under alternative fund distributions and policyholder behaviours. *Scandinavian Actuarial Journal*, 2016(5):446–465, 2016.

[7] A.R. Bacinello, P. Millossovich, A. Olivieri, and E. Pitacco. Variable annuities: a unifying valuation approach. *Insurance: Mathematics and Economics*, 49(3):285–297, 2011.

[8] L. Ballotta and I. Kyriakou. Convertible bond valuation in a jump diffusion setting with stochastic interest rates. *Quantitative Finance*, 15(1):115–129, 2015.

[9] G. Barles and J. Burdeau. The Dirichlet problem for semilinear second-order degenerate elliptic equations and applications to stochastic exit time control problems. *Communications in Partial Differential Equations*, 20:129–178, 1995.

[10] G. Barles and C. Imbert. Second-order elliptic integro-differential equations: viscosity solutions' theory revisited. *Ann. Inst. H. Poincaré Anal. Non Linéaire*, 25(3):567–585, 2008.

[11] G. Barles and P.E. Souganidis. Convergence of approximation schemes for fully nonlinear equations. *Asymptotic Analysis*, 4:271–283, 1991.

[12] D. Bauer, A. Kling, and J. Russ. A universal pricing framework for guaranteed minimum benefits in variable annuities. *ASTIN Bulletin*, 38:621–651, 2008.

[13] C. Belak, S. Christensen, and F.T. Seifried. A general verification result for stochastic impulse control problems. *SIAM Journal on Control and Optimization*, 55(2):627–649, 2017.

[14] E. Benhamou and P. Gauthier. Impact of stochastic interest rates and stochastic volatility on variable annuities. *SSRN Electronic Journal*, 10 2009. Paris December 2009 Finance International Meeting AFFI - EUROFIDAI.

[15] H. Berestycki, R. Monneau, and J.A. Scheinkman. A non-local free boundary problem arising in a theory of financial bubbles. *Philosophical transactions. Series A, Mathematical, physical, and engineering sciences*, 372, 11 2014.

[16] D. Brigo and F. Mercurio. *Interest Rate Models — Theory and Practice: With Smile, Inflation and Credit.* Springer, New York, 2007.

[17] Z. Chen and P. A. Forsyth. A numerical scheme for the impulse control formulation for pricing variable annuities with a Guaranteed Minimum Withdrawal Benefit (GMWB). *Numerische Mathematik*, 109:535–569, 2008.

[18] Z. Chen and P.A. Forsyth. A semi-Lagrangian approach for natural gas storage valuation and optimal control. *SIAM Journal on Scientific Computing*, 30:339–368, 2007.

[19] Z. Chen, K.R. Vetzal, and P.A. Forsyth. The effect of modelling parameters on the value of GMWB guarantees. *Insurance: Mathematics and Economics*, 43:165–173, 2008.

[20] J. Choi. Valuation of gmwb under stochastic volatility. *Journal of Interdisciplinary Mathematics*, 21(3):539–551, 2018.

[21] M. G. Crandall, H. Ishii, and P. L. Lions. User's guide to viscosity solutions of second order partial differential equations. *Bulletin of the American Mathematical Society*, 27:1–67, 1992.

[22] M. Dai, Y.K. Kwok, and J. Zong. Guaranteed minimum withdrawal benefit in variable annuities. *Mathematical Finance*, 18:595–611, 2008.

[23] D.M. Dang, C. C. Christara, K. R. Jackson, and A. Lakhany. A PDE pricing framework for cross-currency interest rate derivatives. *Procedia Computer Science*, 1(1):2371–2380, 2010. ICCS 2010.

[24] D.M. Dang and P.A. Forsyth. Continuous time mean-variance optimal portfolio allocation under jump diffusion: A numerical impulse control approach. *Numerical Methods for Partial Differential Equations*, 30:664–698, 2014.

[25] M. H. A. Davis, X. Guo, and G. Wu. Impulse control of multidimensional jump diffusions. *SIAM Journal on Control and Optimization*, 48:5276–5293, 2010.

[26] K. Debrabant and E.R. Jakobsen. Semi-Lagrangian schemes for linear and fully non-linear diffusion equations. *Mathematics of Computation*, 82:1433–1462, 2013.

[27] S. Demiralp, J. Eisenschmidt, and T. Vlassopoulos. Negative interest rates, excess liquidity and retail deposits:

Banks' reaction to unconventional monetary policy in the euro area. *European Economic Review*, 136:103745, 2021.

[28] M. Dempster and J. Hutton. Numerical valuation of cross-currency swaps and swaptions. *SSRN Electronic Journal*, 02 1996.

[29] B. Dong, W. Xu, and Y.K. Kwok. Willow tree algorithms for pricing guaranteed minimum withdrawal benefits under jump-diffusion and CEV models. *Quantitative Finance*, 19(10):1741–1761, 2019.

[30] R. Donnelly, S. Jaimungal, and D. Rubisov. Valuing guaranteed withdrawal benefits with stochastic interest rates and volatility. *Quantitative Finance*, 14:369–382, 2014.

[31] D.G. Duffy. *Green's Functions with Applications*. Chapman and Hall/CRC, New York, 2nd edition, 2015.

[32] M. Egami. A direct solution method for stochastic impulse control problems of one-dimensional diffusions. *SIAM Journal on Control and Optimization*, 47(3):1191–1218, 2008.

[33] F. Fang and C.W. Oosterlee. A novel pricing method for European options based on Fourier-Cosine series expansions. *SIAM Journal on Scientific Computing*, 31:826–848, 2008.

[34] P. A. Forsyth and G. Labahn. Numerical methods for controlled Hamilton-Jacobi-Bellman PDEs in finance. *Journal of Computational Finance*, 11 (Winter):1–44, 2008.

[35] P. A. Forsyth and G. Labahn. ϵ-monotone Fourier methods for optimal stochastic control in finance. *Journal of Computational Finance*, 22(4):25–71, 2019.

[36] M. G. Garroni and J. L. Menaldi. *Green functions for second order parabolic integro-differential problems*. Number 275 in Pitman Research Notes in Mathematics. Longman Scientific and Technical, Harlow, Essex, UK, 1992.

[37] L. Goudenége, A. Molent, and A. Zanette. Pricing and hedging GMWB in the Heston and in the Black-Scholes with stochastic interest rate models. *Computational Management Science*, 16:217–248, 2016.

[38] L. Goudenége, A. Molent, and A. Zanette. Gaussian process regression for pricing variable annuities with stochastic volatility and interest rate. *Decisions in Economics and Finance*, 06 2020. To be published.

[39] H. Guan and Z. Liang. Viscosity solution and impulse control of the diffusion model with reinsurance and fixed transaction costs. *Insurance: Mathematics and Economics*, (54):109–122, 2014.

[40] N. Gudkov, K. Ignatieva, and J. Ziveyi. Pricing of guaranteed minimum withdrawal benefits in variable annuities under stochastic volatility, stochastic interest rates and stochastic mortality via the componentwise splitting method. *Quantitative Finance*, 19:1–18, 09 2018.

[41] X. Guo and G. Wu. Smooth fit principle for impulse control of multidimensional diffusion processes. *SIAM Journal on Control and Optimization*, 48(2):594–617, 2009.

[42] Y. Huang and P.A. Forsyth. Analysis of a penalty method for pricing a Guaranteed Minimum Withdrawal Benefit (GMWB). *IMA Journal of Numerical Analysis*, 32:320–351, 2012.

[43] Y. Huang, P.A. Forsyth, and G. Labahn. Combined fixed and point policy iteration for HJB equations in finance. *SIAM Journal on Numerical Analysis*, 50:1861–1882, 2012.

[44] Y. Huang, P.A. Forsyth, and G. Labahn. Iterative methods for the solution of the singular control formulation of a GMWB pricing problem. *Numerische Mathematik*, 122:133–167, 2012.

[45] Y.T. Huang and Y.K. Kwok. Analysis of optimal dynamic withdrawal policies in withdrawal guarantees products. *Journal of Economic Dynamics and Control*, 45:19–43, 2014.

[46] Y.T. Huang and Y.K. Kwok. Regression-based Monte Carlo methods for stochastic control models: variable annuities with lifelong guarantees. *Quantitative Finance*, 16(6):905–928, 2016.

[47] Y.T. Huang, P. Zeng, and Y.K. Kwok. Optimal initiation of guaranteed lifelong withdrawal benefit with dynamic withdrawals. *SIAM Journal on Financial Mathematics*, 8:804–840, 2017.

[48] K. Ignatieva, A. Song, and J. Ziveyi. Fourier space time-stepping algorithm for valuing guaranteed minimum withdrawal benefits in variable annuities under regime-switching and stochastic mortality. *ASTIN Bulletin*, 48(1):139–169, 2018.

[49] S. Jaimungal and V. Surkov. Valuing Early-Exercise Interest-Rate Options With Multi-Factor Affine Models. *International Journal of Theoretical and Applied Finance (IJTAF)*, 16(06):1–29, 2013.

[50] E. R. Jakobsen and K. H. Karlsen. A "maximum principle for semicontinuous functions" applicable to integro-partial differential equations. *Nonlinear differ. equ. appl.*, 13:137–165, 2006.

[51] A. Jobst and H. Lin. *Negative interest rate policy (NIRP): implications for monetary transmission and bank profitability in the euro area*. International Monetary Fund, 2016.

[52] A. Kling, F. Ruez, and J. Ruß. The impact of stochastic volatility on pricing, hedging, and hedge efficiency of variable annuity guarantees. *Astin Bulletin*, 41(2):511–545, 2011.

[53] R. Korn. Some applications of impulse control in mathematical finance. *Mathematical Methods of Operations Research*, 50(3):493–518, 1999.

[54] S.G. Kou. A jump diffusion model for option pricing. *Management Science*, 48:1086–1101, August 2002.

[55] M. Kouritzin and A. Mackay. VIX-linked fees for GMWBs via explicit solution simulation methods. *Insurance: Mathematics and Economics*, 81:1–17, 2018.

[56] Jose A Lopez, Andrew K Rose, and Mark M Spiegel. Why have negative nominal interest rates had such a small effect on bank performance? Cross country evidence. *European Economic Review*, 124:103402, 2020.

[57] Y. Lu, D.M. Dang, P.A. Forsyth, and G. Labahn. An ϵ-monotone Fourier method for Guaranteed Minimum Withdrawal Benefit (GMWB) as a continuous impulse control problem. Submitted, 06 2022.

[58] X. Luo and P.V. Shevchenko. Valuation of variable annuities with guaranteed minimum withdrawal and death benefits via stochastic control optimization. *Insurance: Mathematics and Economics*, 62(3):5–15, 2015.

[59] K. Ma and P.A. Forsyth. An unconditionally monotone numerical scheme for the two-factor uncertain volatility model. *IMA Journal of Numerical Analysis*, 37(2):905–944, 2017.

[60] R.C. Merton. Option pricing when underlying stock returns are discontinuous. *Journal of Financial Economics*, 3:125–144, 1976.

[61] M.A. Milevsky and T.S. Salisbury. Financial valuation of guaranteed minimum withdrawal benefits. *Insurance: Mathematics and Economics*, 38:21–38, 2006.

[62] A. Molent. Taxation of a GMWB variable annuity in a stochastic interest rate model. *ASTIN Bulletin*, 50(3):1001–1035, 2020.

[63] J.F. Navas. On jump diffusion processes for asset returns. Working paper, Instituto de Empresa, 2000.

[64] B. Oksendal and A. Sulem. *Applied Stochastic Control of Jump Diffusions*. Springer, 3rd edition, 2019.

[65] D. Ou. *Efficient Nested Simulation of Tail Risk Measures for Variable Annuities*. PhD thesis, 2021.

[66] J. Peng, K.S. Leung, and Y.K. Kwok. Pricing guaranteed minimum withdrawal benefits under stochastic interest rates. *Quantitative Finance*, 12:933–941, 2010.

[67] H. Pham. On some recent aspects of stochastic control and their applications. *Probability Surveys*, 2:506–549, 2005.

[68] A. Picarelli, C. Reisinger, and J. Arto. *Boundary Mesh Refinement For Semi-Lagrangian Schemes: Numerical Methods and Applications in Optimal Control*, pages 155–174. 08 2018.

[69] D.M. Pooley, P.A. Forsyth, and K.R. Vetzal. Numerical convergence properties of option pricing PDEs with uncertain volatility. *IMA Journal of Numerical Analysis*, 23:241–267, 2003.

[70] C. Reisinger and J.R. Arto. Boundary treatment and multigrid preconditioning for semi-Lagrangian schemes applied to Hamilton– Jacobi– Bellman equations. *Journal of Scientific Computing*, 72:198–230, 2017.

[71] Daedal Research. The US Annuity Market: Analysis By Type, By Distribution Channel, By Contract Type, By Investment Category, By Asset Under Management, By Annuity Premium Size and Trends with Impact of COVID-19 and Forecast up to 2022, 2022.

[72] M.J. Ruijter, C.W. Oosterlee, and R.F.T. Aalbers. On the Fourier cosine series expansion (COS) method for stochastic control problems. *Numerical Linear Algebra with Applications*, 20:598–625, 2013.

[73] R.C. Seydel. Existence and uniqueness of viscosity solutions for QVI associated with impulse control of jump-diffusions. *Stochastic Processes and Their Applications*, 119:3719–3748, 2009.

[74] P. Shevchenko and X. Luo. Valuation of variable annuities with guaranteed minimum withdrawal benefit under stochastic interest rate. *Insurance: Mathematics and Economics*, 76:104–117, 07 2017.

[75] P.V. Shevchenko and X. Luo. A unified pricing of variable annuity guarantees under the optimal stochastic control framework. *Risks*, 4(3):1–31, 2016.

[76] P. M. Van Staden, D.M. Dang, and P.A. Forsyth. Mean-quadratic variation portfolio optimization: A desirable alternative to time-consistent mean-variance optimization? *SIAM Journal on Financial Mathematics*, 10(3):815–856, 2019.

[77] P. M. Van Staden, D.M. Dang, and P.A. Forsyth. On the distribution of terminal wealth under dynamic mean-variance optimal investment strategies. *SIAM Journal on Financial Mathematics*, 12(2):566–603, 2021.

[78] P. M. Van Staden, D.M. Dang, and P.A. Forsyth. The surprising robustness of dynamic mean-variance portfolio optimization to model misspecification errors. *European Journal of Operational Research*, 289:774–792, 2021.

[79] P.M. Van Staden, D.M. Dang, and P.A. Forsyth. Time-consistent mean-variance portfolio optimization: a numerical impulse control approach. *Insurance: Mathematics and Economics*, 83(C):9–28, 2018.

[80] O. Vasicek. An equilibrium characterization of the term structure. *Journal of financial economics*, 5(2):177–188, 1977.

[81] V.L. Vath, M. Mnif, and H. Pham. A model of optimal portfolio selection under liquidity risk and price impact. *Finance and Stochastics*, 11:51–90, 2007.
[82] J. Wang and P.A. Forsyth. Maximal use of central differencing for Hamilton-Jacobi-Bellman PDEs in finance. *SIAM Journal on Numerical Analysis*, 46:1580–1601, 2008.
[83] L. Wang, A. Kalife, X. Tan, B. Bouchard, and S. Mouti. Understanding guaranteed minimum withdrawal benefit: a study on financial risks and rational lapse strategy. *Insurance markets and companies: analyses and actuarial computations*, (61):6–21, 2015.

Appendix A Truncation error of Fourier series

As $\alpha \to \infty$, there is no loss of information in the discrete convolution (4.45). However, for any finite α, there is an error due to the use of a truncated Fourier series. Using similar arguments in [35], we have

$$\begin{aligned} |\tilde{g}_{n-l,k-d}(\alpha) - \tilde{g}_{n-l,k-d}(\infty)| \;&\leq\; \frac{2}{P^\dagger}\frac{1}{Q^\dagger}\sum_{s\in[\alpha N^\dagger/2,\infty)}^{z\in\mathbb{Z}}{}^{*} \left(\frac{\sin^2 \pi\eta_s\Delta w}{(\pi\eta_s\Delta w)^2}\right)\left(\frac{\sin^2 \pi\xi_z\Delta r}{(\pi\xi_z\Delta r)^2}\right)|G(\eta_s,\xi_z,\Delta\tau)| \\ &\quad+\; \frac{1}{P^\dagger}\frac{2}{Q^\dagger}\sum_{s\in\mathbb{Z}}^{z\in[\alpha K^\dagger/2,\infty)}{}^{*} \left(\frac{\sin^2 \pi\eta_s\Delta w}{(\pi\eta_s\Delta w)^2}\right)\left(\frac{\sin^2 \pi\xi_z\Delta r}{(\pi\xi_z\Delta r)^2}\right)|G(\eta_s,\xi_z,\Delta\tau)|\,. \end{aligned} \tag{A.1}$$

Using the closed-form expression (4.41), and noting that $\mathrm{Re}\left(\overline{B}(\eta)\right) \leq 1$, $|\rho| < 1$, we then have

$$\begin{aligned} \mathrm{Re}(\Psi(\eta,\xi)) \;&=\; -\frac{\sigma_{Z}^2}{2}(2\pi\eta)^2 - \rho\sigma_{Z}\sigma_{R}(2\pi\eta)(2\pi\xi) - \frac{\sigma_{R}^2}{2}(2\pi\xi)^2 - \lambda + \lambda\mathrm{Re}\left(\overline{B}(\eta)\right) \\ &\leq\; -\left(1-|\rho|\right)\frac{\sigma_{Z}^2}{2}(2\pi\eta)^2 - \left(1-|\rho|\right)\frac{\sigma_{R}^2}{2}(2\pi\xi)^2. \end{aligned} \tag{A.2}$$

Thus, from (A.2), we have

$$|G(\eta,\xi,\Delta\tau)| = |\exp\left(\Psi(\eta,\xi)\Delta\tau\right)| \leq \exp\left(-\left(1-|\rho|\right)\frac{\sigma_{Z}^2}{2}(2\pi\eta)^2\Delta\tau\right)\exp\left(-\left(1-|\rho|\right)\frac{\sigma_{R}^2}{2}(2\pi\xi)^2\Delta\tau\right). \tag{A.3}$$

Let $C_6 = 2\left(1-|\rho|\right)\sigma_{Z}^2\pi^2\Delta\tau/(P^\dagger)^2$ and $C_6' = 2\left(1-|\rho|\right)\sigma_{R}^2\pi^2\Delta\tau/(Q^\dagger)^2$. Taking (A.3) into (A.1), we can bound these infinite sums as follows

$$\begin{aligned} &|\tilde{g}_{n-l,k-d}(\alpha) - \tilde{g}_{n-l,k-d}(\infty)| \\ &\leq\; \left(\frac{2}{P^\dagger}\frac{4}{\pi^2\alpha^2}\sum_{s=\alpha N^\dagger/2}^{\infty} e^{-C_6 s^2}\right)\left(\frac{1}{Q^\dagger}\sum_{z\in\mathbb{Z}}\left(\frac{\sin^2 \pi\xi_z\Delta r}{(\pi\xi_z\Delta r)^2}\right)e^{-C_6' z^2}\right) \\ &\qquad+\left(\frac{2}{Q^\dagger}\frac{4}{\pi^2\alpha^2}\sum_{z=\alpha N^\dagger/2}^{\infty} e^{-C_6' z^2}\right)\left(\frac{1}{P^\dagger}\sum_{s\in\mathbb{Z}}\left(\frac{\sin^2 \pi\eta_s\Delta w}{(\pi\eta_s\Delta w)^2}\right)e^{-C_6 s^2}\right) \\ &\leq\; \frac{8(K^\dagger)^2(1+e^{-C_6'})}{P^\dagger Q^\dagger\pi^4\alpha^2(1-e^{-C_6'})}\frac{\exp\left(-C_6 N^\dagger\alpha^2/4\right)}{1-e^{-C_6 N^\dagger\alpha}} + \frac{8(N^\dagger)^2(1+e^{-C_6})}{P^\dagger Q^\dagger\pi^4\alpha^2(1-e^{-C_6})}\frac{\exp\left(-C_6' K^\dagger\alpha^2/4\right)}{1-e^{-C_6' K^\dagger\alpha}}, \end{aligned}$$

which yields (considering fixed $P^\dagger$ and $Q^\dagger$ here)

$$|\tilde{g}_{n-l,k-d}(\alpha) - \tilde{g}_{n-l,k-d}(\infty)| \;\simeq\; \mathcal{O}\left(e^{-1/h}/h^2\right).$$

Appendix B A proof of Proposition 5.1

Proof of Proposition 5.1. Letting $p = n - l$ and $q = k - d$, we have

$$\begin{aligned} \Delta w\Delta r\sum_{l\in\mathbb{N}^\dagger}^{k\in\mathbb{K}^\dagger}{}^{*}\tilde{g}_{n-l,k-d} \;&\overset{\text{(i)}}{=}\; \frac{P^\dagger}{N^\dagger}\frac{Q^\dagger}{K^\dagger}\sum_{p\in\mathbb{N}^\dagger}^{q\in\mathbb{K}^\dagger}{}^{*}\tilde{g}_{p,q} \\ &\overset{\text{(ii)}}{=}\; \frac{P^\dagger}{N^\dagger}\frac{Q^\dagger}{K^\dagger}\sum_{p\in\mathbb{N}^\dagger}^{q\in\mathbb{K}^\dagger}{}^{*}\frac{1}{P^\dagger}\frac{1}{Q^\dagger}\sum_{s\in\mathbb{N}^\alpha}^{z\in\mathbb{K}^\alpha}{}^{*} e^{2\pi i\eta_s p\Delta w}e^{2\pi i\xi_z q\Delta r}\;\mathrm{tg}(s,z)G(\eta_s,\xi_z,\Delta\tau) \\ &=\; \frac{1}{N^\dagger}\frac{1}{K^\dagger}\sum_{s\in\mathbb{N}^\alpha}^{z\in\mathbb{K}^\alpha}{}^{*}\mathrm{tg}(s,z)G(\eta_s,\xi_z,\Delta\tau)\sum_{p\in\mathbb{N}^\dagger}\exp\left(\frac{2\pi isp}{N^\dagger}\right)\sum_{q\in\mathbb{K}^\dagger}\exp\left(\frac{2\pi izq}{K^\dagger}\right) \\ &\overset{\text{(iii)}}{=}\; G(0,0,\Delta\tau) \;\overset{\text{(iv)}}{=}\; 1. \end{aligned} \tag{B.1}$$

Here, in (i), we use the periodicity of $\tilde{g}_{n-l,k-d}$, i.e. the sequence $\{\tilde{g}_{-N^\dagger/2,k}(\alpha), \ldots, \tilde{g}_{N^\dagger/2-1,k}(\alpha)\}$ for a fixed $k \in \mathbb{K}^\dagger$ is $N^\dagger$-periodic, and similarly, the sequence $\{\tilde{g}_{n,-K^\dagger/2}(\alpha), \ldots, \tilde{g}_{n,K^\dagger/2-1}(\alpha)\}$ for a fixed $n \in \mathbb{N}^\dagger$ is $K^\dagger$-periodic; in (ii), we use the definition of (4.45), noting the term $\mathrm{tg}(s,z)$ is given in (4.44); in (iii),we apply properties of roots of unity; in (iv), we use the closed-form expression (4.41). □

Appendix C ℓ-stability in $\Omega_{\text{in}} \cup \Omega_{a_{\min}}$

We now show the bounds (5.5)-(5.6) for $\Omega_{\text{in}} \cup \Omega_{a_{\min}}$. We note that numerical solutions at nodes in $\Omega \setminus (\Omega_{\text{in}} \cup \Omega_{a_{\min}})$ satisfy the bounds (5.5)-(5.6) at the same $j \in \mathbb{J}$ and $m = 0, \ldots, M$, that is

$$\max_{n \in \mathbb{N}^c \text{ or } k \in \mathbb{K}^c} \left\{v_{n,k,j}^m\right\} \text{ satisfies (5.5)}, \quad \text{and} \quad \min_{n \in \mathbb{N}^c \text{ or } k \in \mathbb{K}^c} \left\{v_{n,k,j}^m\right\} \text{ satisfies (5.6)}. \tag{C.1}$$

Base case: when $m = 0$, (5.5)-(5.6) hold for all $j \in \mathbb{J}$, which follows from the initial condition (4.17) for $n \in \mathbb{N}$

Induction hypothesis: we assume that (5.5)-(5.6) hold for $m = \hat{m}$, where $\hat{m} \leq M - 1$, and $j \in \mathbb{J}$.

Induction: we show that (5.5)-(5.6) also hold for $m = \hat{m} + 1$ and $j \in \mathbb{J}$. This is done in two steps. In Step 1, we show, for $j \in \mathbb{J}$,

$$\left[v_j^{\hat{m}+}\right]_{\max} \leq e^{2\hat{m}\epsilon\frac{\Delta\tau}{T}} e^{C\hat{m}\Delta\tau} \left(\left\|v^0\right\|_\infty + a_j\right) \tag{C.2}$$

$$-2\hat{m}\epsilon\frac{\Delta\tau}{T} e^{2\hat{m}\epsilon\frac{\Delta\tau}{T}} e^{C\hat{m}\Delta\tau} \left(\left\|v^0\right\|_\infty + a_j\right) \leq \left[v_j^{\hat{m}+}\right]_{\min}, \tag{C.3}$$

where $\left[v_j^{\hat{m}+}\right]_{\max} = \max_{n,k} \left\{v_{n,k,j}^{\hat{m}+}\right\}$ and $\left[v_j^{\hat{m}+}\right]_{\min} = \min_{n,k} \left\{v_{n,k,j}^{\hat{m}+}\right\}$. In Step 2, we bound the timestepping result (4.40) at $m = \hat{m} + 1$ using (C.2)-(C.3).

Step 1 - Bound for $v_{n,k,j}^{\hat{m}+}$: Since $v_{n,k,j}^{\hat{m}+} = \max\left((v^{(1)})_{n,k,j}^{\hat{m}+}, (v^{(2)})_{n,k,j}^{\hat{m}+}\right)$, using (4.25), we have

$$v_{n,k,j}^{\hat{m}+} = \sup_{\gamma_{n,k,j}^{\hat{m}} \in [0,a_j]} \left[\mathcal{I}\left\{v^{\hat{m}}\right\} \left(\max\left(e^{w_n} - \gamma_{n,j}^{\hat{m}}, e^{w_{\min}^\dagger}\right), r_k, a_j - \gamma_{n,k,j}^{\hat{m}}\right) + f(\gamma_{n,k,j}^{\hat{m}})\right]. \tag{C.4}$$

As noted in Remark 4.2, for the case $c > 0$ as considered here, the supremum of (C.4) is achieved by an optimal control $\gamma^* \in [0, a_j]$. That is, (C.4) becomes

$$v_{n,k,j}^{\hat{m}+} = \mathcal{I}\left\{v^{\hat{m}}\right\} \left(\max\left(e^{w_n} - \gamma^*, e^{w_{\min}^\dagger}\right), r_k, a_j - \gamma^*\right) + f(\gamma^*), \quad \gamma^* \in [0, a_j]. \tag{C.5}$$

We assume that $\max\left(e^{w_n} - \gamma^*, e^{w_{\min}^\dagger}\right) \in [e^{w_{n'}}, e^{w_{n'+1}}]$ and $(a_j - \gamma^*) \in [a_{j'}, a_{j'+1}]$, and nodes that are used for linear interpolation are $(\mathbf{x}_{n',k,j'}^{\hat{m}}, \ldots, \mathbf{x}_{n'+1,k,j'+1}^{\hat{m}})$. We note that these node could be outside $\Omega_{\text{in}} \cup \Omega_{a_{\min}}$, in $\Omega_{w_{\min}} \cup \Omega_{wa_{\min}}$. However, by (C.1), the numerical solutions at these nodes satisfy the same bounds (5.5)-(5.6). Computing $v_{n,k,j}^{\hat{m}+}$ using linear interpolation results in

$$v_{n,k,j}^{\hat{m}+} = x_a \left(x_w\ v_{n',k,j'}^{\hat{m}} + (1 - x_w)\ v_{n'+1,k,j'}^{\hat{m}}\right) + (1 - x_a)\left(x_w\ v_{n',k,j'+1}^{\hat{m}} + (1 - x_w)\ v_{n'+1,k,j'+1}^{\hat{m}}\right), \tag{C.6}$$

where $0 \leq x_a \leq 1$ and $0 \leq x_w \leq 1$ are interpolation weights. In particular,

$$x_a = \frac{a_{j'+1} - (a_j - \gamma^*)}{a_{j'+1} - a_{j'}}. \tag{C.7}$$

Using (C.1) and the induction hypothesis for (5.5) gives abound for nodal values used in (C.6)

$$\begin{aligned} \left\{v_{n',k,j'}^{\hat{m}}, v_{n'+1,k,j'}^{\hat{m}}\right\} &\leq e^{2\hat{m}\epsilon\frac{\Delta\tau}{T}} e^{C\hat{m}\Delta\tau}(\|v^0\|_\infty + a_{j'}), \\ \left\{v_{n',k,j'+1}^{\hat{m}}, v_{n'+1,k,j'+1}^{\hat{m}}\right\} &\leq e^{2\hat{m}\epsilon\frac{\Delta\tau}{T}} e^{C\hat{m}\Delta\tau}(\|v^0\|_\infty + a_{j'+1}). \end{aligned} \tag{C.8}$$

Taking into account the non-negative weights in linear interpolation, particularly (C.7), and upper bounds in (C.8), the interpolated result $\mathcal{I}\left\{v^{\hat{m}}\right\}(\cdot)$ in (C.5) is bounded by

$$\mathcal{I}\left\{v^{\hat{m}}\right\} \left(\max\left(e^{w_n} - \gamma^*, e^{w_{\min}^\dagger}\right), r_k, a_j - \gamma^*\right) \leq e^{2\hat{m}\epsilon\frac{\Delta\tau}{T}} e^{C\hat{m}\Delta\tau}(\|v^0\|_\infty + (a_j - \gamma^*)). \tag{C.9}$$

Using (C.9) and $f(\gamma^*) \leq \gamma^*$ (by definition in (4.14)), (C.5) becomes

$$v_{n,k,j}^{\hat{m}+} \leq e^{2\hat{m}\epsilon\frac{\Delta\tau}{T}} e^{C\hat{m}\Delta\tau} \left(\|v^0\|_\infty + a_j - \gamma^*\right) + \gamma^* \leq e^{2\hat{m}\epsilon\frac{\Delta\tau}{T}} e^{C\hat{m}\Delta\tau} \left(\|v^0\|_\infty + a_j\right),$$

which proves (C.2) at $m = \hat{m}$.

For subsequent use, we note, since $v_{n,k,j}^{\hat{m}+} = \max\left((v^{(1)})_{n,k,j}^{\hat{m}+}, (v^{(2)})_{n,k,j}^{\hat{m}+}\right)$, (C.2) results in

$$\left\{(v^{(1)})_{n,k,j}^{\hat{m}+}, (v^{(2)})_{n,k,j}^{\hat{m}+}\right\} \ \le \ v_{n,k,j}^{\hat{m}+} \ \le \ e^{2\hat{m}\epsilon\frac{\Delta\tau}{T}} e^{C\hat{m}\Delta\tau}\left(\|v^0\|_\infty + a_j\right). \tag{C.10}$$

Next, we derive a lower bound for $(v^{(1)})_{n,k,j}^{\hat{m}+}$ and $(v^{(2)})_{n,k,j}^{\hat{m}+}$. By the induction hypothesis for (5.6), we have $v_{n,k,j}^{\hat{m}} \ge -2m\epsilon\frac{\Delta\tau}{T}e^{2\hat{m}\epsilon\frac{\Delta\tau}{T}}e^{C\hat{m}\Delta\tau}\left(\left\|v^0\right\|_\infty + a_j\right)$. Comparing $(v^{(1)})_{n,k,j}^{\hat{m}+}$ given by the supremum in (4.25) with $v_{n,k,j}^{\hat{m}}$, which is the candidate for the supremum evaluated at $\gamma_{n,k,j}^{\hat{m}} = 0$, yields

$$v_{n,k,j}^{\hat{m}} \ \ge \ (v^{(1)})_{n,k,j}^{\hat{m}+} \ \ge \ -2\hat{m}\epsilon\frac{\Delta\tau}{T}e^{2\hat{m}\epsilon\frac{\Delta\tau}{T}}e^{C\hat{m}\Delta\tau}\left(\left\|v^0\right\|_\infty + a_j\right), \tag{C.11}$$

which proves (C.3) at $m = \hat{m}$.

For $(v^{(2)})_{n,k,j}^{\hat{m}+}$ in (4.25), we consider optimal $\gamma = \gamma^*$, where $\gamma^* \in (C_r\Delta\tau, a_j]$. Using the induction hypothesis and non-negative weights of linear interpolation, noting $\gamma^* \ge 0$ and assuming $f(\gamma^*) \ge 0$, gives

$$\begin{aligned}
(v^{(2)})_{n,k,j}^{\hat{m}+} \ &\ge \ -2\hat{m}\epsilon\frac{\Delta\tau}{T}e^{2\hat{m}\epsilon\frac{\Delta\tau}{T}}e^{C\hat{m}\Delta\tau}\left(\left\|v^0\right\|_\infty + (a_j - \gamma^*)\right) + f(\gamma^*) \\
&\ge \ -2\hat{m}\epsilon\frac{\Delta\tau}{T}e^{2\hat{m}\epsilon\frac{\Delta\tau}{T}}e^{C\hat{m}\Delta\tau}\left(\left\|v^0\right\|_\infty + a_j\right).
\end{aligned} \tag{C.12}$$

From (C.10)-(C.11) and (C.12), noting $\epsilon \le 1/2$, we have

$$\left\{|\,(v^{(1)})_{n,k,j}^{\hat{m}+}\,|, |\,(v^{(2)})_{n,k,j}^{\hat{m}+}\,|\right\} \le e^{2\hat{m}\epsilon\frac{\Delta\tau}{T}}e^{C\hat{m}\Delta\tau}\left(\|v^0\|_\infty + a_j\right). \tag{C.13}$$

Step 2 - Bound for $v_{n,k,j}^{\hat{m}+1}$: We will show that (5.5)-(5.6) hold at $m = \hat{m}+1$. For all $n \in \mathbb{N}$, $k \in K$, $j \in J$, using (4.34) and (4.38), we have

$$\begin{aligned}
\left(v_{\text{SL}}^{(1)}\right)_{n,k,j}^{\hat{m}+1} \ &= \ \Delta w \Delta r \sum_{l\in\mathbb{N}^\dagger}^{d\in\mathbb{K}^\dagger}{}^{*}\ \tilde{g}_{n-l,k-d}\left(v_{\text{SL}}^{(1)}\right)_{l,d,j}^{\hat{m}+} \\
&= \ \Delta w \Delta r \sum_{l\in\mathbb{N}^\dagger}^{d\in\mathbb{K}^\dagger}{}^{*}\left(\max\left(\tilde{g}_{n-l,k-d}, 0\right) + \min\left(\tilde{g}_{n-l,k-d}, 0\right)\right)\left(v_{\text{SL}}^{(1)}\right)_{l,d,j}^{\hat{m}+}.
\end{aligned} \tag{C.14}$$

Note that $\left(v_{\text{SL}}^{(1)}\right)_{l,d,j}^{\hat{m}+}$ is computed by (4.34), where $\breve{w}_l$ and $\breve{r}_d$ have no dependence on a_j. From (C.14), using the property of linear interpolation and the upper bound (C.13), we have

$$\begin{aligned}
|\left(v_{\text{SL}}^{(1)}\right)_{n,k,j}^{\hat{m}+1}| \ &\le \ \frac{\Delta w \Delta r}{|1+\Delta\tau r_d|}\sum_{l\in\mathbb{N}^\dagger}^{d\in\mathbb{K}^\dagger}{}^{*}\left(\max\left(\tilde{g}_{n-l,k-d}, 0\right) + |\min\left(\tilde{g}_{n-l,k-d}, 0\right)|\right)\left|\mathcal{I}\left\{(v^{(1)})^{\hat{m}+}\right\}(\breve{w}_l, \breve{r}_d, a_j)\right| \\
&\overset{\text{(i)}}{\le} \ (1 + 2\epsilon\frac{\Delta\tau}{T})e^{2\epsilon\hat{m}\frac{\Delta\tau}{T}}\left(1 + \Delta\tau C\right)e^{C\hat{m}\Delta\tau}\left(\|v^0\|_\infty + a_j\right) \\
&\le \ e^{2\epsilon(\hat{m}+1)\frac{\Delta\tau}{T}}e^{C(\hat{m}+1)\Delta\tau}\left(\|v^0\|_\infty + (1+\mu)a_j + c\right),
\end{aligned} \tag{C.15}$$

where in (i), we use (5.1) and (5.4). Similarly, for $n \in \mathbb{N}$, $k \in \mathbb{K}$, $j \in \mathbb{J}$, we also have

$$|\left(v_{\text{SL}}^{(2)}\right)_{n,k,j}^{\hat{m}+1}| \le e^{2(\hat{m}+1)\epsilon\frac{\Delta\tau}{T}}e^{C(\hat{m}+1)\Delta\tau}(\|v^0\|_\infty + a_j). \tag{C.16}$$

Therefore, from (C.15)-(C.16), we conclude, for $n \in \mathbb{N}$, $k \in \mathbb{K}$, $j \in \mathbb{J}$,

$$|v_{n,k,j}^{\hat{m}+1}| \le e^{2(\hat{m}+1)\epsilon\frac{\Delta\tau}{T}}e^{C(\hat{m}+1)\Delta\tau}(\|v^0\|_\infty + a_j).$$

This proves (5.5) at time $m = \hat{m}+1$.

To prove (5.6), similarly with (C.14), for $n \in \mathbb{N}$, $k \in \mathbb{K}$, $j \in \mathbb{J}$, we have

$$
\begin{aligned}
\left(v_{\text{SL}}^{(1)}\right)_{n,k,j}^{\hat{m}+1} &= \Delta w \Delta r \sum_{l\in\mathbb{N}^\dagger}^{d\in\mathbb{K}^\dagger}{}^{*} \tilde{g}_{n-l,k-d} \; \left(v_{\text{SL}}^{(1)}\right)_{l,d,j}^{\hat{m}+} \\
&\geq \Delta w \Delta r \Bigg[\sum_{l\in\mathbb{N}^\dagger}^{d\in\mathbb{K}^\dagger}{}^{*} \max\left(\tilde{g}_{n-l,k-d}, 0\right) \left(v_{\text{SL}}^{(1)}\right)_{l,d,j}^{\hat{m}+} - \sum_{l\in\mathbb{N}^\dagger}^{d\in\mathbb{K}^\dagger}{}^{*} \left|\min\left(\tilde{g}_{n-l,k-d}, 0\right)\right| \left|\left(v_{\text{SL}}^{(1)}\right)_{l,d,j}^{\hat{m}+}\right|\Bigg] \\
&\overset{\text{(i)}}{\geq} \frac{\Delta w \Delta r}{1+\Delta\tau r_d} \sum_{l\in\mathbb{N}^\dagger}^{d\in\mathbb{K}^\dagger}{}^{*} \tilde{g}_{n-l,k-d} \; \left[-2\epsilon\hat{m}\frac{\Delta\tau}{T} e^{2\epsilon\hat{m}\frac{\Delta\tau}{T}} e^{C\hat{m}\Delta\tau}\left(\left\|v^0\right\|_\infty + a_j\right)\right] \qquad \text{(C.17)} \\
&\quad - \frac{\Delta w \Delta r}{1+\Delta\tau r_d} \sum_{l\in\mathbb{N}^\dagger}^{d\in\mathbb{K}^\dagger}{}^{*} \left|\min\left(\tilde{g}_{n-l,k-d}, 0\right)\right| \left[e^{2\epsilon\hat{m}\frac{\Delta\tau}{T}} e^{C\hat{m}\Delta\tau}\left(\left\|v^0\right\|_\infty + a_j\right)\right] \\
&\overset{\text{(ii)}}{\geq} -2\epsilon(\hat{m}+1)\frac{\Delta\tau}{T} e^{2\epsilon(\hat{m}+1)\frac{\Delta\tau}{T}} e^{C(\hat{m}+1)\Delta\tau}\left(\left\|v^0\right\|_\infty + a_j\right), \qquad \text{(C.18)}
\end{aligned}
$$

where, in (i), we used (C.11), (C.13), and the property of linear interpolation; in (ii), we used (4.46), (5.1) and (5.4). Thus, by (C.18), we have

$$
v_{n,k,j}^{\hat{m}+1} \;\geq\; \left(v_{\text{SL}}^{(1)}\right)_{n,k,j}^{\hat{m}+1} \;\geq\; -2\epsilon(\hat{m}+1)\frac{\Delta\tau}{T} e^{2\epsilon(\hat{m}+1)\frac{\Delta\tau}{T}} e^{C(\hat{m}+1)\Delta\tau}\left(\left\|v^0\right\|_\infty + a_j\right),
$$

which proves (5.6) at $m = \hat{m}+1$.